1990

Quantitative Evaluation Of Myocardial Fibrosis Using Polarization-video Microscopy

J Geoffrey Pickering

QUANTITATIVE EVALUATION OF MYOCARDIAL FIBROSIS USING POLARIZATION-VIDEO MICROSCOPY

by

J. Geoffrey Pickering

Department of Medical Biophysics

submitted in partial fulfillment

of the requirements for the degree of

Doctor of Philosophy

Faculty of Graduate Studies

The University of Western Ontario

London, Ontario

March, 1990

ISBN 0-315-59102-1

Abstract

Fibrosis is an essential feature of tissue repair and is characterized by the deposition of collagen. Fibrosis in the myocardium is prevalent among patients with heart disease and can significantly impair cardiac function. The evaluation and treatment of myocardial scarring is however limited by a lack of quantitative and practical methods for studying fibrosis. My thesis was that both the amount and the relative maturity of fibrotic collagen could be quantified directly from histologic sections by taking advantage of the birefringent properties of collagen and assessing these with computer-based image analysis. A system, using polarized light microscopy and video microscopy, was therefore developed.

To quantify fibrosis, the high brightness intensity of collagen stained with picrosirius red was exploited. Using color filtering and image processing, a digital video image of myocardium was generated in which only collagen was visible. The collagen was quantified as the area-fraction of visible pixels. This video approach was compared to that of hydroxyproline analysis using samples from 14 autopsy hearts. A strong correlation (r=0.98) between the two techniques was demonstrated. Also, in 22 endomyocardial biopsy specimens, the collagen content determined by the video technique was shown to correlate well with the collagen content determined by stereology (r=0.95).

To quantify the relative maturity of fibrosis, the increasing birefringence of maturing fibrotic collagen was utilized. The median grey-level of all pixels depicting collagen served as the index of collagen brightness and reflected fiber birefringence. I measured the brightness of collagen in the scar that formed after superficial injury to the rat gracilis muscle. In this model, the diffuse arrangement of the collagen fibers was similar to that in interstitial myocardial fibrosis. Collagen brightness increased progressively over a 63-day period. I also measured brightness in the scar that formed

after myocardial infarction in dogs and found that collagen brightness in 6-week infarcts was greater than that in 3-week infarcts ($p<0.01$).

The clinical utility of the system was confirmed by two studies in which fibrosis in the human transplanted heart was studied. In the first study, I examined the relationship between the length of time the heart was not perfused during transport from donor to recipient (graft ischemic time), and the amount of fibrosis present one week after transplantation. Collagen content was measured in endomyocardial biopsy samples from 36 transplant recipients and found to be linearly related to graft ischemic time ($r=0.60$). In the second study, I examined the relationship between allograft rejection and the amount and activity of fibrosis in five transplant patients. Serial biopsy samples, taken over a period of up to 1.5 years after transplantation, were evaluated. The collagen content of samples taken one year after surgery did not correlate with the frequency or severity of rejection. However, the activity of fibrosis was greatest in the early weeks (<12) after transplantation which was time when most of the rejection episodes had occurred.

In conclusion, both the content and the activity of myocardial fibrosis can be quantified using the polarization-video microscopy technique.

Acknowledgements

Several individuals have made important contributions to this work. I would like to thank Dr. D.R. Boughner for introducing me to the biophysics of cardiovascular diseases and for his skillful supervision of this research. I also acknowledge the support and sound advice that I received from the members of my advisory committee, Dr. C. Ellis and Dr. M.R. Roach.

I would also like to thank Dr. C. Guiraudon, Dr. W.J. Kostuk, Dr. P.W. Pflugfelder, and Dr. P. Whittaker for providing tissue. Dr. Whittaker's comments regarding this research were also valuable as were those of Dr. I. Vesely.

I also extend gratitude to Mrs. J. Dixon for her expert preparation of the histologic samples, Mr. W. Chung for performing the hydroxyproline assay, and Mrs. R. Pegg for her secretarial expertise.

Finally, I acknowledge the financial support from Dr. Boughner's research grant from the Heart & Stroke Foundation of Ontario, and the fellowship funding for myself from the Heart & Stroke Foundation of Canada.

Table of Contents

List of Photographic Plates

List of Figures

List of Tables

Chapter 1 Introduction

1.1 Introduction of the Problem

Collagen is the most abundant protein in the human body (Grant and Prockop 1972). In the myocardium, as in most tissues, it may be considered in two contexts: health and disease. In the healthy heart collagen constitutes a major component of the extracellular space of the myocardium but in many diseases of the heart excess collagen is deposited in the myocardium - a process termed fibrosis. In the past decade advances in the anatomy and biochemistry of normal myocardial collagen have greatly enhanced our understanding of the role this fibrous network plays in the function of the healthy heart (Caulfield and Borg 1979, Borg and Caulfield 1981, Medugorac et al 1983, Robinson et al 1987, Factor and Robinson 1988). In contrast, our knowledge of cardiac fibrosis remains limited and successful methods of influencing the process do not exist. This poor understanding is, in part, due to a paucity of satisfactory techniques available for the study of myocardial fibrosis. In this thesis I address this deficiency and present a technique that I have developed for the quantitative evaluation of myocardial fibrosis.

1.2 Functional Importance of Myocardial Fibrosis

Fibrosis is a nonspecific response to tissue injury and may occur in any organ (Gillman 1968). Its occurrence in the heart is of particular significance for a number of reasons. Firstly, cardiac muscle cells have no capacity to regenerate (Robbins and Cotran 1979, p 92). The universal response to myocyte death is therefore resorption of the necrotic debris followed by reparative fibrosis. Secondly, the primary function of the heart is a mechanical one and, as elaborated below, the deposition of excess fibrillar collagen can dramatically affect cardiac performance.

Presently, two general categories of cardiac fibrosis are recognized - replacement fibrosis and interstitial fibrosis. The former is typically seen following a myocardial infarction. When blood flow through a coronary artery ceases for a critical period of time, a large proportion of the myocytes supplied by that vessel will die. In the ensuing weeks collagen, synthesized by myocardial fibroblasts, is secreted and organizes to form a scar (Plate 1.1). The adequacy of scar formation will influence the geometric changes of the left ventricle that take place following the infarction (Jugdutt and Amy 1986) and is thus an important determinant of the immediate and long term hemodynamic performance of the heart (Pfeffer et al 1988).

Interstitial fibrosis, in contrast, is a more diffuse process in which collagen becomes deposited between individual myocytes and myocyte bundles (Plate 1.2). Muscle cell death may be the initiating event but is not associated with all cases of interstitial fibrosis (Abrahams et al 1987). Like replacement fibrosis, the functional effects of this type of fibrosis are important. Given the high elastic modulus of collagen (10^9 dynes.cm^{-2} per 100% elongation (Burton 1954)) its presence in excess can augment chamber stiffness and thereby impair filling of the ventricles during the diastolic phase of the cardiac cycle. This alteration in the passive pressure-volume relationship of the ventricle may contribute to the development of myocardial ischemia (Brutsaert et al 1986), decreased exercise tolerance (Topel et al 1985), and ultimately heart failure (Grossman 1986). Interstitial fibrosis may also interfere with the important diastolic function of normal myocardial collagen. The normal collagen architecture is such that collagen fibers encircling and bridging individual myocytes become stretched as myocytes shorten during systole (Robinson et al 1986, Factor and Robinson 1988). With the onset of ventricular relaxation, the now unloaded collagen fibers return to their unstretched state. This elastic behavior is believed to enhance chamber relaxation and contribute to the diastolic "suction" phenomena first described in 1956 by Brecher.

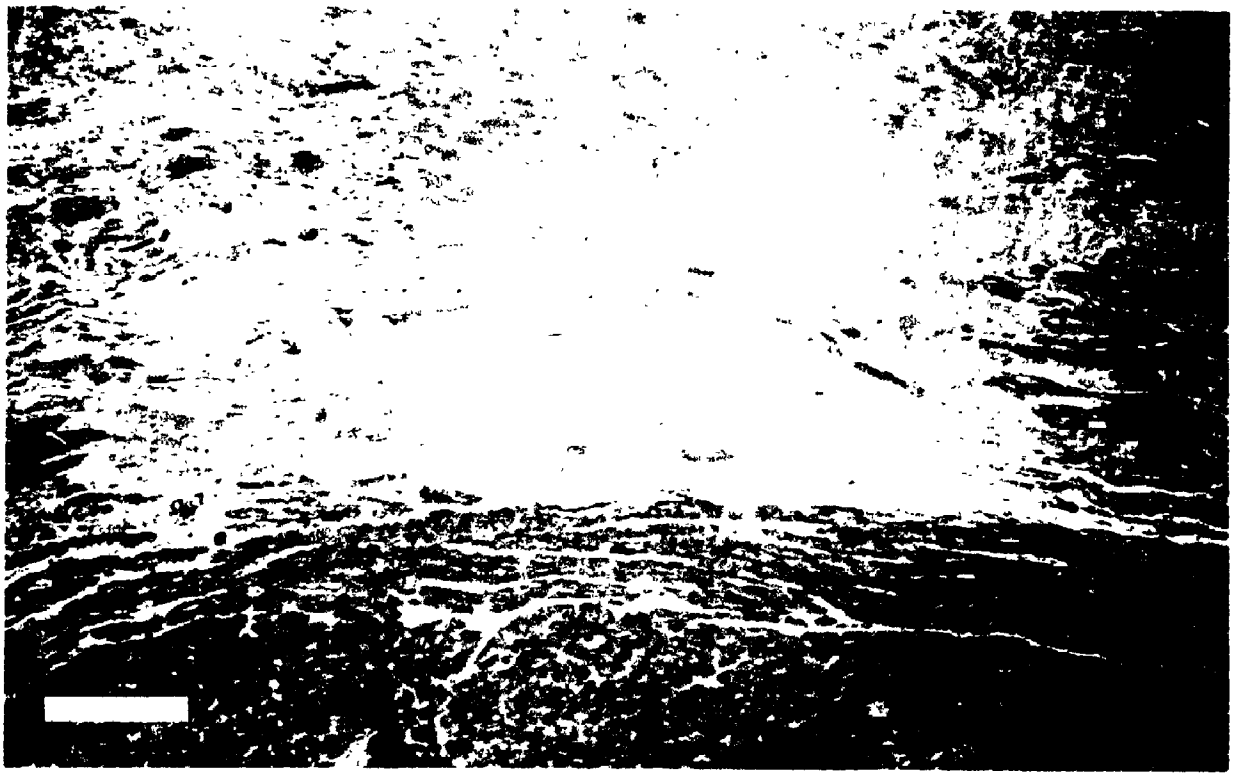

Plate 1.1: Photomicrograph of a region of infarcted myocardium. Dead myocytes have been replaced by a zone of fibrotic tissue (scar) which appears blue-green. Masson's trichrome. Bar, 300 μm.

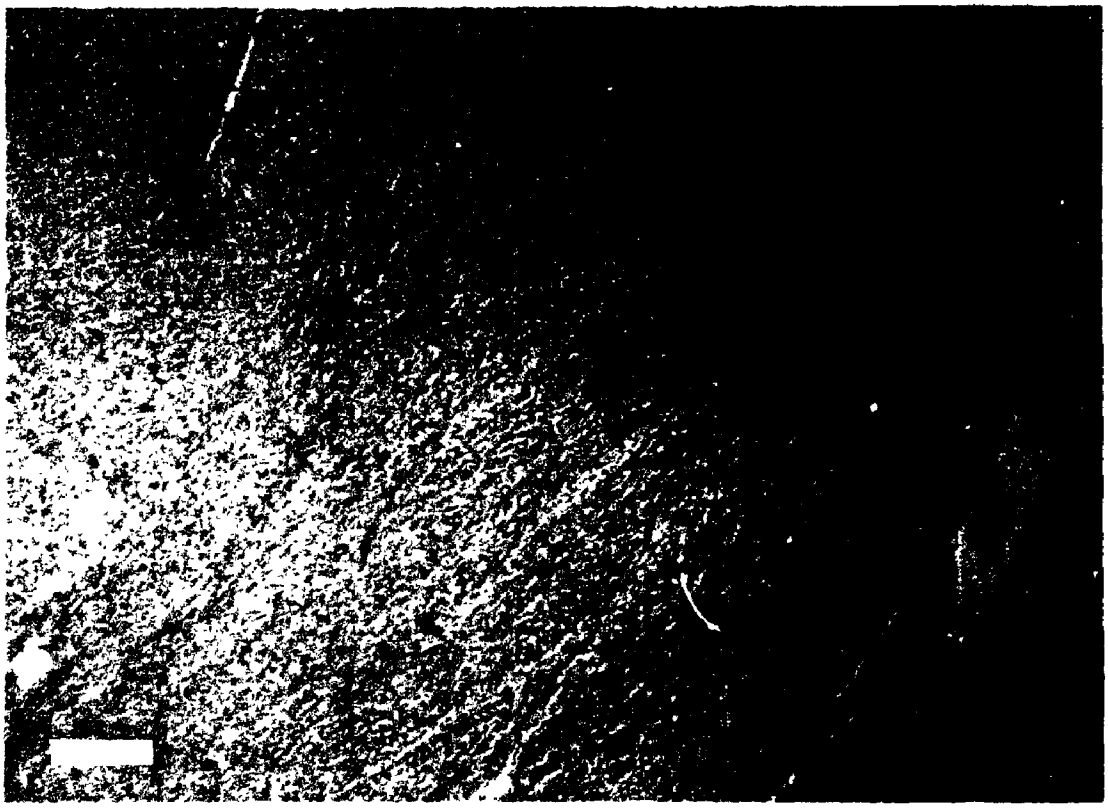

Plate 1.2: Trichrome-stained section of myocardium showing interstitial fibrosis. In contrast to replacement fibrosis, the collagen has been deposited diffusely and between groups of myocytes. Bar, 300 μm.

Disruption of the normal collagen architecture by the deposition of fibrotic collagen can limit or possibly obliterate this important recoil phenomena.

The systolic or contractile function of the heart may likewise be affected. By connecting adjacent myocytes and myocyte bundles (Borg and Caulfield 1981) the collagen framework coordinates the delivery of force to the ventricular chamber and prevents misalignment or slippage between individual myocytes (Weber 1989). Excess collagen may impair this coordinated activity and reduce the effectiveness with which the heart ejects blood.

Finally, interstitial fibrosis is believed to be a critical factor in the generation of malignant ventricular arrhythmias (Richards et al 1984). Foci of fibrosis may serve as the morphologic substrate for electrical re-entry, a phenomena frequently associated with life threatening tachycardias (Gardner et al 1984).

1.3 Methods Employed to Study Myocardial Fibrosis

Given the functional importance of myocardial scarring and its prevalence among patients with heart disease it would clearly be beneficial to have therapies targeted directly at this problem. This could include preventing the development of fibrosis, modulating the rate of collagen deposition, or facilitating its regression. Prior to addressing these issues, however, one must have the tools with which to obtain accurate information on the quantity and nature of fibrosis within the heart. For instance, before one can correlate interstitial fibrosis with potential etiologies there must be a reliable and practical method for detecting cardiac fibrosis. Likewise, if techniques are to be developed to accelerate or decelerate fibrosis, methods for characterizing the activity of a fibrotic process must exist. Because the major component of fibrosis is collagen (Prockop et al 1979a), these requirements may be restated in terms of fibrotic collagen. I

have therefore proposed two fundamental questions to be addressed when attempting to characterize cardiac fibrosis:

1) Is fibrosis present and if so to what extent? Simply, what is the collagen content* of the tissue?
2) How active is the observed fibrotic process?

The degree and manner to which these questions can be addressed with present techniques is reviewed below.

1.3.1 Quantification of Myocardial Collagen

The generally recognized "gold standard" approach to determining tissue collagen content is measurement of the amino acid hydroxyproline. Hydroxyproline comprises approximately 16% of the amino acid residues of the collagen polypeptide chain and the mass-ratio of hydroxyproline to collagen, while somewhat dependent on the type of collagen, is relatively constant at 7.5 (Neuman and Logan 1950). Furthermore, this particular aminoacid has been found in only a few other vertebrate proteins. This includes the C1q component of the complement system (Porter and Reid 1978), acetylcholinesterase (Prockop 1979b), and a small quantity (6 residues per 1000) has been found in elastin (Grant and Prockop 1972). Biochemical assay for hydroxyproline is thus a relatively specific approach for tissue collagen determination. Several assays have been developed (Neuman and Logan 1950, Prockop and Udenfriend 1960, Woessner 1961, Chiarello et al 1986) and investigators have employed these, or a modification of them, to study the connective tissue content of the human autopsy heart (Oken and Boucek 1957, Lenkiewicz et al 1972, Caspari et al 1977). The chief drawback to the biochemical approach, however, is the need for tissue homogenization.

---

* The term "collagen content" is used throughout this thesis to denote the concentration of collagen within a tissue.

Because of this, regional differences in collagen content cannot be ascertained. If excess cardiac collagen is found it remains unknown if this has been deposited in a perivascular, intermyocyte or subendocardial location. In addition, tissue degradation eliminates the opportunity to simultaneously evaluate other features of the myocardium such as muscle size and integrity, and cellular infiltration. This "economical" consideration has gained importance in recent years with the advent of the endomyocardial biopsy procedure. By obtaining small samples of the wall of the ventricle, morphologic assessment of the diseased heart can be made with minimal inconvenience or patient discomfort (Mortensen and Baandrup 1987). Previously this assessment was restricted to autopsy hearts or surgical specimens. However a limited number of biopsy specimens are taken from a given patient. It would be undesirable therefore if one or more specimens had to be digested solely to determine collagen content.

It is for these reasons that a histologic approach to quantifying myocardial collagen is desired. Without question, the most widely employed approach is to subjectively evaluate the tissue using light microscopy. The value of the results, however, is highly dependent on the experience of the interpreter. In an effort to improve the reliability of this type of assessment, several investigators have employed a "semi-quantitative" scoring system for fibrosis, e.g., 0 to 4+ (Shanes et al 1987, Herskowitz et al 1987, Nakayama et al 1987, Yonesaka et al 1987). There remain no data to support any real benefit of such an approach. Indeed, the unreliability of this method has recently been illustrated by Shanes et al (1987). They examined the interobserver variability among seven internationally-recognized cardiac pathologists examining identical slides of heart biopsy specimens from patients with dilated cardiomyopathy. A scale of 0 to 3+ was employed. They found that the median coefficient of variation was 74.4%, 114.8%, and 170.8% for endocardial, interstitial, and perivascular fibrosis respectively. If the assessments were divided into significant fibrosis (score of 2+ or greater) versus insignificant fibrosis (below 2+), the reported

prevalence in the patient population ranged from 25 to 69%. These results clearly demonstrate the serious limitations of a qualitative assessment of cardiac fibrosis. Even under the relatively controlled circumstances of a clinical study, the interobserver variability is exceedingly high and the utility of this approach, even in the most routine setting, must be seriously questioned.

Quantitative approaches to the histologic assessment of collagen content have been employed. Estimates of volumetric density, by point counting techniques described by Weibel (1963), have been utilized by a number of investigators. An important drawback of this approach, however, is the time required to yield an accurate determination of the collagen content. Pearlman et al (1982) have estimated that to obtain a 5% standard error in the estimated connective tissue content of the human left ventricle, approximately 20,000 points should be counted. The magnitude of this requirement precludes widespread or routine use of the stereologic approach to quantifying myocardial collagen. Indeed, even for study purposes such strict criteria are rarely followed, particularly when investigators are examining small amounts of myocardial tissue as in the case of biopsy material (Oldershaw et al 1980, Baandrup et al 1982, Mall et al 1982, Schwartz et al 1983, Unverferth et al 1983).

A second factor that can limit the value of the stereologic approach to collagen measurement concerns the precise nature of the material that is being counted. The fibrous component of the heart has been variably described as the nonmuscular cardiac components (Schwartz et al 1983, Hess et al 1984, Fuster et al 1986, Krayenbuehl et al 1989), interstitial connective tissue (Moore et al 1982, Pearlman et al 1982), and interstitial collagen (Baandrup et al 1982). Collagen content will clearly be overestimated if other components of the extra muscular tissue (elastin, water, mucopolysaccharides, blood vessels, and interstitial tissue cells) are included. Efforts to distinguish these elements from collagen, however, are often limited by the stain employed. A commonly employed stain for the detection of collagen is the trichrome stain (Masson's or

Gomori's) which imparts a blue or green color to collagenous structures (Drury and Wallington 1976). Its ability to differentiate interstitial mu opolysaccharides and collagen, however, is poor (Baandrup et al 1982). Hematoxylin and eosin, and toluidine blue are similarly not specific for collagen (Krayenbuehl et al 1989). Thus, while many stains reliably distinguish muscular from nonmuscular tissue, precise identification of collagen fibers is often not possible.

The sensitivity of many stains for collagen is also suboptimal. Van Gieson's stain, while its red color is reportedly specific for collagen (Baandrup et al 1982), is not able to stain young fibers and, in general, has a tendency to fade (Drury and Wallington 1976). Also, reticulin, an important component of which is type III collagen (Wolman and Kasten 1986), can only be completely demonstrated with routine microscopy by metallic impregnation techniques (Drury and Wallington 1976).

It can be seen therefore that stereologic techniques, while theoretically sound, become limited in value by practical constraints, statistical considerations, and imperfections in the commonly employed stains. The significance of these factors is borne out when one considers that the reported collagen volume fraction of normal myocardium, assessed stereologically, ranges from 2% (Pearlman et al 1982) to 25% (Moore et al 1980).

In recent years, newer technologies have been utilized in an effort to quantify myocardial fibrosis in histologic sections and also to offer a degree of practicality through automation. In 1972, Lenkiewicz et al utilized an electronically-controlled microscope in which a focal beam of light originat g from a cathode ray tube scanned the field and the transmitted light was measured by a photomultiplier. Using Lendrum's picromallory stain, he determined the normal area fraction of myocardial collagen to be 20-35%. Fuster et al (1976) found a similar value of 32.2% using a TV camera and computer system to digitize photomicrographs of myocardium. In this instance, the entire interstitial space was highlighted with white pen and muscle with black pen. The

reported value therefore refers to all interstitial components and ignores the effect of myocyte shrinkage commonly associated with fixation. Tanaka et al (1986) employed a similar technique of manually tracing photomicrographs and determining fibrous area with a camera and microprocessor. In this case, samples were stained with Masson's trichrome and the fibrous content was determined to be $1.1 \pm 0.5\%$ - in great contrast to the above two studies but much closer to the stereologic study of Pearlman et al (1982). Finally, Hoyt et al (1984) used the technique of video microscopy and determined the collagen content on the basis of grey levels of the digitized image. They also employed a trichrome stain but found the collagen content of biopsies of two normal left ventricles to be 6 and 13%.

The use of image analysis to quantify collagen is attractive, particularly if, as in the study by Hoyt et al (1984), this can be done directly from the microscope image (video microscopy). The enormous variability in the above results however attest to the need for improvements in this type of approach. As with stereologic methods, there are problems with imprecise demarcation of fibrous tissue due to the imperfect and variable sensitivity and specificity of stains for collagen. This problem may be compounded once the image is digitized. Components that are readily distinguishable to the eye on the basis of color are very often poorly distinguishable following digitization and representation by grey levels (Jarvis 1988).

In summary, while quantification of collagen is fundamental to the assessment of cardiac fibrosis, present methods have not proved satisfactory.

1.3.2 Assessment of Activity of Myocardial Fibrosis

While the ability to quantify collagen would allow one to determine the presence and extent of cardiac fibrosis, it would offer little in the way of useful data from the therapeutic standpoint. To treat fibrosis, one requires the capacity to influence the fibrotic process itself. This might mean accelerating it, for example, following

myocardial infarction where rapid tissue repair is desirable, or it may entail decelerating the process, as may be required to retard the deterioration associated with idiopathic dilated cardiomyopathy. Successful development and employment of these types of therapy, however, is dependant on the ability of investigators to gauge the activity of fibrosis within a tissue bed. For example, fibrosis that is found to be in an early, or active stage is more likely to be reversible (Baily and Light 1985). Also, by following the activity of fibrosis over time, one might determine if a therapeutic intervention has in fact influenced fibrosis. Thus fibrosis should be considered not simply as the presence of scar tissue, but as a biologic process.

To understand how this process may be studied, one should be aware of the specific events occurring during fibrosis. Generally these are considered in terms of collagen synthesis, secretion of collagen into the extracellular space, and the subsequent formation of collagen fibers which mature over time. Synthesis of fibrillar collagen in the heart takes place in the fibroblast (Eghbali et al 1989) where α-chain polypeptide precursors of collagen are formed by translation of the appropriate genetic material. As these chains are being produced, enzyme-mediated modifications to the aminoacid constituents occur. This includes hydroxylation of proline and lysine, and the addition of various sugar moieties (galactose, glucose, and mannose) (Prockop and Kivirikko 1984). Once these translational and posttranslational modifications are complete, the carboxy terminals of three polypeptide chains are bridged together by disulphide bonds (Prockop et al 1979a). The product, the procollagen molecule, consists of a central helical domain and two globular nonhelical domains at each terminal (Prockop et al 1979a, Goldberg and Rabinovitch 1983). This molecule is secreted into the interstitial space following which the globular propeptide terminals are cleaved. At this point the molecules spontaneously assemble into fibrils. The three-dimensional features of fibril packing remain to be fully elucidated (Goldberg 1983, Nimni and Harkness 1988). However, the two-dimensional organization is traditionally described by the "quarter

stagger" model in which there is a constant axial displacement of adjacent molecules (Prockop et al 1979b, Nimni 1980). Under routine light microscopy, these fibers appear similar to mature collagen, yet they remain highly susceptible to degradation and do not have the necessary tensile strength or viscoelasticity to perform a structural role. For this to occur, the fiber must be stabilized and this occurs primarily through covalent intermolecular crosslinking (Nimni 1980).

A complete description of the chemistry of crosslinking is not necessary for this discussion; however the functional importance of these bonds are emphasized. Introducing covalent crosslinks to an immature collagen fiber increases its tensile strength, renders the fiber less soluble, and decreases its susceptibility to enzyme-mediated proteolysis (Goldberg and Rabinovitch 1983). As maturation proceeds, the chemical nature of these crosslinks change from a reducible to nonreducible form (Bailey and Light 1985). This change in the type of crosslink has been associated with decreased solubility in organic acids (Light and Bailey 1980), increased shrinkage temperature, and an increase in the isometric tension generated during thermal contraction (Allain et al 1978, Nimni and Harkness 1988). An increase in the number of crosslinks during maturation is also believed to occur (Nimni 1980) although evidence for this to date remains indirect. Butzow and Eichorn (1968) have found that the number of collagen subunits obtained during solubilization of rat tail tendon decreased with age, suggesting a time-dependent increase in the number of intramolecular crosslinks.

Other events, besides crosslinking, may serve to stabilize the fibers over time. Nimni and Harkness (1988) have suggested there is a progressive exclusion of water molecules from the fiber. This would allow newly exposed nonpolar surfaces of adjacent collagen molecules to interact, forming new hydrophobic bonds and enhancing fiber stability. As adjacent molecules move closer to each other, existing ionic bonds

would also be strengthened. An age-related decrease in interstitial ground substance also serves to augment molecular and fibrillar packing with time (Sibert 1973).

Another feature of aging fibrotic lesions is a change in the type of collagen deposited. The initial response to injury is the rapid synthesis of type III collagen (Clore et al 1979). Later, the cells revert to synthesizing type I collagen (Bailey and Light 1985) which forms thicker fibrils (40-60 nm versus 20-40 nm) in a denser network than those of type III (Wolman and Kasten 1986).

Thus, the fibrotic process entails a series of highly regulated events which, when examined, could provide a basis for determining the activity of scar formation and its relative age. Currently, biochemical studies are generally felt to be more quantitative than classic microscopal procedures, as is the case for determining collagen content. One such approach is measurement of the posttranslational enzymes. Increased levels of proline hydroxylase have been found in liver biopsy specimens from patients with active hepatic disease and progressive fibrosis (Brunner and Schubothe 1976, Mezey et al 1976). This approach has not been applied to the heart although its potential value is limited by the need for tissue destruction. Increased serum levels of this enzyme (Prockop et al 1979a) or of glucosyl transferase (Anttinen et al 1977) have also been proposed as markers of active fibrosis.

Sensitive radioimmunoassays have been developed for the terminal portion of procollagen I and III and could likewise be used to study serum antigen levels in fibrotic diseases (Timpl 1980). Elevated levels of procollagen type III have been found in patients with chronic active hepatitis suggesting that the assay can detect active scarring. An important disadvantage of any method using serum measurements is the lack of organ specificity. While this may be relatively unimportant for the liver, which is a large organ that can become severely fibrotic with disease, its utility in heart disease is unclear. The "total" fibrotic activity of the diseased heart is likely to be sufficiently low, even

though clinically important, that a serum measurement would not accurately reflect the events in that organ.

Wide angle x-ray diffraction may also be used to monitor collagen aging (Sinex 1968). As the aging network becomes increasingly packed there is progressive alignment of fibers and molecules and the structure becomes more crystalline. Unfortunately, this technique lacks practicality and, to date, has not been employed on fibrotic collagen.

The role of histologic assessment of fibrotic activity is likewise limited. In spite of the substantial changes that occur in the collagen of a developing scar, its appearance with routine microscopal techniques is nondescript. Connective tissue stains that employ silver impregnation, referred to as reticulin stains, may facilitate the identification of recently deposited collagen in granulation tissue (Drury and Wallington 1976). Immunostains specific for type III collagen may also be helpful in this regard (Timple 1980, Williams et al 1984). Both of these approaches, however, provide only qualitative data.

In summary, cardiac fibrosis is an important pathologic process that contributes to considerable morbidity and mortality among patients with heart disease yet practical and quantitative methods for evaluating this process are lacking. In this thesis, I will outline the technique that I have developed to quantitatively study myocardial fibrosis in histologic sections. Both content and activity are examined using an approach that combines the techniques of polarized light microscopy and computer image analysis. The rationale for this approach and an overview of the developed technique are presented in the following chapter. Validation of these methods will subsequently be presented. Finally, the utility of the developed technique will be illustrated by studies of cardiac fibrosis in the human transplanted heart.

Chapter 2 Methods

To evaluate cardiac fibrosis, I set out to develop a method combining the techniques of polarized light microscopy and video image analysis. In this section, these two modalities will be reviewed with reference to their application in the histological assessment of cardiac tissue. Additionally, the manner in which they can be combined to quantitatively study myocardial fibrosis is described.

2.1 Polarized Light Microscopy

2.1.1 Theory

Although no one really knows what light consists of (Shurcliffe 1964, p 7), much is known about its behavior. Light can be described as a series of waves, or as a group of energy particles (photons). Wave theory is generally best suited for the description of the nature of polarized light. Light is thus considered as waves with their electromagnetic displacements oscillating perpendicular to the line of travel. At any one point in time, the electric displacement is perpendicular to the magnetic displacement and only one component is therefore necessary to describe the wave. By convention, the electric vector is considered. In unpolarized light, this vector oscillates transversely in all planes. If one removes all of the oscillating components except those with vectors vibrating in one particular plane, the remaining light is said to be linear (or plane-) polarized. Thus, as suggested by Shurcliffe (1964, p 7), polarized light is merely simplified light.

In the polarizing microscope light from the light source contacts a polarizer situated below the condenser apparatus. This polarizing plate allows light vibrating in only one particular plane to pass through it thereby converting the incident light to a linearly polarized form. A second polarizing plate, referred to as the analyzer, is situated

just above the objective lens. For analysis, the transmission axis of the analyzer is oriented perpendicular to that of the polarizer. Under these conditions alone no light will reach the eyepiece and the field appears dark (Figure 2.1).

For a specimen on the stage to be visualized, it must have the ability to alter the state of polarization of the transmitted light such that a component of the light will pass through the analyzer to the eyepiece. This phenomena will occur if the constituents of the material interacting with the light are not randomly distributed but have a preferred spatial orientation, i.e., are anisotropic (Bennett 1950). One property of anisotropic material is the phenomenon of birefringence. Birefringence is the characteristic of an object in which light, polarized in different planes, will travel through the object at different velocities (Wolman 1975). This occurs because the material, being anisotropic, will have multiple refractive indices (Bennett 1950) (Figure 2.2).

When plane-polarized light enters a birefringent structure, it is resolved into two rays which oscillate in mutually perpendicular planes. One ray travels in the plane of maximum refractive index (the slow ray) and the second in the plane of the minimum refractive index (the fast ray). The fast ray emerges from the object first and is followed by the slow ray which enters the air θ wavelengths behind a corresponding point in the fast ray. The difference between the two rays is the retardation (Γ) which may be described either in terms of the path difference (in nanometers) or the difference in phase angle (in degrees or radians). When the two components exit the specimen, they recombine to form a new electric vector, the course of which is dependent on the phase retardation and the relative amplitudes of the two component waves (Bennett 1950). In general, this resultant vector forms an ellipse, although under certain conditions of either retardation and/or relative amplitudes, the resultant vector will form a straight line or a circle.

The intensity of brightness of a birefringent material examined under crossed polars will be determined by the amount of light that passes through the analyzer. This is

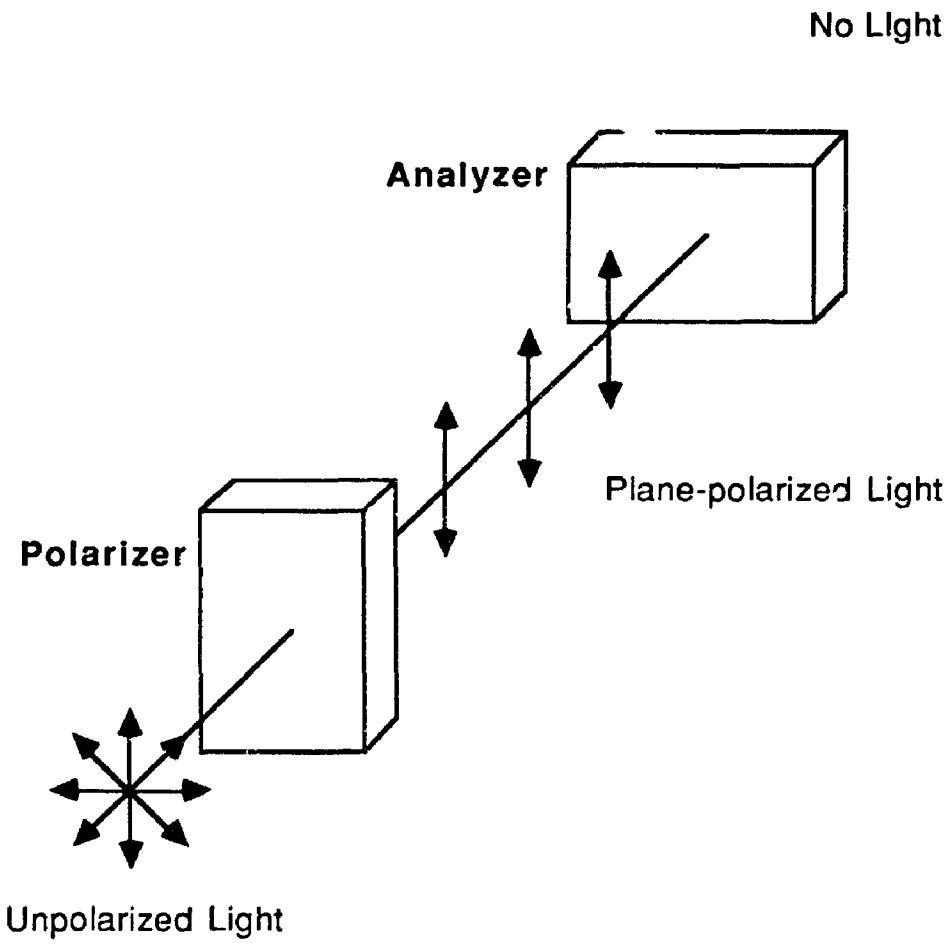

Figure 2.1: Schematic diagram showing the effect of crossed polars. Ordinary unpolarized light is converted to plane-polarized light by the polarizer. The analyzer, oriented 90^{0} to the polarizer, absorbs the remaining light. A birefringent specimen located between the polars will rotate the plane of polarization allowing some light to pass through the analyzer.

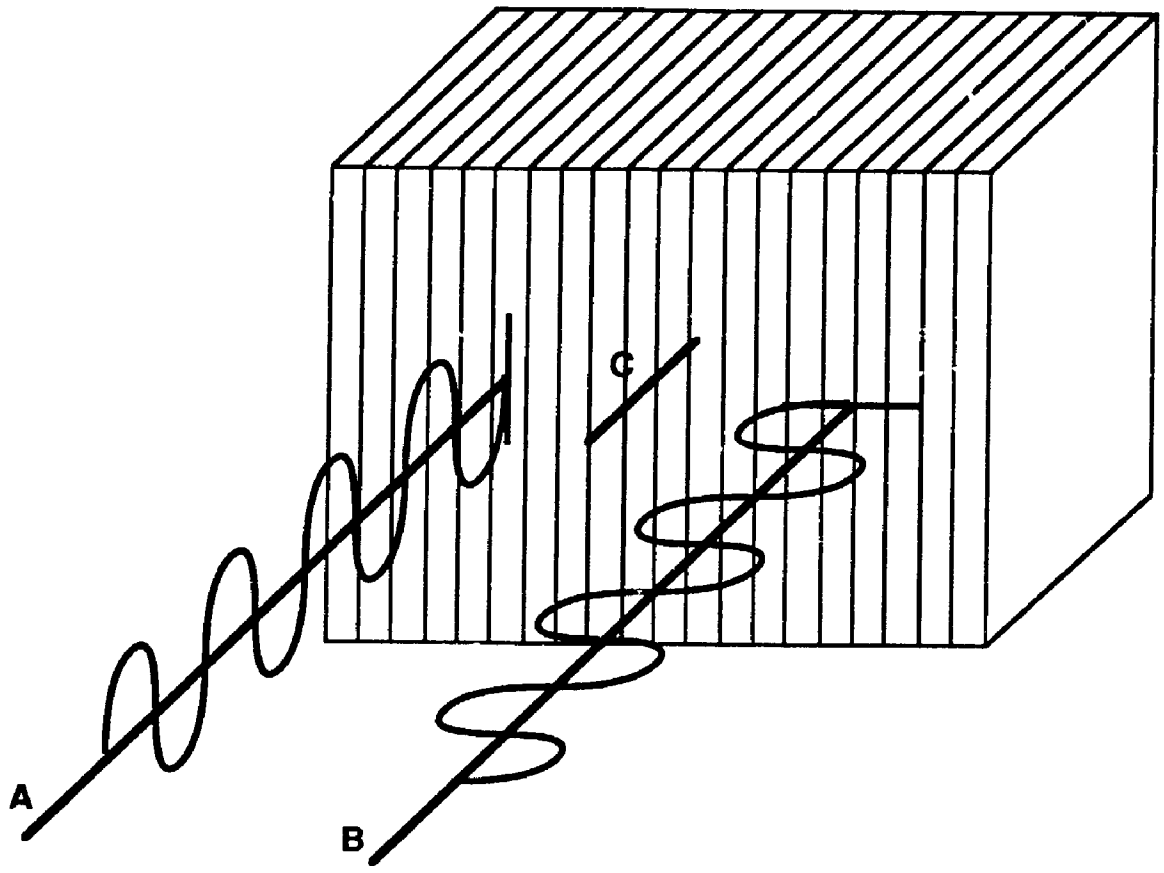

Figure 2.2: Stylized model of a birefringent material. Optically dense molecules are vertically aligned within the box. Polarized ray A interacts with a medium of low refractive index and will exit the box sooner than ray B. If the plane of polarization lies between the 2 rays (C) it is resolved into the 2 orthogonal components. Adapted from Wolman 1970, p 387.

determined by the principal axes and azimuth of the ellipse, which in turn, depend on specimen retardation and the amplitude of the two rays prior to recombining. For a given retardation, the amount of light transmitted by the analyzer will be maximum when the polarization axes of the material are oriented at 45° to the crossed polars. Retardation itself will be dependent on the thickness of the specimen and the intensity of birefringence in accordance with the difference between the two refractive indices (Wolman 1970).

Theoretical considerations of polarized light microscopy can be expanded depending upon the particular application. For this work, however, the primary features of interest are the visibility of birefringent biologic structures when viewed with the polarizing microscope, and the intensity of brightness of these structures.

2.1.2 Assessment of Myocardium With Polarizing Microscopy

Myocardium is well suited to study by polarized light since both collagen and cardiac muscle are anisotropic. Birefringence in the myocyte is limited to the A-(anisotropic) band of the sarcomere, in which myosin filaments are arranged parallel to each other with partial overlap with actin filaments. Although collagen birefringence has been recognized for almost two centuries (Wolman 1975), in contrast to muscle, correlation with structure was not made until recently (Wolman 1986). The collagen molecule consists of three polypeptide chains each wound to form a left-handed helix. The angle of inclination between successive turns is 36° to the width of the molecule. Stacking of helical chains of this configuration generally results in little if any birefringence since the alignment of components in the front chains are largely compensated by the near-perpendicular direction of components of chains behind them. In collagen, however, each of the three chains is twisted in a right-handed superhelix. The angle between subsequent turns of the superhelix is such that aminoacids become

aligned approximately parallel to the molecular axis thereby providing a high degree of anisotropy at the molecular level (Plate 2.1). Structural order will increase as neighboring molecules and fibers become packed together (Nimni 1980). The result is a highly aligned fibrillar protein with a birefringence that is significantly more intense than that of cardiac muscle (Wolman 1975).

The natural birefringence of biologic material can be influenced by staining with dyes. A particularly impressive enhancement of collagen birefringence occurs when it is stained with picrosirius red (Constantine and Mowry, 1968). The sirius red molecule of this stain is an elongated, strongly acidic dye that binds to collagen, which is a basic protein (Junquiera et al 1982). Specifically, the sulphonic acid groups of sirius red are believed to interact with the amino groups of lysine and hydroxylysine, and the guanidine groups of arginine (Junquiera et al 1979). Bonding occurs such that the long axis of the sirius red molecules are parallel to that of the collagen fiber. Birefringence is thus enhanced by at least 700% (Junquiera et al 1979).

Constantine and Mowry (1968) first used the picrosirius-polarization microscopy technique to study dermal collagen and it has since been employed to study the fibrous network of a number of tissues (Junqueira et al 1979, Perez-Tamayo and Montford 1980, Josza et al 1984, Whittaker et al 1989, Vesely and Boughner 1989). While the stain is not entirely specific for collagen (Weathorford 1972) the combination of picrosirius red plus polarization microscopy is a highly specific method for identifying collagen in the interstitial space (Junqueira et al 1979). The sensitivity of this method is generally regarded as high (Weber 1989) although this has not been quantitatively demonstrated. Dolber and Spach (1987) used the picrosirius-polarization technique to study the fine collagen network surrounding individual heart muscle cells. Their findings are consistent with those of investigators using scanning electron microscopy (Borg and Caulfield 1981, Robinson et al 1983).

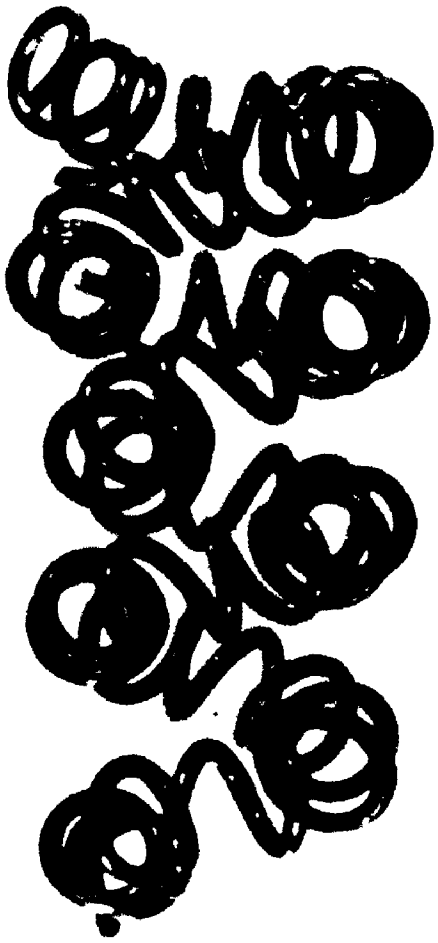

Plate 2.1: A model showing the helical configuration of a collagen polypeptide chain. The left-handed coiling is compensated by right-handed supercoiling of a similar angle. The aminoacid chains are thus aligned parallel to the molecular axis. (Reproduced with permission from Wolman and Kasten (1986))

Several investigators have noted that the color of collagen under these circumstances may be either orange-red or green (Junquiera et al 1978, 1979, Jozsa et al 1984, Perez-Tamayo 1980, Pick et al 1989). It was initially proposed that the yellow-orange color indicated the presence of type I collagen and green depicted type III collagen (Junquiera 1978). It has subsequently been appreciated that such differences in color are also associated with variations in section thickness (Junquiera et al 1982) and fiber diameter (Perez-Tamayo and Montford 1980). The consistent feature however is the association between color and retardation (Szendroi et al 1984) whereby fibers with less retardation appear green and those with more have the orange-yellow appearance. Cardiac muscle, which is less birefringent than collagen, appears dull green (Whittaker et al 1989).

2.1.3 Tissue Preparation

All specimens studied were immersion-fixed in 10% neutral buffered formalin for a minimum of 48 hours. They were subsequently dehydrated in a graded series of alcohol, cleared with chloroform, and embedded in paraffin. Sections were cut at either 5 or 7 μm. Specimens were stained with picrosirius red according to the technique of Constantine and Mowry (1968). All histologic processing was performed by Mrs. J. Dixon (Department of Medical Biophysics, U.W.O.) or by Histology Services, University Hospital, London, Ontario.

2.2 Video Microscopy

2.2.1 Introduction

By combining the techniques of microscopy and microcomputer image analysis, new opportunities exist for the histologic assessment of biologic structures. Transferring a microscope image to digital format provides the potential to rapidly and

quantitatively assess morphologic features. It can thus overcome the practical constraints of traditional quantitative microscopy techniques. Also, the ability of video to enhance contrast in an image may further optimize analysis. Because of these advantages video microscopy can strengthen the role of the histologic approach in diagnosis. Recently, a videodensitometric technique has been developed to measure nuclear DNA content to diagnose malignancy (Jarvis 1985). This assessment has traditionally been done with flow cytometry although this approach requires a much larger sample than does a microdensitometric approach. Thus, while not yet widely employed, video image analysis can increase the utility of presently employed histologic techniques and can form the basis of new analytical methods of tissue characterization.

The ultimate value of videomicroscopy will depend on the reliability of each component of the system. Good quality microscope images are a prerequisite and each component of the video system must process the signal reliably and optimally .

2.2.2 Video Equipment

A schematic of the video-polarizing microscopy technique is shown in Figure 2.3 and individual components are described below.

Polarizing Microscope

The microscope used was a Nikon Optiphot polarizing microscope. The stage was circular and rotatable and illumination was with a 12 volt - 50 Watt halogen lamp (Osram). The eyepiece tube was trinocular with an optical path change-over system. With the change-over knob inserted, 100% of the light is transmitted to the two observations oculars. In the out position, 14% of the light is transmitted to the observation oculars and 86% is directed to the face plate of the camera. A x1 TV relay lens was positioned in the photo tube to converge the image onto the plane of the camera detector.

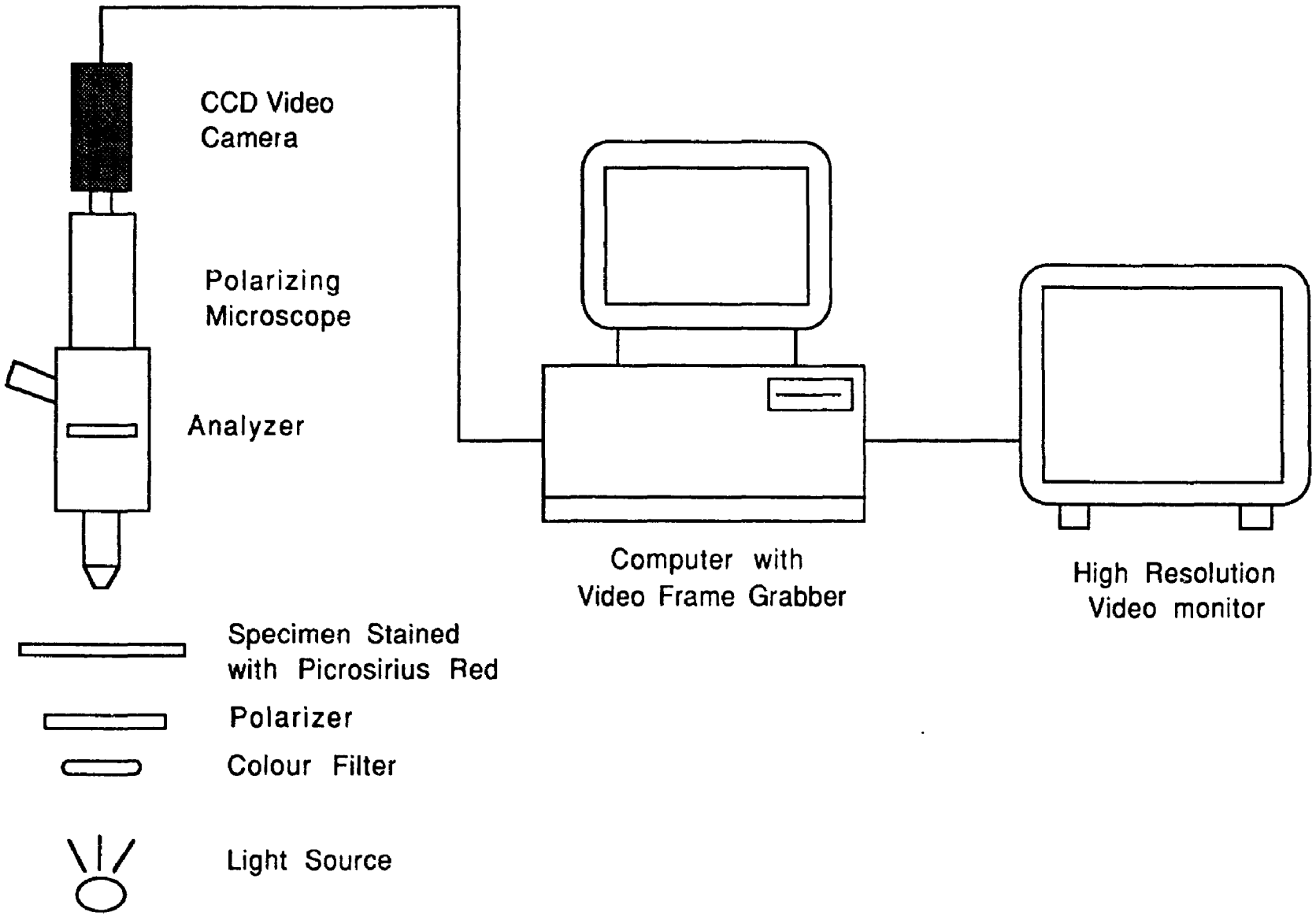

Figure 2.3: Components of the polarization-video microscopy system.

The microscope was equipped with strain-free objectives and a strain-free achromatic condenser. The absence of strain in these components is necessary to avoid the phenomenon of stress birefringence which would brighten the background of the image.

The degree to which the crossed polars can darken the field is termed the extinction factor (EF) and is defined by the relationship:

$$EF = \frac{I_{pa}}{I_{pe}} \qquad \text{(Eqn. 1)}$$

where I_{pa} is the luminance or intensity of the field with the polarizer and analyzer parallel and I_{pe} is the intensity when the polarizer and analyzer are crossed (Inoué 1981). Using a Nikon UFX light meter I found the extinction factor of this microscope to be 1.2×10^4.

Camera

The camera employed was a solid-state CCD (charge-coupled device) monochromatic camera (Series 4810, COHU, San Diego, California). Vacuum tube technology has long dominated video camera design, however, recent developments in semiconductor circuit elements have led to the development of this compact and sensitive type of camera. Individual sensor elements (silicon photodiodes) are built into a small chip at the camera face-plate as a 754 (horizontal) by 488 (vertical) matrix of photosites. While the resolution of this camera may be less than that of high quality tube cameras, it has the advantage of minimal geometric distortion and resistance to transient or permanent after images on exposure to excessively bright light (burn) (Jarvis 1988).

The gamma (the exponent that defines the curve describing the output versus input characteristics) was set to 1.0 via a jumper on the video board of the camera. In this way, the video output signal is linearly related to the face-plate illumination. The camera also has automatic gain control and automatic black level (automatic pedestal

control) circuits. Both of these features can serve to automatically enhance image contrast but in doing so will modulate the output signal without the awareness of the operator. For quantitative measurements this is not desirable and both features were therefore switched to manual control. Specific adjustments are described in the appropriate sections.

Video Digitizer

The video digitizer was a PCVISION-plus Frame Grabber (Imaging Technology, Woburn, Massachusetts) with a single memory buffer. Image resolution was 640 (horizontal) x 480 (vertical) pixels with square-pixels (aspect ratio (y:x) 1.007). Pixel intensity was depicted using 8-bit (256) grey levels and a stored image occupied 307 kilobytes of memory. A PC-AT (Delta Technologies) was the host computer. The digitized image was displayed on a RGB monitor (model 3479, Mitsubishi, Torrance, California). Unless otherwise indicated, a x10 microscope objective was employed yielding a pixel size of 1.82 μm^2.

Software

Two commercial software packages provided the programming basis for image acquisition, enhancement, and analysis. One, the Software Development Package (SDPPC, Infrascan, Richmond, BC) was developed with compiled C and included a library of image analysis subroutines written in C and assembly language (ITEX-PC, Imaging Technologies, Woburn Mass). The second, Jandel Video Analysis Software (JAVA, Jandel Scientific, Corte Madera, California) did not provide source code or library routines; however it allowed for definition of areas of interest through mouse-interaction. Furthermore, grey-level data could be easily converted to ASCII format and accessed for mathematical analysis and graphical display. While use of these two packages was sufficient for some applications, it was necessary for me to develop

further software, specific to quantifying collagen and evaluating the relative intensities of pixels depicting collagen. These were written in C and utilized the ITEX-PC subroutines. When combined with SDPPC, fairly rapid image analysis could be performed since the time associated with "stepping" through the various components of the commercial packages was eliminated.

2.2.3 Evaluation of Video Components

By design, the primary function of the video system was to differentiate and characterize morphologic features on the basis of light intensity (grey-levels). In this regard, several characteristics of the system, required evaluation to ensure that the digitized image reliably reflected the microscope image.

1) Video Response to Light Intensity

With solid state CCD cameras, the electric charge is expected to be linearly related to the incident light. To confirm this, and to test for any deviation from linearity caused by the analogue to digital converter in the digitizing board, the relation between grey-level of a digitized image and intensity of illumination was determined. Microscope illumination was set just below the point of image saturation (recognized by a sudden "whitening" of the image as pixels simultaneously acquire grey-level of 255) and was sequentially reduced by placing neutral density filters (Nikon) in the light path. The respective optical densities (O.D.) of the filters were confirmed by a densitometer (model 301, X-Rite, Grand Rapids, Michigan). The mode of the grey-level histograms for each light setting was determined.

As shown in Figure 2.4, the relationship between relative light transmittance ($10^{-O.D.}$) and grey-level was found to be linear. Variations in the gain or black-level offset of the videosystem will change the slope and Y intercept respectively but not the linearity of the function.

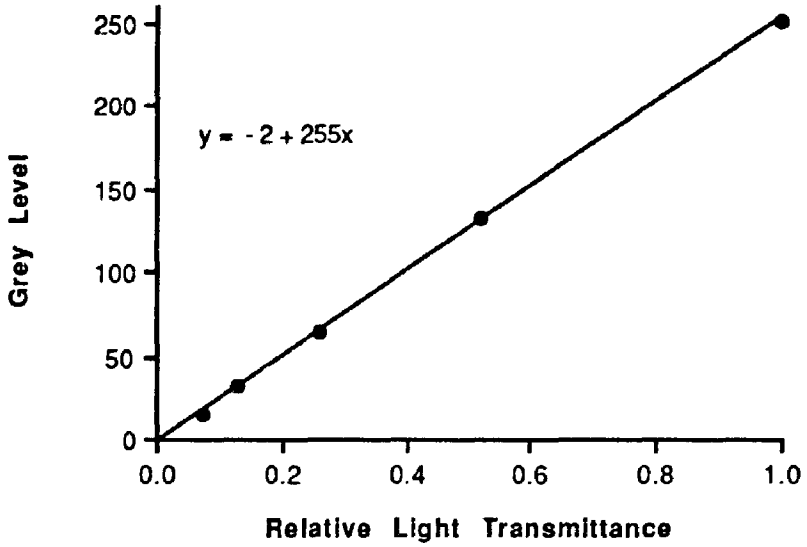

Figure 2.4: Relation between filter transmittance and grey-level of the digitized image, showing linear response of the video system.

2) Variation in Background Illumination

Uneven illumination of the background can impair reliable differentiation of image components. With bright field microscopy, this can be corrected by subtracting a background image from the image of the specimen. With polarizing microscopy, however, the background image (i.e. no specimen and crossed polars) may not be visible to the video system. The background of the bright field image may be used, but, illumination conditions will be different since light intensity must be increased when polarization microscopy is employed. Since the absolute difference between grey-levels within the background image will change with illumination conditions, image subtraction is not appropriate. Instead, the image of the specimen can be divided by the bright background and multiplied by a constant (e.g., the minimum grey-level of the specimen image). In the absence of an assembly language subroutine for this (as was available for image subtraction) this operation becomes exceedingly time consuming (approximately 20 minutes) and was not an attractive alternative.

Fortunately, if attention is paid to the microscope set up, background heterogeneity can be minimized. I found that using Köhler illumination and ensuring the aperture of the condenser iris was not greater than the diameter of the exit pupil of the objective, a uniform background image could be obtained. This is demonstrated in Figures 2.6a and 2.6b which show grey-level profiles across the length and width of a background image at multiple locations.

3) Variation in Light Intensity Due to Fluctuations in Line Voltage

Fluctuations in the lamp intensity will occur with minor fluctuations in line voltage. This can lead to marked differences in intensities of identical microscope images. To address this problem I used a voltmeter (Micronta, Radio Shack) to

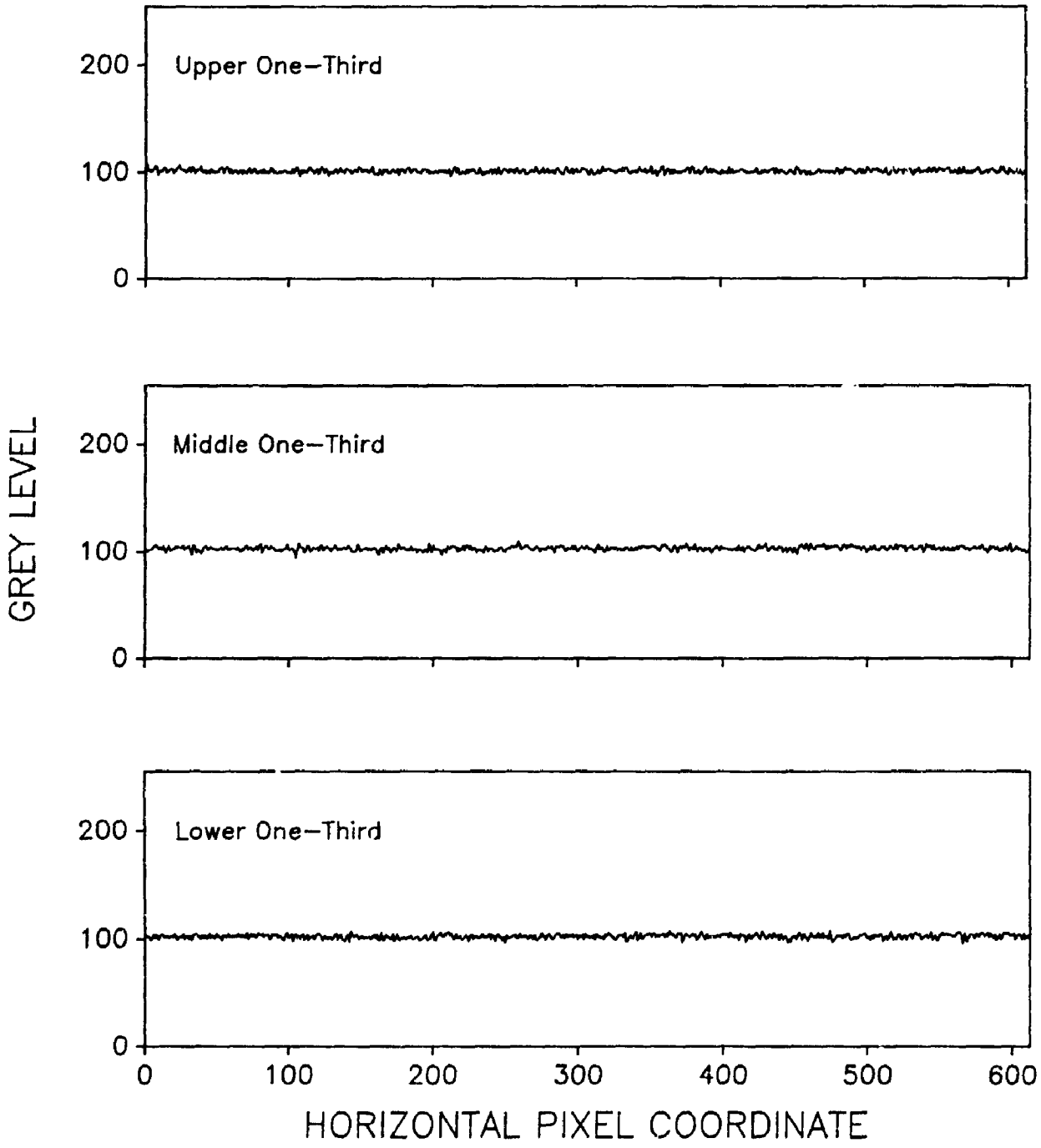

Figure 2.5a: Grey-level profile along the width of a blank image at three different locations. The grey-level remains relatively constant.

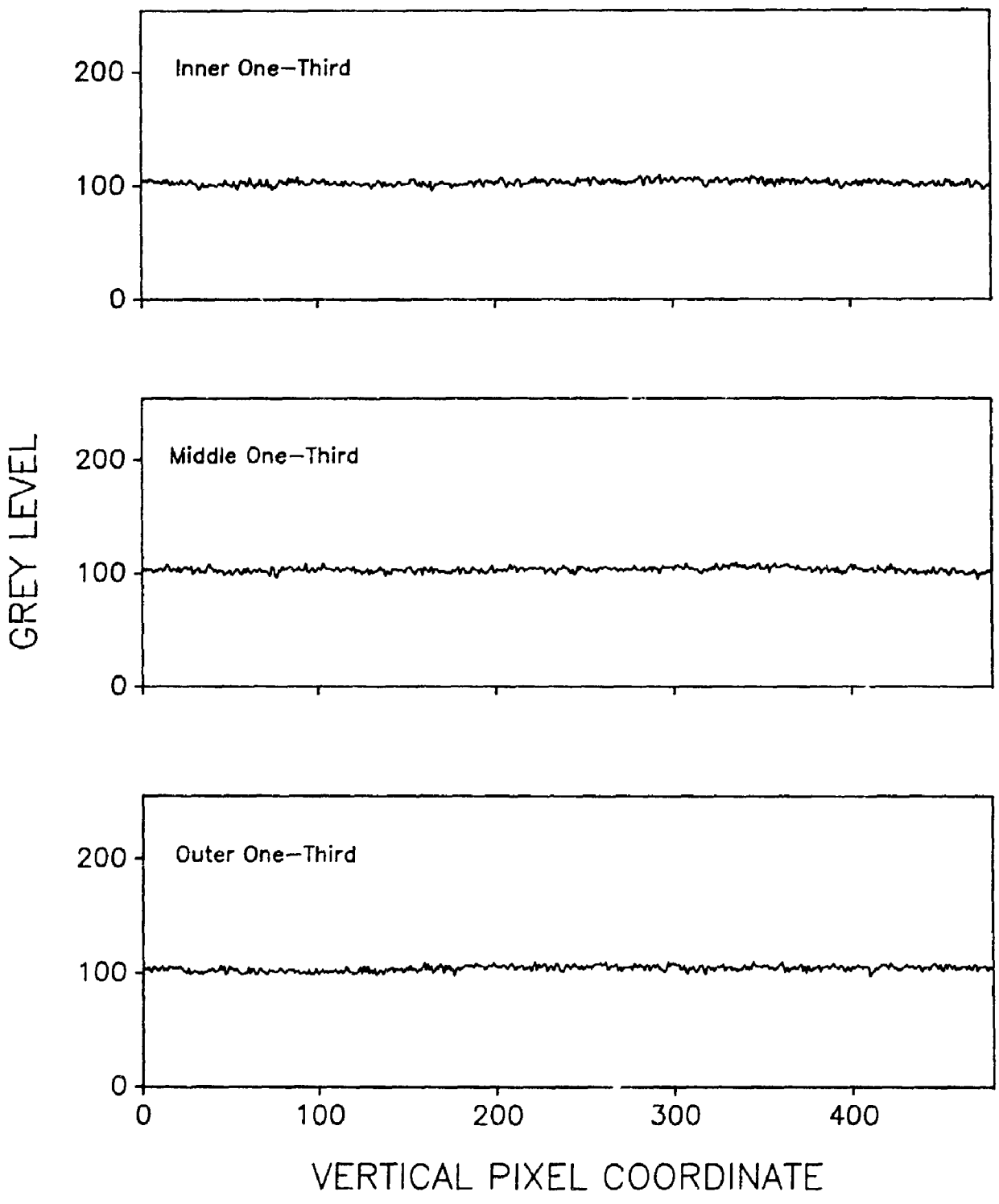

Figure 2.5b: Vertical grey-level profiles across a blank image.

continuously measure voltage across the microscope lamp. As expected changes in grey-level of an image closely correlated with the lamp voltage (Figure 2.6).

To determine if the relationship between lamp voltage and the corresponding grey-level was stable with time, the mode of the grey-level histogram of a blank image was determined on three or more occasions over a 2-day period, for each of 12 different lamp voltages. The mean (± SD) coefficient of variation in the grey-levels was 1.7 ± 1.4 % indicating a stable relationship. Therefore, the voltmeter served as a simple tool to monitor fluctuations in line voltage which could then be corrected by adjusting lamp intensity to maintain a constant voltage. With time a residue may build up within the lamp and decrease its output independent of voltage. For this reason, the grey-level of the background image was documented as a reference for each study.

2.3 Video and Polarizing Microscopy

Both polarized light microscopy and video microscopy have been utilized to study biologic materials. There is, however, little experience with the combination of these techniques and no published data with respect to analysis of myocardium. I believed that the demonstrated role of polarized light microscopy in identifying and characterizing collagen (Whittaker et al 1989, Weber 1989) could be enhanced by the quantitative powers of videomicroscopy. In combining the two techniques, two unique problems presented and are discussed below.

Image Contrast

The challenge of video microscopy is to optimize contrast between features in the image. The appeal of polarization microscopy is that it offers an approach based purely on differences in light intensity rather than color differences which may have poor contrast in light intensity (Jarvis 1988). Yet although the appearance of a birefringent

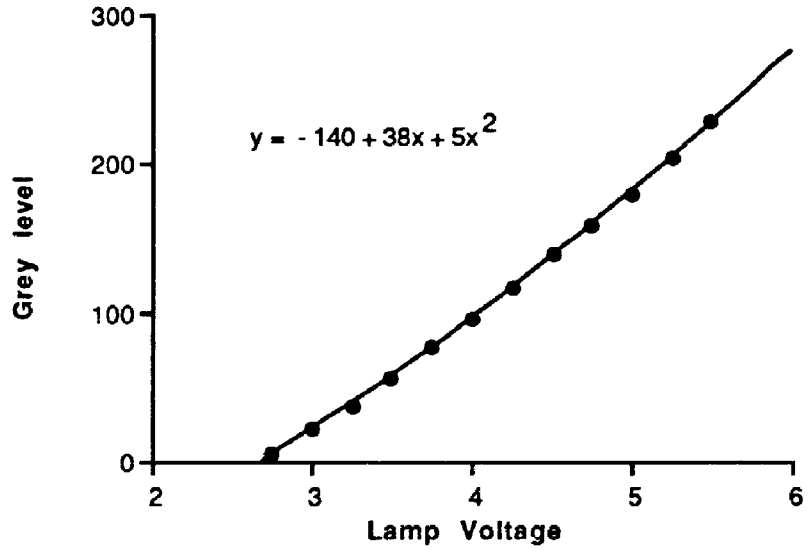

Figure 2.6: Relation between the grey-level of a blank image and the corresponding voltage of the microscope lamp.

material to the eye is that of a bright structure on a dark background, the absolute difference in intensity between the two components may not be great. This is because with polarizing microscopy, the light exiting the birefringent specimen is only a minute fraction of the original light. If Γ is specimen retardation in degrees, the luminance or intensity (I) of a birefringent specimen oriented 45° to the polars is described by:

$$I = I_{pa} \times \sin^2(\Gamma/2) + I_{pe} \qquad \text{(Inoué 1981)} \quad \text{(Eqn. 2)}$$

where I_{pa} is luminance of the field with the polarizer and analyzer parallel and I_{pe} is the intensity when the polarizer and analyzer are crossed.

Since $$EF = \frac{I_{pa}}{I_{pe}} \qquad \text{(Eqn. 1)}$$

equation 2 may be restated:

$$I = I_{pa} \times \{\sin^2(\Gamma/2) + 1/EF\} \qquad \text{(Eqn. 3)}$$

In my experience retardation of light by collagen in sections 4-7 μm thick and stained with picrosirius red is in the order of 15-70°. As noted above the extinction factor of the Nikon polarizing microscope was 1.2×10^4 and with respect to retardation can be considered to approach zero.

Thus, intensity of the specimen is in the order of 10^{-2} of that of the transmittance of a parallel pair of polarizing filters. To detect this degree of illumination, the background must be sufficiently dark. Although a relatively black background is a fundamental principle of polarization microscopy, a certain amount of stray light does pass through to the eyepiece (or camera). This is because at every oblique-incidence light interface located between the crossed polars (eg lenses, slides, cover slips), the plane of polarization will rotate slightly (Inoué and Hyde 1957). Thus, even with strain-

free lenses and slides, some light will transmit through the analyzer even though it has not traversed a birefringent structure (in this case collagen). To the eye, this reduction in contrast between background and collagen may appear minor yet when a CCD camera is used as the sensing device, a significant amount of light will be detected. This is due to the high sensitivity of this camera to light of near infrared wavelength, which is emitted in abundance by the halogen microscope lamp.

Some approaches to this problem have been proposed. Inoué and Hyde (1957), developed a polarization rectifier which reportedly corrected the unwanted rotation of light by the microscope components . Alternately, a retardation bias, can be introduced by inserting a quarter-wave plate and rotating the analyzer (Allen et al 1981, 1983). While this will cause a further increase in the intensity of the background, its effect on birefringent material is proportionally greater (Inoué, 1981). Finally, the use of heat filters to exclude infrared light has been suggested (Inoué, 1986). There remains some controversy as to the best approach. The optimum optical parameters will likely depend on the specific characteristics of the video system.

The assessment of myocardial collagen presents a further challenge since cardiac muscle is also birefringent. Not only is distinct contrast therefore necessary between collagen and background but also between collagen and muscle. Because the tissue was being stained, I considered an alternate approach to attain this contrast . If the specimen could be illuminated with light of wavelengths that were transmitted almost exclusively by collagen then the amount (intensity) of both stray light and light coming from cardiac muscle would be markedly decreased without compromising collagen brightness. A narrow band-pass type of interference filter was consider appropriate since this would also exclude infrared light.

To determine the appropriate wavelength, a monochrometer (Bausch and Lomb) was positioned between the polarizing microscope and a fiber optic light source (Leitz). Band width was set at 15 μm and the illuminating wavelength was varied from 45 to 800

nm in 5-10 nm increments. Three specimens were studied: rat achilles tendon sectioned at 7 μm; an adjacent section cut at 1 μm; and a section of rat skeletal muscle cut in long section. All three were stained with picrosirius red. When viewed with the polarizing microscope, the thicker tendon appeared yellow-orange, the thinner bright green, and muscle appeared dull green. The three specimens were therefore considered representative of the collagenous and muscular components of the myocardium. For each illuminating wavelength, the grey-level histogram (grey-level versus number of pixels in the specimen) was obtained and the median grey-level determined. As shown in Figure 2.7, muscle intensity did not vary considerably with illuminating wavelength. In contrast, both the orange-red and green collagen were brightest when illuminated with light of wavelength 600 nm and maximally distinct from muscle. Background light did not result in visible (non zero) pixels at any wavelength suggesting that the 15 nm band-width was sufficiently narrow to prevent a response to stray light under these illuminating conditions.

On the basis of these results, a 600±5 nanometer band-pass filter (Optikon) was used for all collagen measurements. It is recognized that collagen commonly transmits a wider range of wavelengths than this (indicated by the green color of some fibers when illuminated with white light and viewed with a polarizing microscope) and its absolute intensity may be decreased somewhat by this filter. The important feature, however, is the contrast between image components which becomes optimized at this particular wavelength.

Using this filter, contrast between collagen, muscle, and nonbirefringent structures including nontissue background was visibly much improved although muscle cut in long section was still visible. The visible muscle components were therefore subtracted electrically by adjusting the offset (black-level) potentiometer of the camera

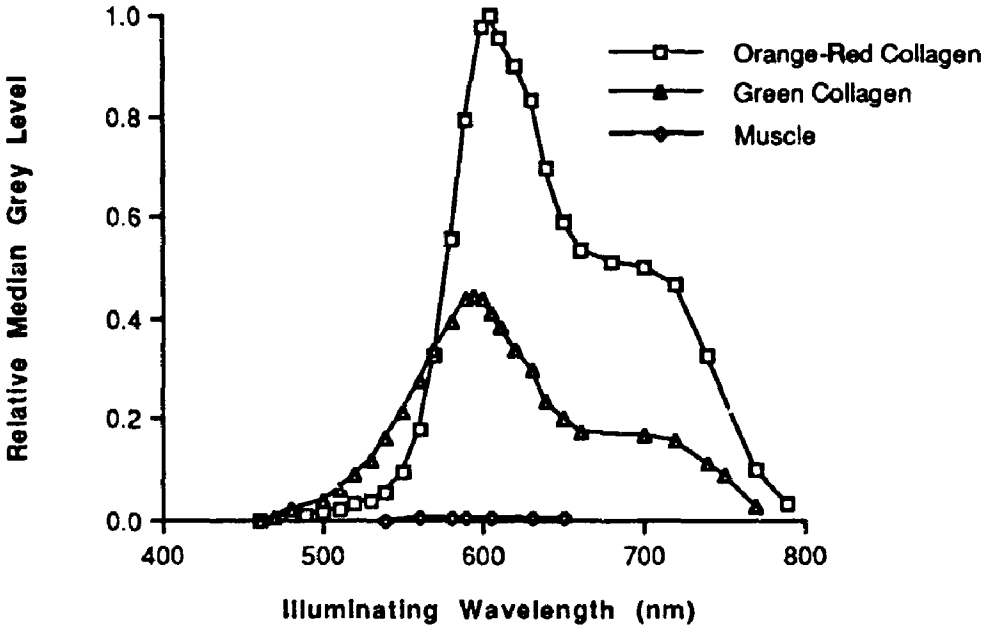

Figure 2.7: Effect of illuminating wavelength on the relative intensity of brightness of tendon sectioned at 7 μm, tendon sectioned at 1 μm, and skeletal muscle. Collagen-muscle contrast is greatest at 600 nm.

video board.* Specifically, while viewing a real-time digitized image of myocardium, the black-level was increased to the point where all muscular components became black. As muscle occupies the bulk of the specimen and has a relatively uniform birefringence, the transition point was relatively abrupt and easily discernable. Thus, the final digitized image consists of two components: noncollagenous material appearing black (grey-level 0), and collagen appearing in various degrees of brightness (grey-level 1-255) (Plates 2.2 and 2.3, Figure 2.8). Collagen content can thus be expressed as the area-fraction of bright pixels. Validation of this approach to collagen quantification is presented in Chapter 3.

The collagen network may also be characterized in terms of the frequency distribution of the collagen grey-levels, which will describe overall collagen brightness. In this context it must be recalled that the black-level has been set above 0 and the "true" intensity of brightness will be greater by an amount equal to the grey-level offset of the video system. This in turn may be determined from the plot of grey-level versus light transmittance (e.g., Figure 2.4). In any event the brightness profile of fibrotic collagen may provide important information on the nature of the fibrotic process. This is explored further in Chapters 4 and 5.

Image Saturation

As evidenced by the histogram shown in Figure 2.8, a proportion of pixels that depict collagen are "stacked" at grey level 255 indicating that the range of intensity of brightness of collagen fibres exceeded the intensity limits imposed by the video system. This was found to occur despite 1) setting the gain of the camera to minimum and 2) electrical subtraction of grey-levels (through the offset adjustment) so that the lower end of the range of collagen intensities was "assigned" to a grey-level of 1. I also found that,

* A similar adjustment in the offset can be made using the "toolbox" software supplied with the video board (Infrascan)

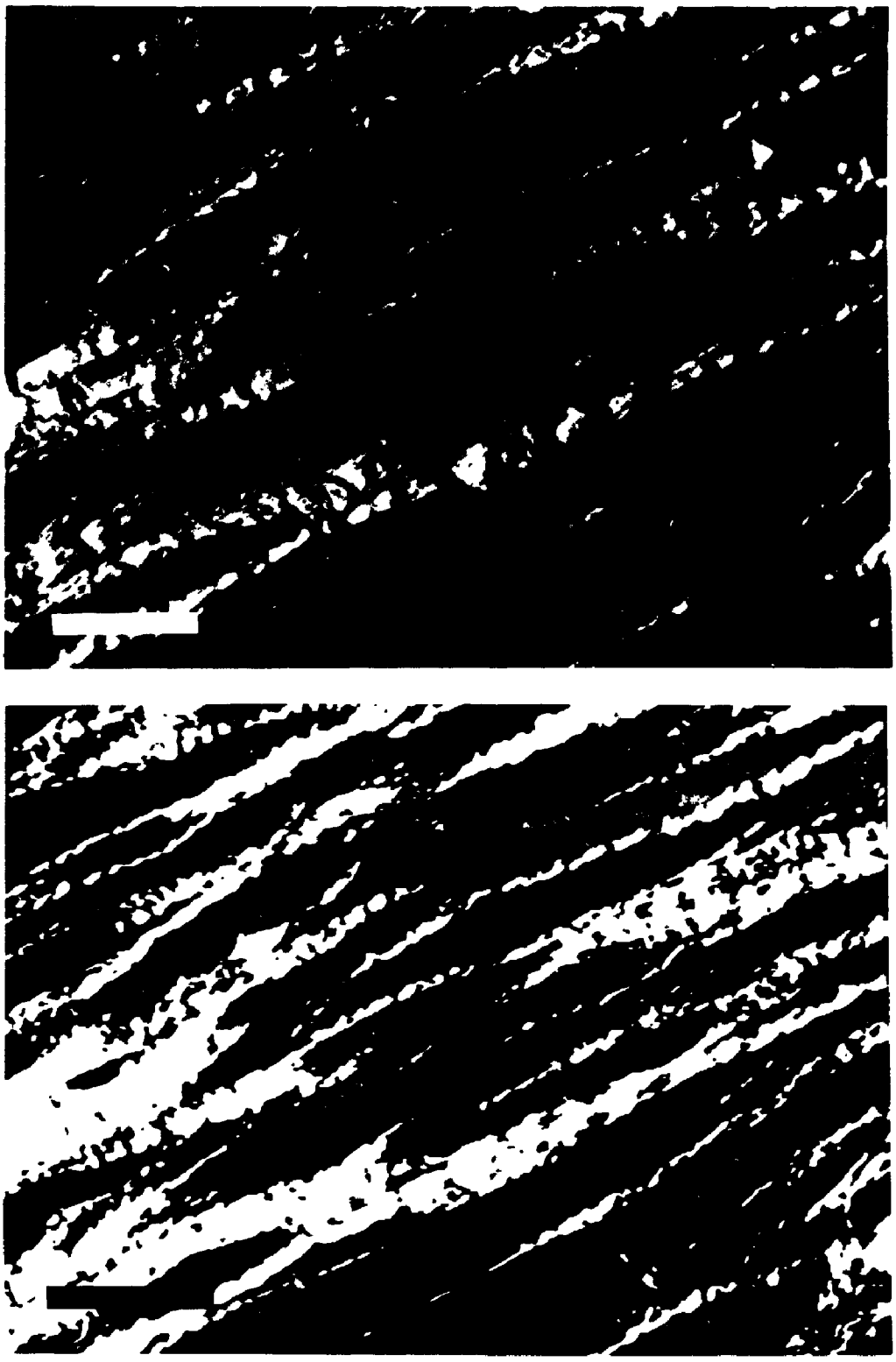

Plate 2.2: (Top panel) Photomicrograph of a section of interventricular septum stained with picrosirius red and viewed through the polarized light microscope. Collagen appears either bright yellow-orange or bright green, while muscle is faintly visible appearing dull green. **Plate 2.3:** (Bottom panel) The digitized image of the same section. Image thresholding has been applied so that all grey-levels above 0 (black) are set to 255 (maximum brightness), illustrating the two-component nature of the image. Polar orientation is ⊕. Bar, 75μm.

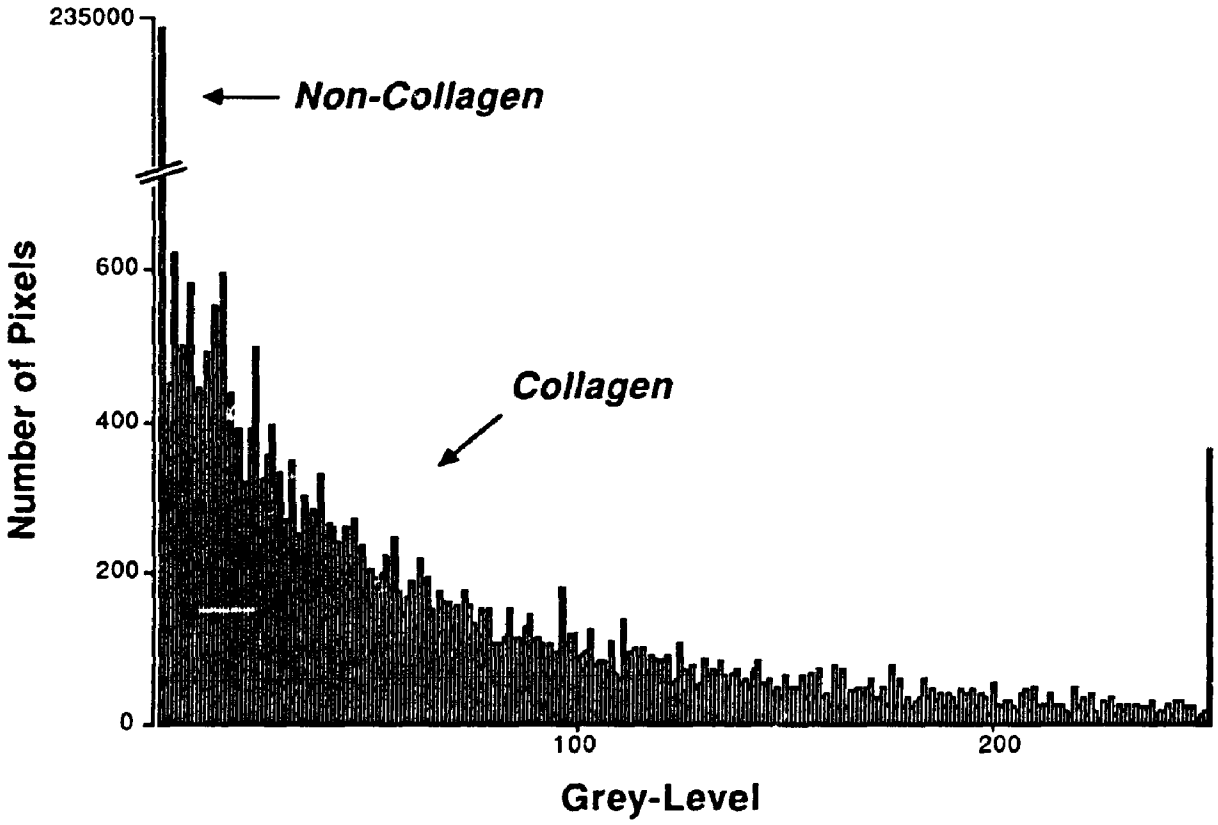

Figure 2.8: Grey-level hi ,togram of a digitized image of myocardium stained with picrosirius red and illuminated with polarized light of 600-nm wavelength. Collagen is represented by all nonzero pixels. Note that the number of pixels at grey-level 0 is much greater than the number of pixels at grey-level 1, allowing for easy distinction of collagen.

under these conditions, the dynamic range of the camera and of the video frame-grabber board were similar (as evaluated using an oscilloscope to compare the minimum and maximum voltage signal of the camera with those associated with the minimum and maximum grey-levels of the digitized image). Thus both the camera and digitizer respond to a window of light intensities much narrower than that transmitted by a network of fibrotic collagen. It would appear therefore that saturation of a proportion of the image may be unavoidable given the apparent wide range of collagen birefringence.

With this finding, it was important to ascertain if there were drawbacks to image saturation. The spilling of light into adjacent pixels ("blooming") is seen with some tube-cameras, and with some CCD cameras vertical white stripes flanking the image have been noted (Inoué 1986, p 221). A section of rat tail tendon, sectioned at 7 µm, and stained with picrosirius red was used to evaluate this. The tendon was oriented at 45° to the polars and the grey-level profile (grey-level versus pixel location) through a column of pixels was obtained. This was done with illumination set both below and above the point of image saturation. As evident from Figure 2.9, there was no detectable effect on the grey-level of adjacent noncollagenous tissue. Therefore, the size and shape of the collagenous components of the image are unaffected by the occurrence of grey-level saturation.

2.4 Summary

I have utilized and combined the techniques of polarization microscopy, video microscopy, and microcomputer image processing to develop a single investigative tool for the quantitative study of myocardial fibrosis. Identification of collagen was based on its high degree of birefringence and image contrast was enhanced by color filtering, digitization, and adjustment of the video signal. Preliminary studies have confirmed that the digitized image accurately reflects the microscope image. Thus using tissue sections

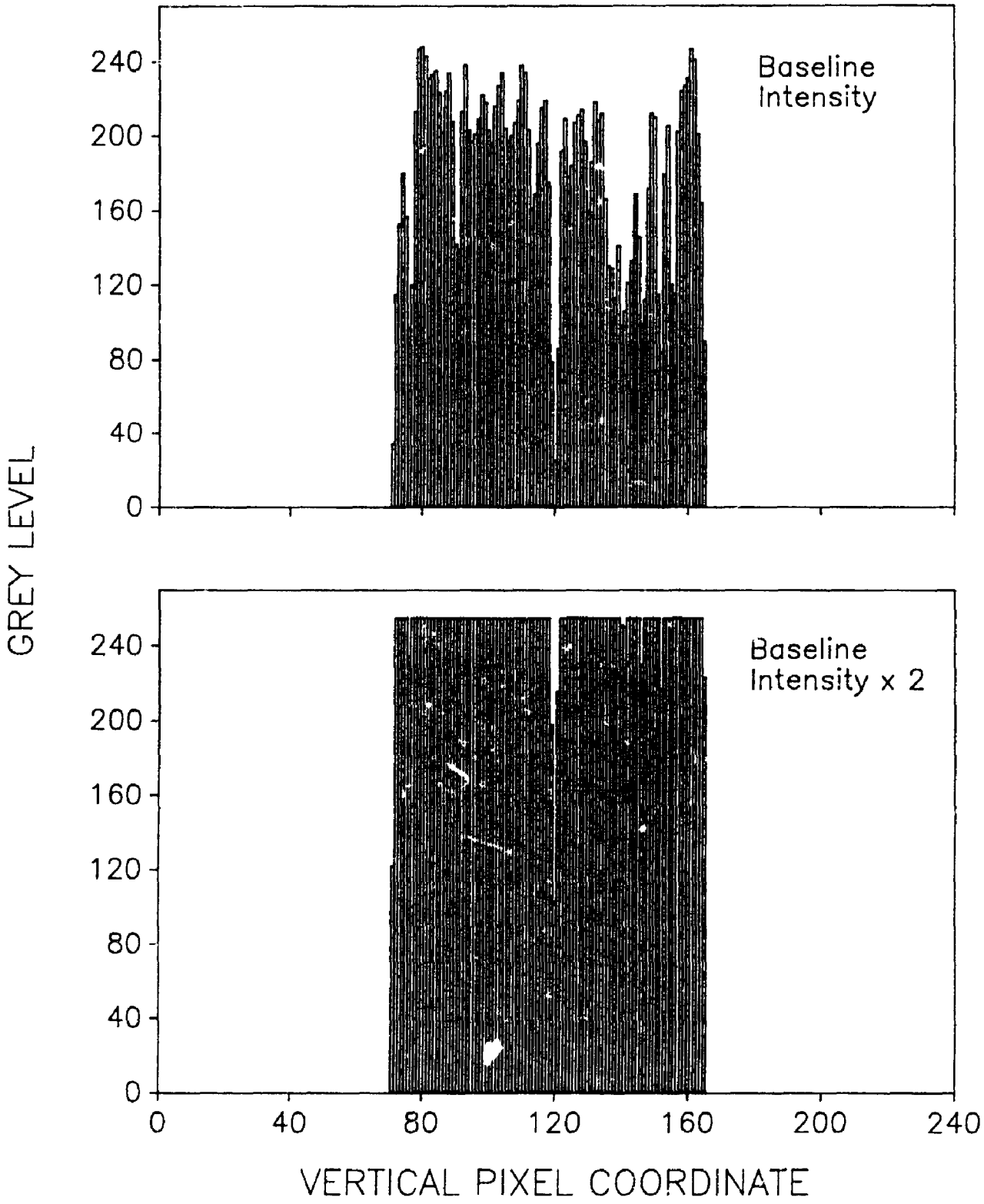

Figure 2.9: Grey-level profiles across an image of rat tail tendon stained with picrosirius red and imaged under crossed polars. The tendon occupies the midportion of the image. When the light intensity is increased (bottom panel), the pixels depicting collagen become saturated at maximum brightness. The adjacent pixels depicting background, however, are unaffected and remain black.

prepared for routine light microscopy, collagenous components of myocardium can be readily and quantitatively evaluated.

Chapter 3 Quantification of Myocardial Collagen

3.1 Introduction

This chapter reviews the specific manner in which the polarization-video microscopy technique can be used to quantify myocardial collagen and it addresses the overall validity of the approach.

To evaluate the heart histologically, specimens of myocardium may be procured in one of two ways: 1) by excising a portion of a postmortem heart or 2) by endomyocardial biopsy of a patient under investigation. While identical information is generally sought from the two types of specimens, the physical nature of the tissue samples can be quite different. Biopsy specimens are smaller than autopsy material (Baandrup et al 1982), and more likely to contain artificial gaps within the myocardium. In addition, the orientation of muscle and collagen fibers within a given biopsy section is more variable than in autopsy specimens. This is relevant to tissue assessment by polarization microscopy because of the phenomenon of "extinction". If a fiber has been sectioned with its long axis in the plane of the section, the fiber will not be visualized if it is aligned parallel or perpendicular to the transmission axis of the polarizer (which determines the plane of polarisation). This occurs because the light incident on the specimen will "see" only one refractive index and its state of polarization will not be changed. In sections from autopsy hearts, collagen extinction can be easily avoided by rotating the microscope stage as necessary. In biopsy specimens, however, collagen orientation is likely to be variable and rotating one collection of fibers out of extinction may cause another group to be extinguished.

Because of the physical differences between the two types of specimens, I felt it was important to test the validity of the collagen videodensitometry technique in both settings. Using myocardium from autopsy hearts, the collagen estimate was compared

with measurements of hydroxyproline content.* For assessment of endomyocardial biopsy samples, hydroxyproline analysis was not feasible because of the small size of the sample and the variable amount of endocardial collagen. To circumvent this problem I examined three separate aspects of collagen quantification in the biopsy specimens: 1) reproducibility of the estimate with successive measurements, 2) dependence of the collagen estimate on sample orientation with respect to the polarization axes, and 3) correlation of the estimate with a stereologic assessment.

3.2 Methods

3.2.1 Comparison of Collagen Measurements by Videodensitometry with Hydroxyproline Content Measurements

Specimens from 14 autopsy hearts were provided by the Department of Pathology, University Hospital, London, Ontario. Five were from patients with no clinical evidence of heart disease, 6 from patients with a history of myocardial infarction and 3 from patients with a dilated cardiomyopathy. Each heart had been fixed in 10% neutral buffered formalin. Endomyocardial samples were excised from the interventricular septum and divided, into two pieces, perpendicular to the endocardial surface. The endocardium itself was dissected free of the specimen to avoid the possibility of unequal distribution of endocardial collagen. One of the two portions was then embedded in paraffin and the cut surface sectioned. All 14 sections thus produced were simultaneously stained with picrosirius red.

To quantify the total area of myocardium for each section that was being histologically analyzed, the slides were studied using brightfield microscopy with a green (λ=540 $\pm$ 5 nm) filter (Optikon) positioned at the plane of the field diaphragm. In this way, the nontissue background, including artifactual gaps in each sample, was

* This study forms part of a publication (Pickering and Boughner 1990).

readily distinguishable from the remainder of the sample based on grey-levels (Figure 3.1). Collagen content was then determined after switching to the red filter (λ=600 ± 5 nm) and inserting the analyzer. The specific steps for the histologic analysis are as follows:

1. Stable illumination conditions were established. Lamp voltage, generally between 8 and 9 volts, was recorded as was the grey-level of a background image.

2.* The specimen was illuminated with green-filtered light and viewed with the analyzer withdrawn from the light path. (bright-field microscopy).

3. Using SDPPC (Software Development Package, Infrascan), a video image was digitized and displayed on the monitor.

4. Using the "density slice" function a grey-level threshold was defined such that grey-levels below threshold depicted background and grey-levels above threshold identified the specimen. The density slice program displays the image in binary format (grey-levels 0 and 255) and the transition grey-level is set by rolling the mouse.†

5. The SDPPC program was terminated and a program to determine the total specimen area, based on the grey-level threshold, was run.

6. The green filter was replaced with the red filter and the analyzer was inserted into the light path.††

7. The polarization image was digitized and displayed.

8. A program to determine the collagen area was run. This assumes a grey-level threshold of 1 unless otherwise specified.

9. Steps 2-8 were repeated until the entire specimen was analyzed. With each run, the values for specimen and collagen area were stored in a data file and summed at the completion of the experiment.

---

* If the specimen routinely occupied all of the digitized image and had no artifactual tears, then steps 2-5 can be eliminated. Total specimen area would be calculated as the total image area (307,200 pixels) multiplied by the number of fields analyzed.

† This procedure was also used to assess homogeneity of the background image. If variations existed, illumination conditions (lamp position, field diaphragm and condensor iris apertures, position of condensor lens) were adjusted accordingly.

†† Illumination through crossed polars generally requires more light than bright-field illumination. This was adjusting using neutral-density filters; lamp voltage was held constant.

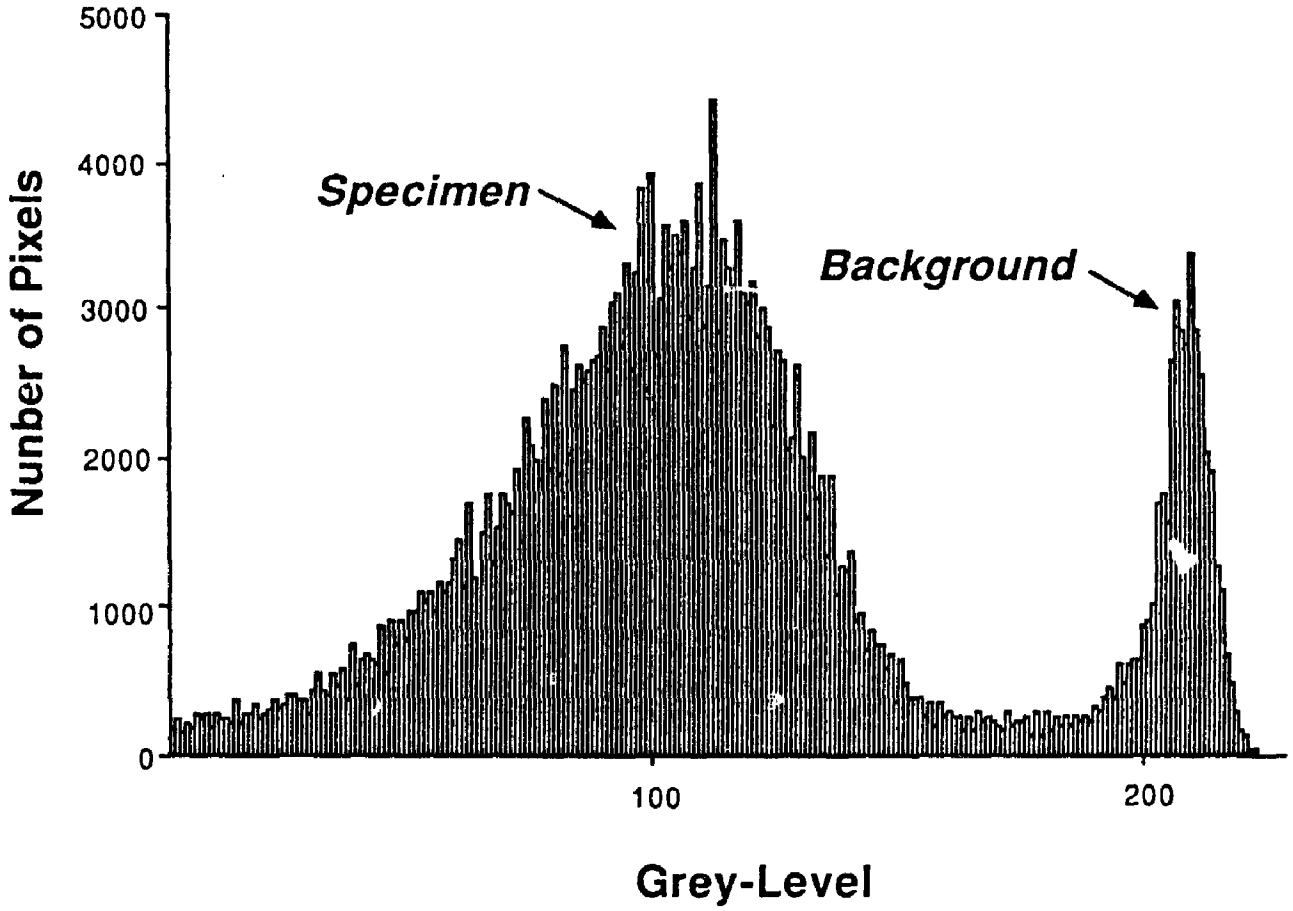

Figure 3.1: Grey-level histogram of myocardium illuminated with green-filtered light and with the analyzer withdrawn from the light path (bright-field microscopy). The background is distinctly brighter than the tissue components.

All of the computer-based steps were linked together in a single batch file allowing rapid transition from one step to the next. Determination of the area-fraction of collagen or of background required 8 seconds of computer processing.

The second portion of each sample was dried at 60° to a constant weight, hydrolyzed in 6N hydrochloric acid at 105°C, and dried under vacuum. Hydroxyproline analysis was performed according to Chiariello et al (1986). Briefly, specimens were oxidized with a chloramine-T solution followed by addition of Erlich's reagent in perchloric acid. Absorbance was measured at 558 nm and results were expressed as nanomoles of hydroxyproline per milligram of dry weight. This analysis was performed by Mr. W. Chung, Department of Biochemistry, UWO. The two quantification procedures were performed without knowledge of the results of the alternate approach.

3.2.2 Variability of Collagen Estimate With Successive Measurements

Although videodensitometry is essentially an objective assessment, some aspects of the procedure might lead to variability. For instance, endocardial collagen should be excluded. Normally, this is not difficult but sectioning of small biopsies may place the endocardium in an unusual location (e.g., "within" the myocardium). Another potential source of variability may be the definition of the grey-level threshold distinguishing tissue from background and artifactual space.

I therefore quantified the myocardial collagen content of 10 biopsy specimens on two occasions, separated by at least eight weeks. These specimens were from heart transplant patients and were taken at least one year after surgery. Fibrosis in the transplanted heart has been identified by several investigators (Billingham 1981, Gokel et al. 1985, Pomerance et al 1985, Bieber et al 1970) and it was anticipated that specimens taken later than one year from the time of transplantation would show a range

of severity of fibrosis. Specimens were provided by the Department of Cardiology, University Hospital, and histologic processing was done by Mrs. J. Dixon.

3.2.3 Dependence of Collagen Estimate on Orientation of the Specimen With Respect to the Microscope Polars

Endomyocardial biopsies from 11 heart transplant recipients, at least one year from the time of surgery, were studied. For each biopsy, the collagen estimate was first determined with the slide oriented at 0^{o} (parallel to the transmission axis of the polarizer). The stage was then rotated 5^{o} and the measurement was repeated. This was repeated until the slide had been rotated through a full 90^{o} for a total of 18 different orientations. In this way, all fibers that were lying in the plane of the cutting section would at some point be positioned at or close to the point of extinction. To ensure that identical areas of myocardium were studied at each orientation, a program utilizing a circular area of interest was written. The diameter of the field was 480 pixels corresponding to an image area of 0.33 mm^2. The quantification procedure was otherwise as outlined in Section 3.1. Up to 5 areas per biopsy section were studied. The estimate for each orientation was therefore the sum of the estimates at that particular orientation for the slide.

A wide range of collagen estimates would suggest that there was a significant proportion of fibers lying parallel to the sectioning plane and that there was a preferred orientation of these fibers. Assessment at a single randomly chosen orientation might therefore result in an underestimation of the total collagen content. A narrow range of estimates would imply either that the arrangement of fibers was sufficiently disorganized that very few fibers were lying in the plane of section, or, that at any orientation the percentage of fibers at extinction was relatively constant, but not necessarily zero.

3.2.4 Comparison of Videodensitometry With Stereology

To further evaluate the video approach as applied to biopsy specimens, I compared it with a stereologic method. Five-µm thick paraffin sections from 22 endomyocardial biopsy specimens from heart transplant recipients were studied. These were provided by the Department of Pathology, University Hospital and had been stained, as a matter of routine, with Masson's trichrome stain. A slide adjacent to each trichrome-stained slide was stained with picrosirius red for the purpose of this study. Slide labels were covered with tape.

The trichrome-stained sections were viewed with a x40 objective and x10 ocular. Volume fractions were determined by intersection-point counting using a 100-point eyepiece grid. All blue-stained interstitial material was counted as collagen. Muscle, interstitial space, and noncollagenous components of the interstitium (cells, capillaries) were also counted. The endocardium and artifactual gaps in the tissue were not included. Approximately 1000 intersection points were counted for each specimen (948±286). I wrote a short program in C so that counts could be input via the computer keyboard and tallied by the computer.

The collagen content of the picrosirius red-stained sections was determined using the polarization-videodensitometry technique.

3.3 Statistics

Values are presented as mean ± standard deviation. Relations between the various methods of quantifying collagen were tested by linear regression analysis. Variability between the two successive measurements of identical biopsies was expressed as the coefficient of variation. Orientation-dependency was described by the range of the 18 collagen estimates for a given sample.

3.4 Results

A wide range of values of hydroxyproline content existed in myocardial samples from the 14 autopsy hearts (19.2-268.8 nmol/mg dry weight). The histologic features included normal myocardium, varying degrees of interstitial fibrosis, and areas with dense scar tissue. The collagen volume fraction, determined by videodensitometry, ranged from 3.7 to 50.4%. As depicted in Figure 3.2, there was good correlation between the hydroxyproline content and the collagen estimate by videodensitometry ($r=0.98$, $p<0.001$).

The first set of collagen estimates of the biopsy samples used to assess the repeatability of the measurement ranged from 2.3-18.3 %. There was excellent reproducibility of these results on the second measurement with a mean coefficient of variation of 2.7±2.2% (range 0.7-7.2%).

For the 11 specimens in which the orientation effect was studied, the mean collagen volume fraction ranged from 2.6-17.4 %. The mean variability within a sample (i.e. the range of the 18 values) was 0.32±0.19 % (range 0.10-0.86 %). When expressed in terms of the mean collagen content of the sample, this variability was 5.1±3.3 % (range 1.5-12.6 %). There was no correlation between the magnitude of variability and the amount of fibrous tissue ($r=0.56$, p=N.S.) although there was a weak negative correlation between the range, expressed as a percent of the total fibrous tissue, and the degree of fibrosis ($r=-0.60$, $p=0.05$) (Figure 3.3).

Of the 22 biopsy specimens studied by both stereology and videodensitometry, the collagen volume fraction estimated by intersection point counting was 5.5±3.4 % (range 1.0-15.8 %). As shown in Figure 3.4, there was good correlation between these data and the values obtained by videodensitometry ($r=0.95$, $p<0.01$). From the point count data, the volume fraction of myocytes, interstitial space, and the other interstitial components was 82.3±5.7 %, 7.6±3.8 %, and 4.5±1.8 % respectively. The collagen

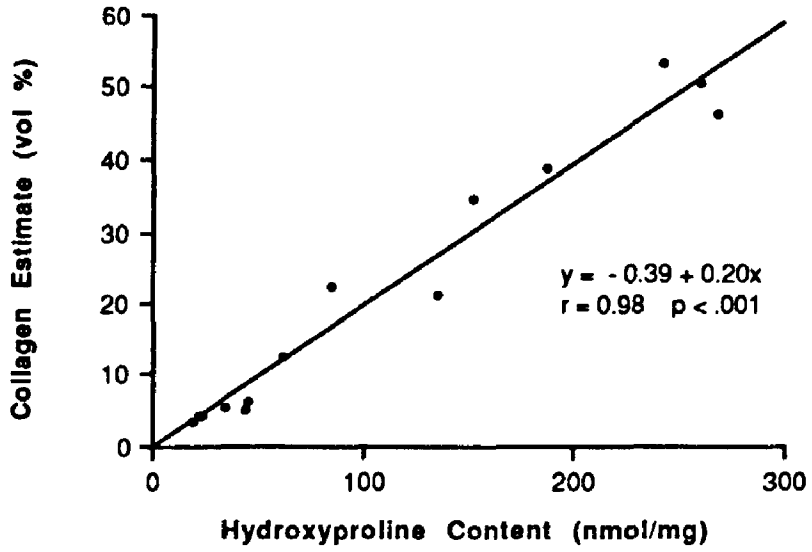

Figure 3.2: Relation between collagen content determined by hydroxyproline analysis and videodensitometry from myocardial samples from 14 autopsy hearts. Good correlation exists between the two techniques.

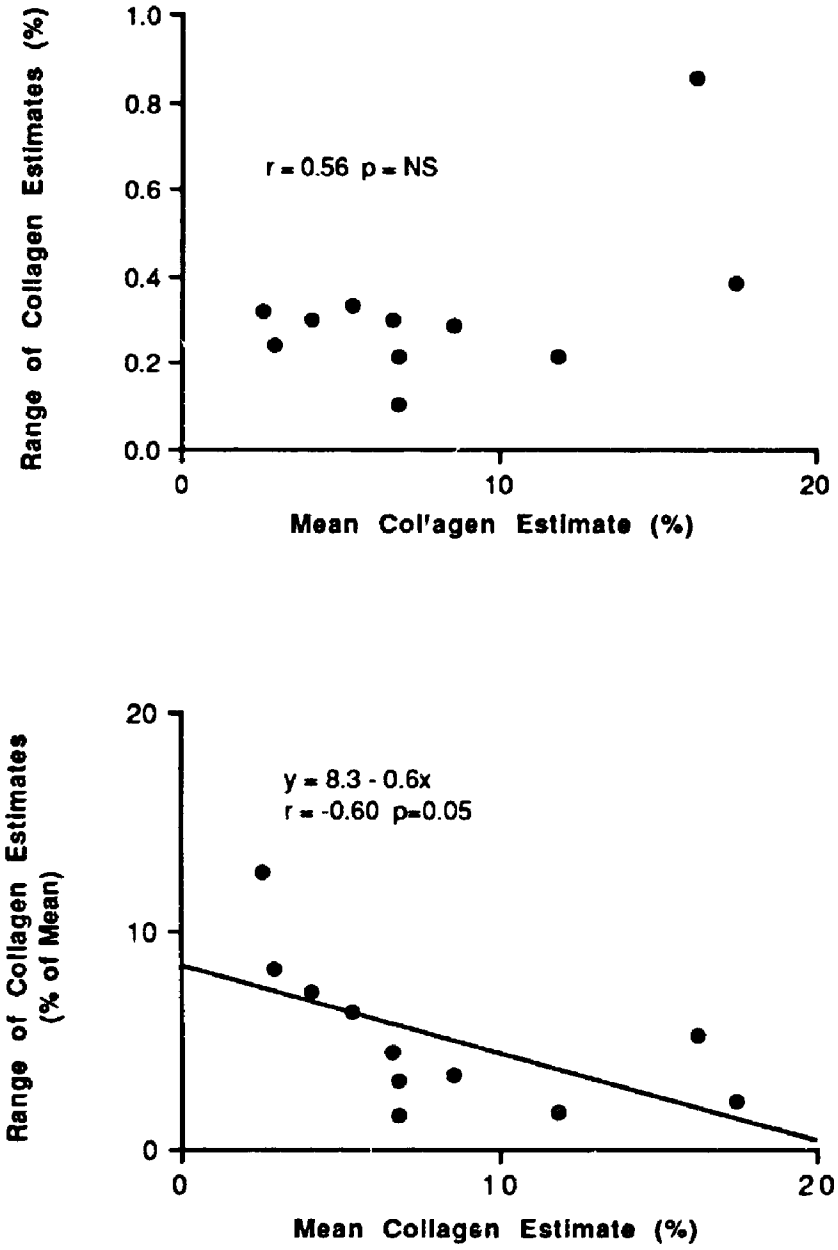

Figure 3.3: Dependence of collagen estimate using the polarization-videodensitometry technique on the orientation of the slide. The top graph shows the absolute range of the 18 estimates of each biopsy and indicates no relation with collagen content. The bottom graph shows the range as a percentage of the overall mean of the 18 results and suggests that the variability decreases with increasing collagen content.

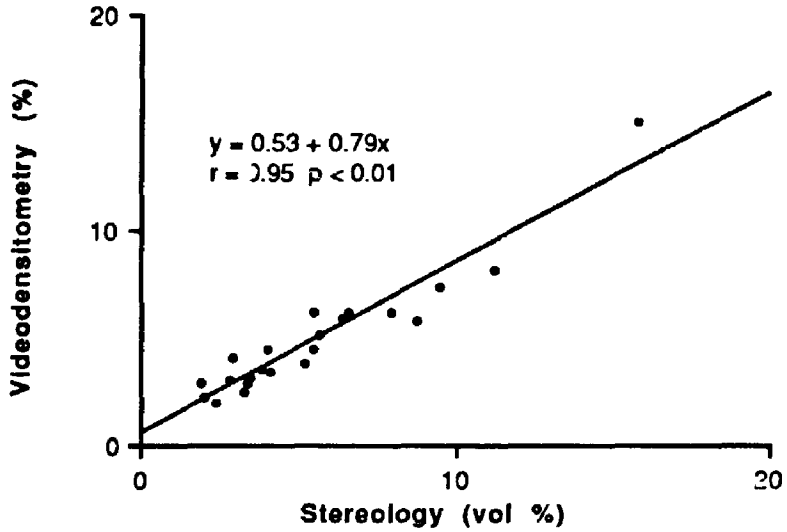

Figure 3.4: Relation between collagen content determined by videodensitometry and by stereology from 22 endomyocardial biopsy specimens.

volume fraction did not correlate with the amount of interstitial space (r=0.03, p=N.S.) or the fraction of the other interstitial components.

3.5 Discussion

The primary means of validating the collagen videodensitometry system was the comparison with chemical estimation of the collagen content. Hydroxyproline is present in abundance in collagen but in very few other proteins (Grant and Prockop 1972). Measurement of this aminoacid is thus considered the best biochemical method of quantifying collagen. Although chemical analysis of tissue is generally performed on fresh specimens, Caspari et al (1977) have shown that measurement of hydroxyproline in the heart is not affected by fixation in 10% formalin. Using formalin-fixed specimens, we found an excellent correlation between hydroxyproline content and the estimate of collagen content by videodensitometry. The chief advantage of the latter technique is that structural integrity of the sample is preserved.

The recent development of the myocardial bioptome has provided a safe means of obtaining heart specimens from patients with cardiac disease (Mortenson and Baandrup 1987). As a consequence, histologic analysis of this type of myocardial specimen is pervasive and increasing. Mason and O'Connel have estimated that at least 20,000 endomyocardial biopsies were done in the U.S. in 1987 excluding those done to monitor transplant rejection. The latter indication likely accounted for a further 15,000 in that year.* Given this high prevalence and the unique structural characteristics of biopsy specimens, it is important to determine if morphometric techniques retain their validity when used for biopsy analysis.

---

* I estimated this number assuming 10 biopsies per year for patients in the first year after transplantation. There were 1436 transplants performed in the U.S. in 1987 (Fragomeni 1988).

By assessing the collagen content of biopsies on two remote occasions, I found the reproducibility of the estimate to be very good. It is expected that the variability of collagen estimates for autopsy specimens would be even lower since the specimens are larger and there is no difficulty in distinguishing endocardial from myocardial collagen. Variations in the measurement of the area of nontissue background of autopsy sections are also likely to be lower since the proportion of tissue with artifactual separations will be small or nonexistent.

The results of the orientation study indicate that although the collagen estimate varies somewhat with the orientation of the specimen on the microscope stage, this is very small. In terms of collagen content, the mean range of values was only 5%. It is emphasized that this refers to the maximum possible difference between any two orientations. It is therefore reasonable to conclude that if a preferred alignment of fibers is not obvious to the observer, collagen measurement can be made at any single orientation with respect to the polars.

As noted previously, this lack of variability suggests that the proportion of fiber in biopsy samples that are both highly aligned with each other and are lying in the plane of the section is relatively low. Alternately, it may reflect a relatively equal number of fibers, or parts of fibers, becoming extinguished at all orientations. While the latter possibility cannot be ruled out entirely, its contribution is likely to be small. As discussed below, there was no evidence that the videodensitometry technique significantly underestimated the amount of collagen quantified by stereology. As well, Dolber and Spach (1987), using the picrosirius-polarization technique to study dog myocardium, have observed that the only collagenous components in which visibility was significantly dependent on orientation were the very thin (0.2-0.5 μm) septa that ensheathed individual myocytes. Thicker septa did not show this phenomenon suggesting that the constituent fibrils are oriented in nonparallel planes. Qualitatively, I

found this also to be the case for patches of fibrotic collagen present in the biopsy specimens.

The ultimate test for reliability of a procedure is, of course, comparison with an independent technique. Unfortunately, chemical analysis of homogenized tissue is not well suited to endomyocardial biopsy material. Given the small size of the sample, it is not possible either to remove the endocardium or to divide the sample so that both portions contain equal amounts of this collagen-rich material. Stereology was therefore used as the method of comparison. A good correlation was observed over a range of collagen volume fractions of 1.0-15.8 %. The major drawback of the point counting method is the time required to yield an accurate result. Since a high magnification is required (Pearlman et al 1982) only a small area can be analyzed at a time. With the video approach the size of a single digitized image was 0.56 mm^2 and determination of the area-fraction of collagen required about 10 seconds of computer processing. The time required to establish appropriate illumination conditions and determine the specimen area will add to this; however it remains a substantially faster and less laborious procedure than point counting.

A second finding of the point counting study concerns the proportion of the noncollagenous constituents of the cardiac interstitium. In total, the volume fraction of the nonmuscular myocardial elements was approximately 18%. This is somewhat less than that found by Fuster et al (32%) and Moore et al (25%) and the difference may be due to avoidance in my approach of artifactual tissue spaces. Of the total cardiac interstitium, noncollagenous structures such as cells and blood vessels occupied approximately 25 %, and interstitial space (water and ground substance that did not take up stain) occupied approximately 40 %. For the population studied, there was no relationship between the fibrous content and either of these components. It can be seen therefore that methods of quantifying collagen that do not distinguish other components

of the interstitium will be unreliable. Collagen is the only component of the interstitium that is both stained by picrosirius red and is birefringent (Junquiera et al 1979).

In summary, the technique of polarization microscopy of myocardium stained with picrosirius red has provided the basis for an accurate and rapid videodensitometric method of quantifying cardiac fibrosis. It may be successfully employed to study both autopsy and biopsy specimens. Thecretical concerns regarding the effect of collagen extinction, in practice become relatively unimportant. Unless there is an obvious high degree of fiber alignment, orientation of the specimen with respect to the polars need not be considered.

Chapter 4 Assessment of Replacement Fibrosis

4.1 Introduction

Fibrosis has traditionally been regarded as the final and irreversible stage of tissue injury (Robbins and Cotran 1979, p 103). It is not surprising therefore that although myocardial fibrosis can severely impair cardiac function, specific treatment of cardiac fibrosis is almost nonexistent. In recent years however, basic research in the biology of collagen has elucidated an extensive series of events that take place as fibrotic collagen is deposited and structurally organized (Prockop and Kivirikko 1984). This has prompted investigators to develop agents that alter the rate of one, or several, of these steps in an effort to obtain a degree of control over the fibrotic process. Although several approaches have been proposed the available results are conflicting or inconclusive (Prockop et al 1979a). No technique to date has been successfully incorporated into clinical practice with the possible exception of the topical application of epidermal growth factor to enhance skin wound healing (Brown et al 1989). One reason for this limited success may be the lack of suitable methods for evaluating the effect of a proposed treatment. Investigators would be aided considerably if they could readily determine the activity of fibrosis and its state of maturation.

The practical and nondestructive nature of histologic assessment makes it a desirable approach for this type of assessment. However, when stained and examined using routine microscopy, collagen has a rather uniform appearance and an active process is difficult to identify. Immunostains may identify type III collagen (Timpl 1980, Williams et al 1984) present in early fibrotic lesions (Bailey and Light 1985), as may argyrophilic reticulin stains (Goldberg and Rabinovitch 1983), but these techniques provide only qualitative data.

In contrast, polarized light microscopy has been utilized to demonstrate quantitative differences in collagen birefringence at various stages of the healing process (Wolman et al 1972, Mello et al 1975, Whittaker et al 1989). This is because as a fibrotic network matures, a series of molecular and macromolecular events ensue which increase the anisotropy of the network (Figure 4.1). Polarized light microscopy can serve as a tool to monitor this process. Whittaker et al (1989) have recently illustrated this by examining the collagen laid down after myocardial infarction. In spite of their report, and that of others (Wolman and Gillman 1972, Mello et al 1975) who successfully used quantitative polarizing microscopy to characterize fibrosis, the technique has not been widely employed. This may be partly due to the laborious nature of the assessment, as individual measurements of retardation must be made on a large number of collagen fibers to adequately characterize the tissue. I hypothesized that the assessment could be simplified, yet retain its validity, if the relative brightness of collagen were quantified rather than its birefringence. In this way, zones of fibrosis could be rapidly evaluated using video techniques. Theoretical considerations regarding the use of collagen intensity as an index of its state of maturation are considered below.

4.2 Theory

The intensity of brightness of a birefringent material viewed with polarization microscopy is determined by two factors: retardation and orientation (Wolman 1975). As noted previously, the relationship between the intensity of brightness, I, and retardation of a specimen oriented 45^{o} to the polars is described by

$$I = I_{pa} \times \sin^2(\Gamma/2) + I_{pe} \qquad \text{(Inoué 1981)} \quad \text{(Eqn. 2)}$$

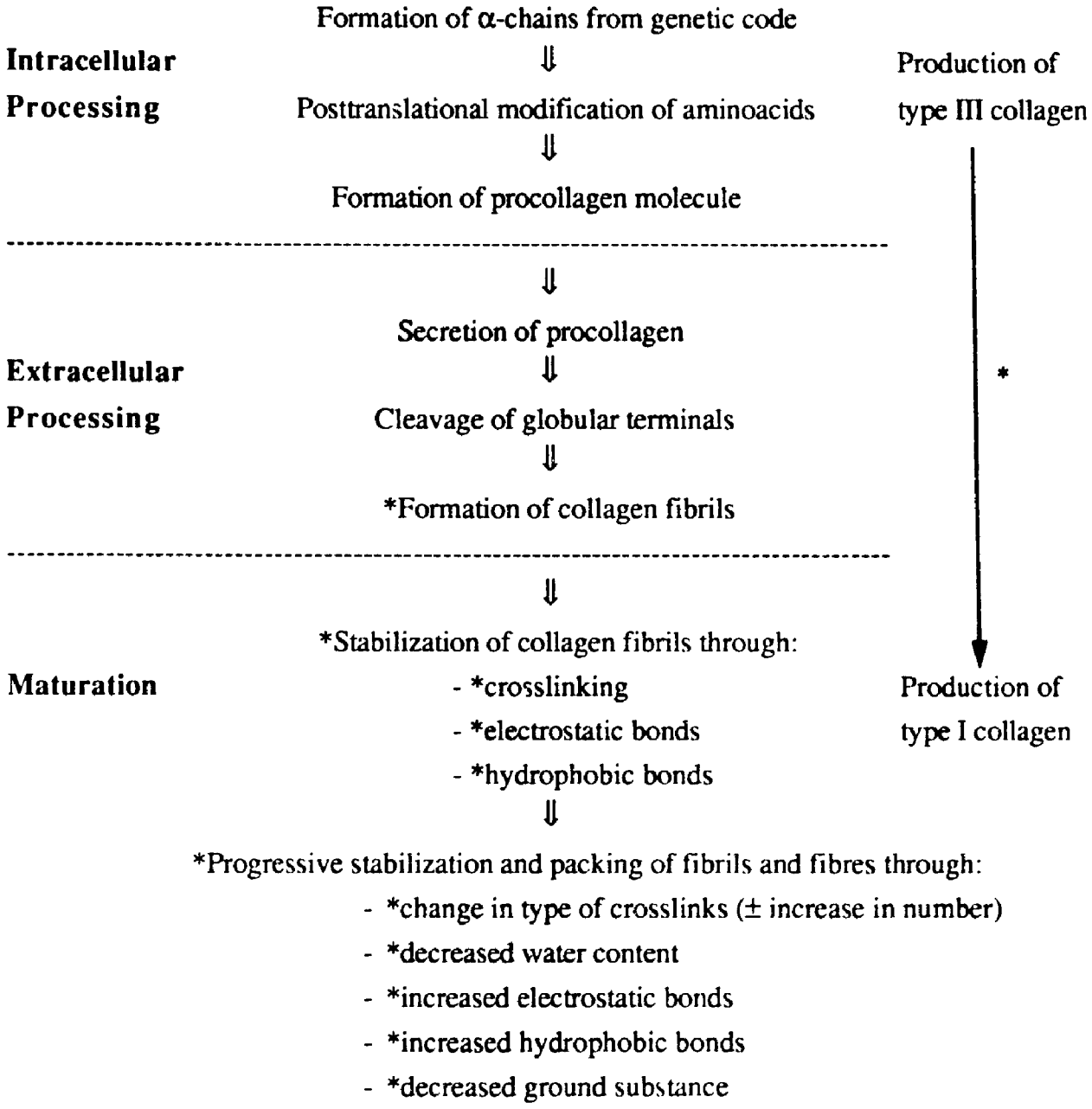

Figure 4.1: Steps in the formation and maturation of fibrotic collagen. The '*' denotes events that may increase the anisotropy of a fibrotic network.

where Γ is retardation, I_{pa} is luminance of the field with the polarizer and analyzer parallel, and I_{pe} is the intensity when the polarizer and analyzer are crossed. With the polarization-video microscopy system that I developed, extinction is effectively perfect. Thus

$$I = I_{pa} \sin^2(\Gamma/2) \qquad \text{(Eqn. 4)}$$

It can be seen that an increment in retardation will only produce an increase in the intensity of brightness if retardation lies between 0 and 180^{o}. Ideally, values should be well within these extremes, so that they are away from the "flat" portions of the curve. To determine if this was the case for collagen stained with picrosirius red, I measured both retardation and intensity of brightness of a series of sections of rat tail tendon. The tendon was dissected from a 300-gram male Sprague-Dawley rat after it had been sacrificed as part of an approved protocol (see Chapter 5). A 2-cm portion of the tendon was excised, fixed in 10% phosphate-buffered formalin, and strained in an Instron by 5%. Straining effectively removed the waviness of the fiber enhancing measurement of retardation. The tendon was embedded in paraffin wax and sectioned at 2, 4, 6, 8, and 10 μm thickness. Slides were stained with picrosirius red. Ten measurements of retardation (see Appendix for a description of this method) were made on each section. The intensity of brightness was determined from the digitized image as the median grey-level of the nonzero pixels. The range of retardation values was 40 - 105^{0} and the relation with brightness approximated the theoretical relation (Figure 4.2).

The relationship between the intensity of brightness and the orientation with respect to the polarization axes is described mathematically as:

$$I = 4\, I_{pa}\, \sin^2\theta \cos^2\theta \qquad \text{(Slayter 1971, p322)} \quad \text{(Eqn. 5)}$$

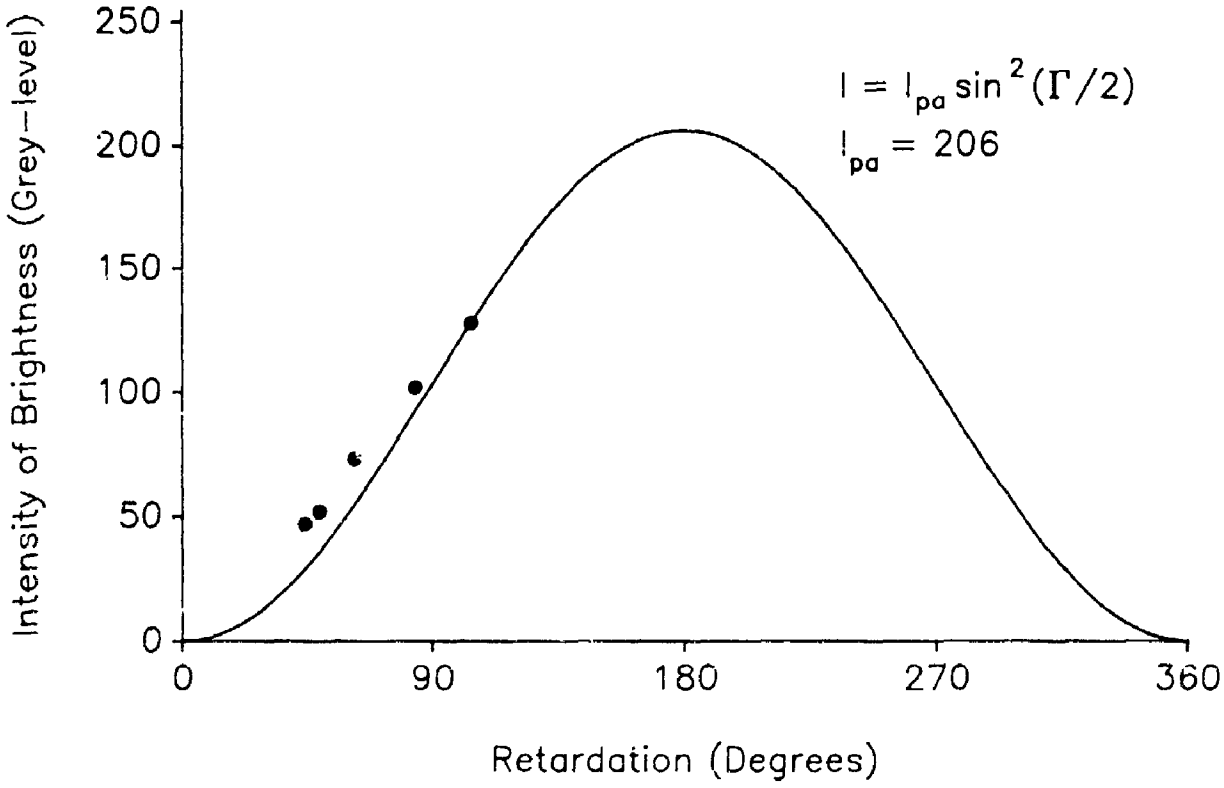

Figure 4.2: Relation between intensity of brightness (I) of rat tail tendon and retardation (Γ). The theoretical relation is superimposed on the data points. Intensity of brightness was measured as the median grey-level of the pixels depicting collagen. I_{pa} is the intensity of the field when the polarizer and analyzer are parallel, which for this study was grey-level 206.

where θ is the angle between the polarization azimuth of the incident light, and one of the two polarization planes of the specimen. (By convention it is the plane perpendicular to the optical axis of the specimen. For collagen, however, it is easier to consider the plane parallel to the optical axis since this is also parallel to the fiber's morphological axis.) Intensity of a fiber will be minimum (zero if extinction is perfect) when aligned parallel to one of the two planes of polarization ($\sin\theta$ or $\cos\theta = 0$). Brightness of a fiber will be maximum when oriented at 45° to the polars since in this case $I = 4\ I_{pa}\ (1/\sqrt{2})^2\ (1/\sqrt{2})^2 = I_{pa}$. Clearly, in order to compare the intensity of brightness of different specimens, collagen orientation with respect to the polars must be similar.

It should also be noted that fiber orientation with respect to the plane of the section will also affect collagen brightness. Whittaker (1986) has emphasized that retardation measurements will be lower if made on fibers that have been sectioned obliquely.

The dependence of brightness on the three-dimensional fiber orientation is pertinent to the assessment of the two types of fibrosis (replacement and interstitial) seen in the heart. In replacement fibrosis, collagen is deposited as a closely packed network with fibers running parallel to the long axis of the preexisting muscle (Whittaker 1989). Sectioning parallel to these fibers can easily be done and comparison of the brightness of various specimens can be made by aligning the fibers at an identical angle to the polars. Ideally, this would be at 45° since this would produce the maximum brightness and thereby increase the likelihood of detecting differences between samples.

In interstitial fibrosis the process is much more diffuse and a high degree of organization is generally not seen . Specimens therefore are more likely to be sectioned so that fiber orientation, with respect to the cutting plane and with respect to each other, is variable. Provided that the overall orientation approaches a random distribution, a comparison may still be made. However, one cannot make meaningful comparisons of the intensity of brightness between the two types of fibrosis.

In this chapter, I examine the relation between brightness and relative maturity of a network of replacement fibrosis as determined using the video-polarization apparatus. For this the collagen deposited in the canine heart, three and six weeks after myocardial infarction is studied. In the subsequent chapter, the relation between intensity of collagen brightness and fibrotic maturity is studied in a model of interstitial fibrosis.

4.3 Methods

The infarct zones of dog myocardium taken three weeks (n=3) and six weeks (n=3) following ligation of the left anterior descending coronary artery were studied. The surgery was performed by Dr. H Hammerman in Dr. Kloner's lab (Harper Hospital, Detroit, Michigan). Coronal sections of the left ventricular wall were fixed in formalin and embedded in paraffin. These were provided by Dr. P. Whittaker.

Tissue blocks were sectioned at 7 μm and stained with picrosirius red. The sections were cut perpendicular to the long axis of the ventricular chamber and the circumferential fibers that occupy the midmyocardial zone of the scar lay predominantly in the plane of the section. Collagen in the subendocardium was sectioned obliquely. The scar did not generally extend to the subepicardial layers (which is typically the case for experimental infarction in the canine heart (Jugdutt and Amy 1986)). For this study, only the midmyocardial fibers were analyzed.

After digitizing the image, the appropriate portion of the myocardium was demarcated using the area-of-interest program in the Jandel video analysis software (JAVA). The scar was systematically analyzed and a grey-level histogram was generated for each area. These histograms were then summed to create a single histogram and the overall median grey-level, excluding grey-level zero (noncollagenous material), was calculated. All measurements were made with the collagen aligned at 45° to the polarization axes.

In some sections, more than 50% of the pixels depicting collagen had a grey-level of 255, precluding an accurate determination of the median level of brightness. In these cases, illumination was reduced, by placing a neutral density filter in the light path. The resulting median grey-level was then converted to a value corresponding to the original light conditions by multiplying by a factor equal to the reduction in light intensity by the filter and adding the grey-level offset of the video system.

To avoid differences in collagen brightness due to variations in staining conditions, the median grey-level from three to four regions of the visceral pericardium was determined for each specimen . Thus,

$$\text{Relative brightness of fibrotic collagen} = \frac{\text{Median grey-level of infarct collagen}^{*}}{\text{Median grey-level of pericardial collagen}^{*}}$$

Collagen content was determined as the sum of all non-zero pixels divided by the area of myocardium studied.

The age of the infarct was not known during the measurements. Comparisons between the three- and six-week infarcts were made with an unpaired t-test.

4.4 Results

At three weeks, the midmyocardial region of the infarct consisted of a mixture of necrotic myocytes, blood vessels, and collagen. These fibers were loosely packed and with polarization microscopy appeared green or yellow-orange (Plate 4.1). In contrast, the sections of the six-week infarct territories consisted almost entirely of densely packed collagen that appeared yellow-orange (Plate 4.2).

---

* Corrected by the grey-level offset

Digitized, color-encoded images of the three- and six-week infarct zones are shown in Plates 4.3 and 4.4 with the corresponding grey-level histograms (Figures 4.3 and 4.4). Grey-level 0 is encoded by black, and grey-levels 1-255 by red to blue. For the 3-week specimen shown, the majority of collagen was depicted by pixels that were relatively less bright, with a median grey-level of 72. Just under 10 % of the total collagen was at maximal detectable brightness. In contrast, in the six-week specimen, the proportion of pixels at any given brightness was relatively uniform, or slightly increasing, up to the spike at 255 which represented 39 % of the total collagen area. The median grey-level in this case was 225. The average median brightness value, expressed in terms of median grey-level of pericardial collagen, was significantly greater at six weeks postocclusion than at three weeks following the infarction ($p<0.01$) (Figure 4.5). The area fraction of midmyocardial collagen was also significantly greater in the six-week sample ($p<0.02$) (Figure 4.5).

4.5 Discussion

The preliminary study of rat tail tendon indicated that the intensity of brightness of collagen can be ascertained, using the polarization-video microscopy technique, by characterizing the frequency distribution of grey-levels. I have used the median grey-level as the descriptor of this distribution given that it is generally not Gaussian. This measure approximated the predicted value of intensity of brightness based on the theoretical relation between brightness and retardation. Furthermore, for the specimen used, the data points fell within a near-linear portion of the sinusoidal relationship. Thus a biophysical property of collagen – optical anisotropy – is reflected by its brightness and may be readily assessed with this approach.

The data from the video analysis of dog myocardial infarcts suggests firstly that significant collagen deposition continues between three and six weeks. This is consistent

Plate 4.1: Midmyocardial section of the infarct territory of canine myocardium, 3 weeks after occlusion of the left anterior descending coronary artery. The collagen appears as green or yellow-orange fibres amongst a bed of necrotic myocytes which are nonbirefringent. Polar orientation is ⊗. Picrosirius red. Bar, 200 μm.

Plate 4.2 Midmyocardial section of a 6-week infarct. Compared to the 3-week specimen collagen fibres are thicker, more densely packed, and appear brighter. Polar orientation is ⊗. Picrosirius red. Bar, 200 μm.

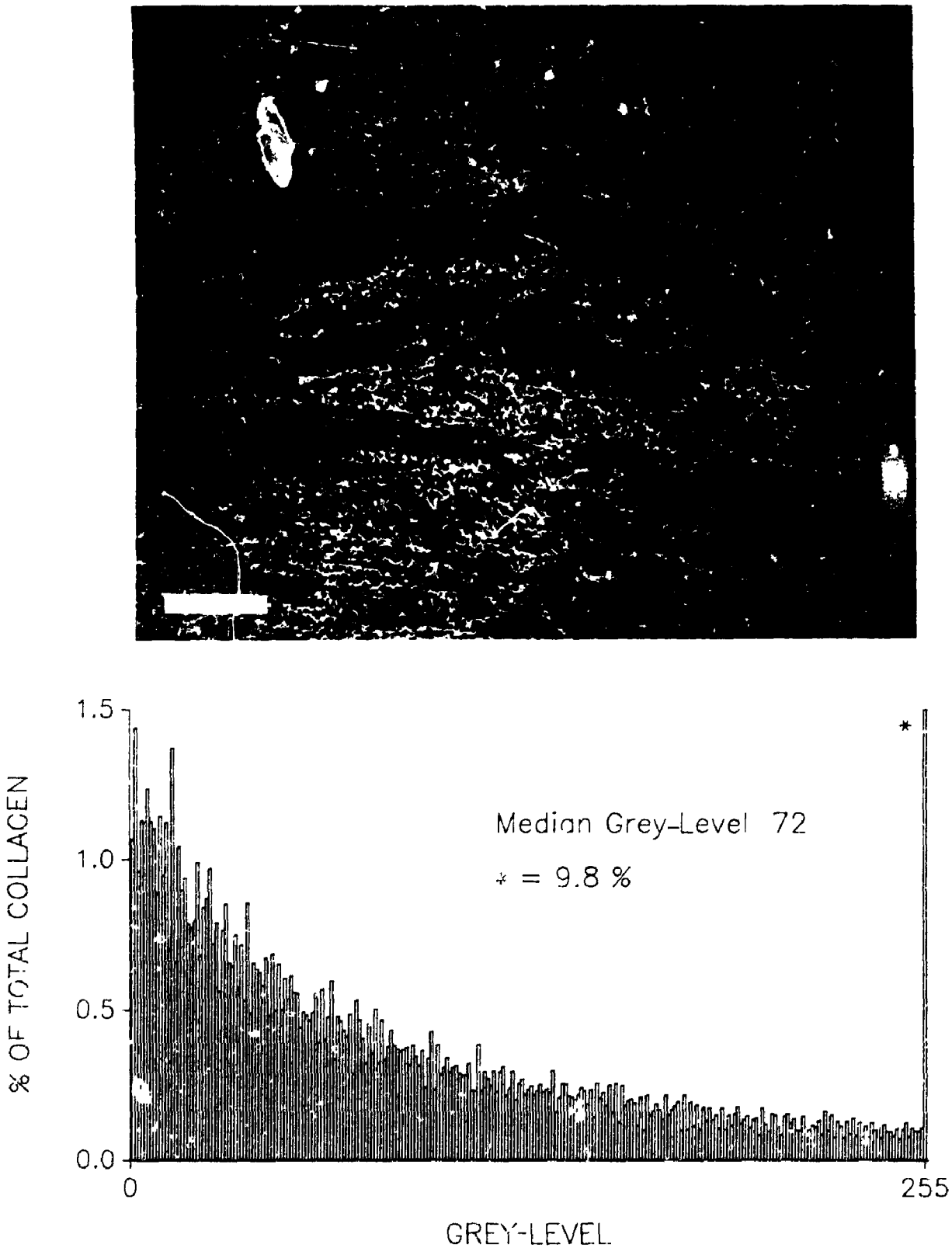

Plate 4.3: (Top panel) Digitized colour-encoded image of the section of the 3-week infarct shown in Plate 4.1. Bar, 100 μm. **Figure 4.3:** (Bottom panel) The corresponding grey-level histogram. The majority of fibres are of low pixel intensity.

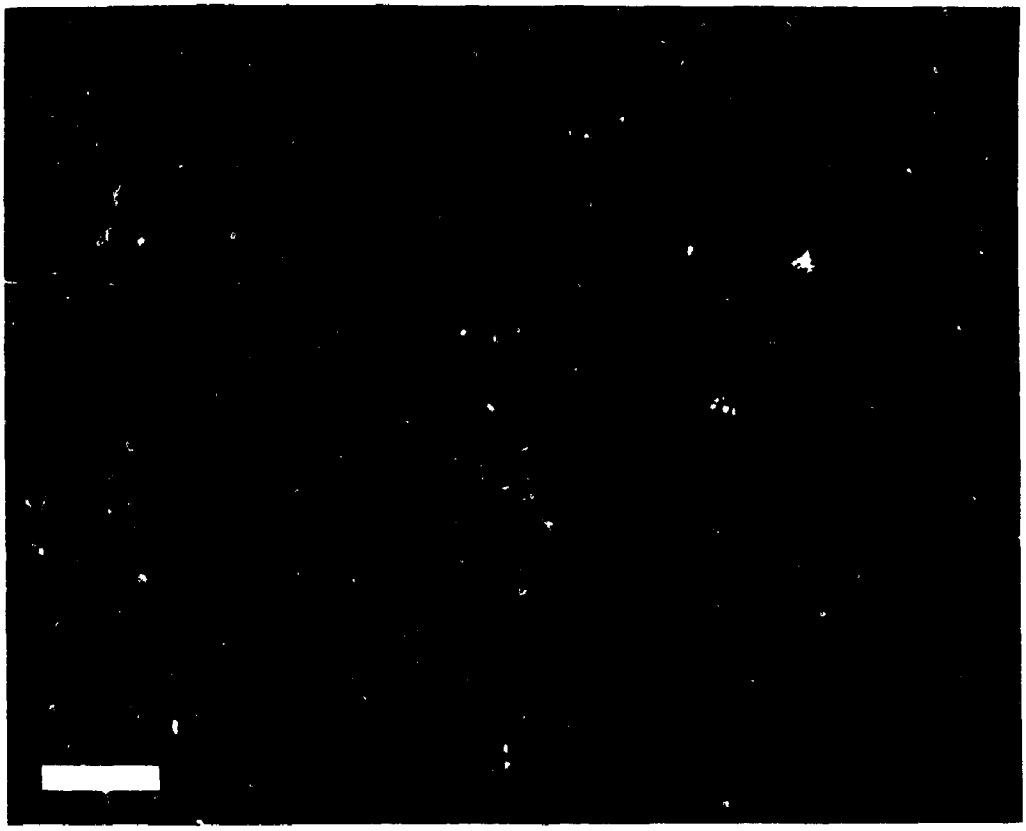

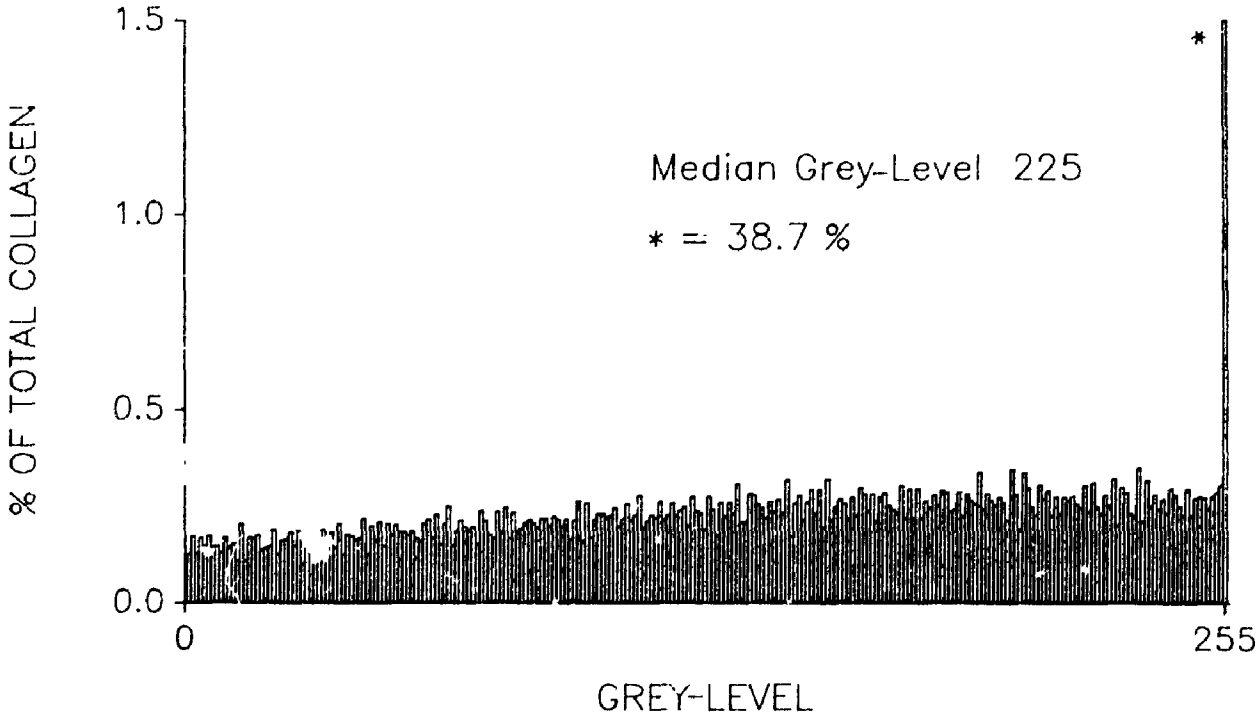

Plate 4.4: (Top panel) Digitized colour-encoded image of the section of the 6-week infarct shown in plate 4.2. Bar, 100 µm. **Figure 4.4:** (Bottom panel) The corresponding grey-level histogram. The distribution has shifted toward brighter fibres.

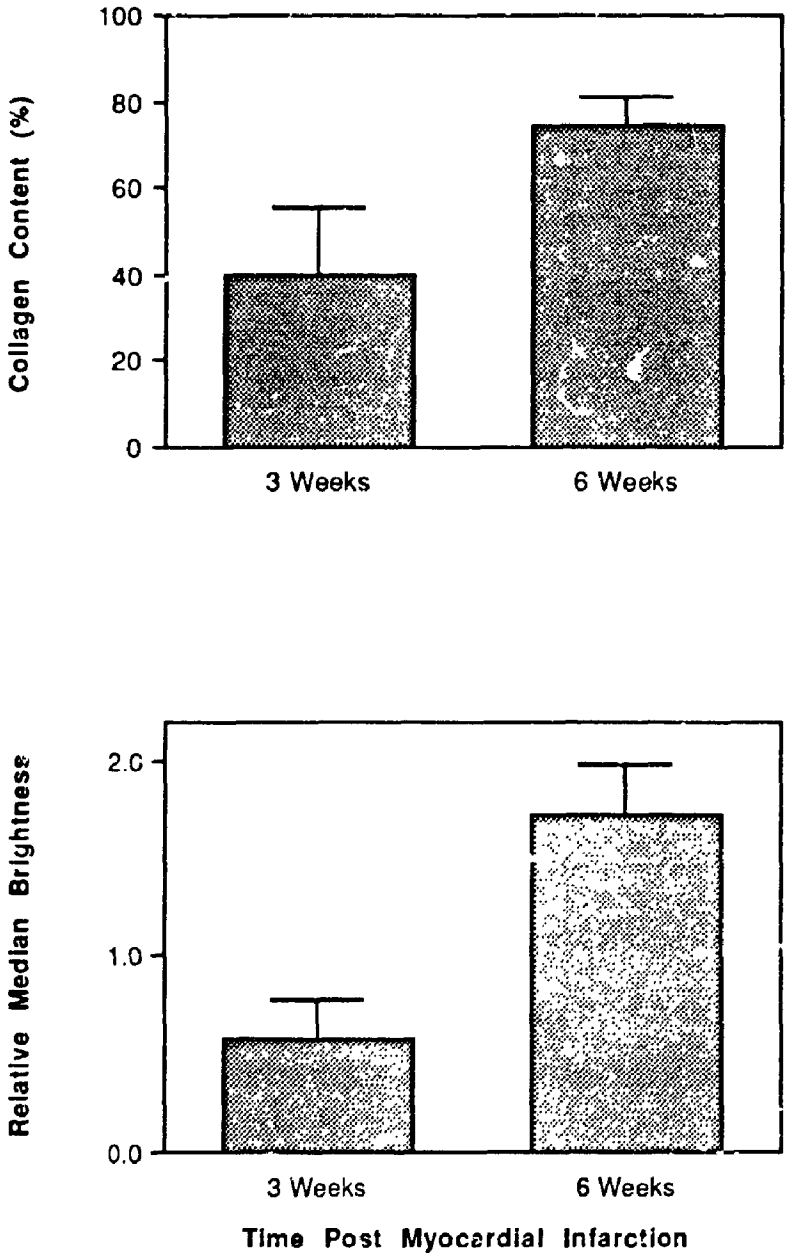

Figure 4.5: Content (top panel) and relative brightness (lower panel) of collagen in the midmyocardial region of canine myocardium, three (n=3) and six (n=3) weeks following occlusion of the left anterior descending coronary artery.

with the findings of Jugdutt and Amy (1986) who showed a progressive increase in canine infarct hydroxyproline up to six weeks. Healing in human infarcts may continue beyond 6 weeks (Mallory 1939).

Secondly, there were quantifiable differences in the intensity of brightness of collagen between the three-week and six-week infarcts. The brightness of collagen in the six-week scar was approximately three times that of the collagen in the three-week scar. Two types of changes occurring in the network may have accounted for this rise in brightness. First, packing of adjacent fibers could increase the amount of collagen present in the volume of tissue "beneath" a given pixel. This would increase retardation and thus the measured intensity of brightness.* Second, increased organization at the molecular and fibrillar level, e.g., through intermolecular crosslinking, may have contributed to the increased brightness. While these latter changes are well recognized (Kastelic and Bayer 1980), it cannot be said for certain that the video technique has detected them. This possibility is further explored in Chapter 5.

The ability to characterize an infarct in this manner could be of benefit when evaluating the efficacy of measures designed to enhance infarct healing. While no agents are presently in clinical use, there is evidence that increasing the rate of collagen deposition following a myocardial infarction may reduce morbidity and mortality. Rupture of the ventricular free wall occurs in 4-24 % of all fatal myocardial infarctions and is lower in patients with preexisting myocardial fibrosis (Bates et al 1977). In the rabbit, collagen synthetic activity has been identified within the first eight days after infarction and it has been suggested that a more rapid rate of deposition may decrease the rupture-related mortality rate (Lerman et al 1983).

Another important sequelae of myocardial infarction is early expansion of the infarct zone. This may adversely influence long term survival by altering the normal

---

* Variations in the proportion of the section thickness occupied by collagen may explain the wide range of collagen grey-levels associated with any one state of maturation.

geometry and loading conditions of the ventricle (Pfeffer et al 1988). Jugdutt and Amy (1986) have found in the dog model that much of the cavity dilatation occurs within the first seven days, prior to significant collagen deposition. Subsequent scarring may render these changes permanent and further alter ventricular topography through thinning and contraction of the infarct zone. A prompt deposition of collagen, with rapid maturation, (e.g. by the addition of cofactors) may protect the ventricle from progressive dilatation. This hypothesis remains to be tested however.

The present studies suggest that the polarization-video microscopy technique can characterize the intensity of brightness of collagen in a bed of replacement fibrosis and provide an index of maturity and activity of scar formation following acute myocardial infarction. It is therefore well suited to the evaluation of measures aimed at modifying the healing process following experimental myocardial infarction.

Chapter 5 Assessment of a Model of Interstitial Fibrosis

5.1 Introduction

Increased myocardial collagen may be present in a number of pathologic conditions besides myocardial infarction. This includes dilated and nondilated cardiomyopathies (Olsen 1975, Dick et al 1982, Tanaka et al 1986), senescent myocardium (Lenkiewicz et al 1972, Tomanek et al 1972) and ventricles that have been subjected to sustained pressure overload from hypertension (Weber et al 1987, Oldershaw et al 1980, Pearlman et al 1982) or aortic valve stenosis (Caspari et al 1977, Krayenbuehl et al 1988). The term interstitial fibrosis is generally used to describe the increased collagen seen in these conditions, since it is typically found coursing between groups of myocytes or between individual myocytes. Scattered microscopic foci of scar tissue may also be referred to as interstitial fibrosis even though they may have "replaced" focal myocyte necrosis.

While the precise arrangement of collagen fibers in interstitial fibrosis may depend on the etiology, collagen fiber orientation typically is variable and at times may form a complex mesh (Pick et al 1989). Thus in a random section, fibers will generally be oriented in various directions. This is pertinent to study by polarized light particularly when comparing fiber brightness between specimens. Provided that a large enough area of the tissue is analyzed the variable effect of orientation on brightness may "average out". However in the absence of parallel fibers that can be oriented at 45° to the polars, the magnitude of brightness of the network will be less than maximum. Brightness may further be reduced if fibers lie obliquely in the section since retardation will be lower. It may therefore be difficult to detect differences in brightness between samples in which collagen birefringence is different.

To determine if the polarization-video microscopy method could detect age-related differences in diffusely oriented fibrotic collagen, I studied the scar formed by trauma to the surface of rat gracilis muscle.

5.2 Methods

After preliminary study, I found that a superficial injury to the gracilis muscle of the rat produced a scar in which the collagen fibers were diffusely oriented. With time, progressive alignment of the fibers was not a prominent feature as occurs with tendon repair (Mello et al 1975, Williams et al 1984). This was therefore chosen as the method of fibrosis induction.

The surgical procedure was approved by the Animal Ethics Committee at the University of Western Ontario, London, Canada. Twelve, male Sprague-Dawley rats weighing 250 grams, were anesthetized with sodium pentobarbitol (40 mg/kg). A 1.5 cm incision to the skin over the medial aspect of the left thigh was made exposing the gracilis muscle. With the use of an operating microscope (American Optical) a partial thickness elliptical incision of the gracilis muscle was made using iridectomy scissors. The skin was then oversewn with absorbable sutures. Of the 12 animals studied, two were sacrificed on each of 5, 9, 14, 21, 42, and 63 days after the injury and the healing tissue was recovered. During this procedure, the loose connective tissue immediately beneath the skin was carefully dissected away until the underlying gracilis muscle, with a zone of superficial scarring could be identified. This portion of the muscle was freed from the adjacent tissues, excised, and immediately placed in a solution of 10% neutral buffered formalin.

Specimens were fixed in formalin for a minimum of 48 hours, cleared with chloroform, and embedded in paraffin. Sections were cut perpendicular to the length of the muscle at 7-μm thickness and stained with picrosirius red. Sections were evaluated

with the polarization-video microscopy equipment and 8 to 10 images were digitized and analyzed for each specimen. Collagen content was determined by the area-fraction of nonzero pixels and the median grey-level of these pixels served as the index of collagen brightness. To avoid variations in collagen brightness due to different staining conditions, the fascial covering of the muscle opposite the scarred region served as control tissue. This also served to normalize changes due to aging of the rat as opposed to aging of the wound.

All collagen measurements were made without knowledge of the age of the injury. The results are expressed as mean ± standard deviation. Comparison between groups were done using one-way analysis of variance and Scheffés multiple range test.

5.3 Results

Qualitatively, the injured regions at five days consisted of granulation tissue with abundant blood vessels, thrombi, and a loosely packed network of collagen. With polarization microscopy, the fibers appeared green or orange-red with a diameter of approximately 1-3 μm (Plate 5.1). With time, collagen became more predominant with thicker fibers (up to 14 μm) that were densely packed and appeared orange-red under crossed polars (Plate 5.2). This process appeared to start in the region immediately adjacent to the muscle.

By five days, collagen occupied 16±2 % of the granulation tissue. This increased significantly by days 14 and 21 after which a plateau was evident. This sigmoidal response is depicted in Figure 5.1.

Digitized, color-encoded images of typical collagen networks 5 and 63 days after injury and the corresponding grey-level histograms are depicted in Plates 5.4 and 5.5 and Figures 5.2 and 5.3 respectively. Of the colored regions, the blue portion, which corresponds to higher grey-levels, increased with time. This shift in

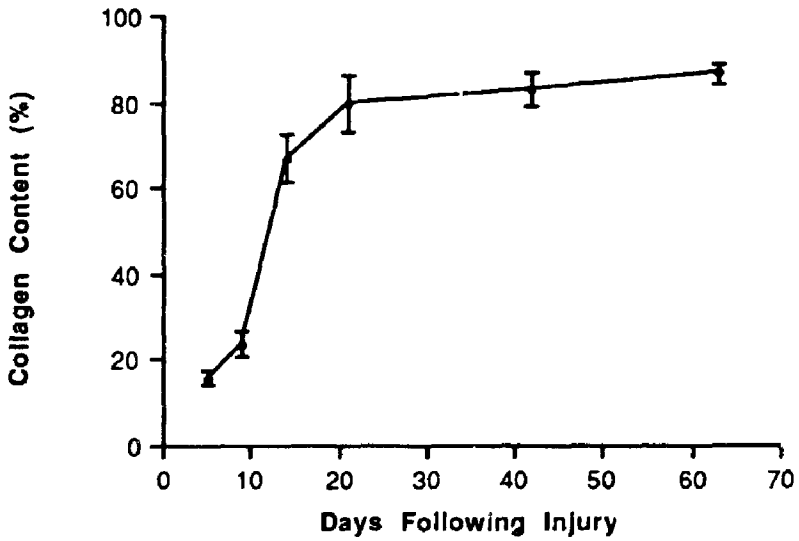

Figure 5.1: Time-course of collagen content of the scar forming on the surface of injured gracilis muscle.

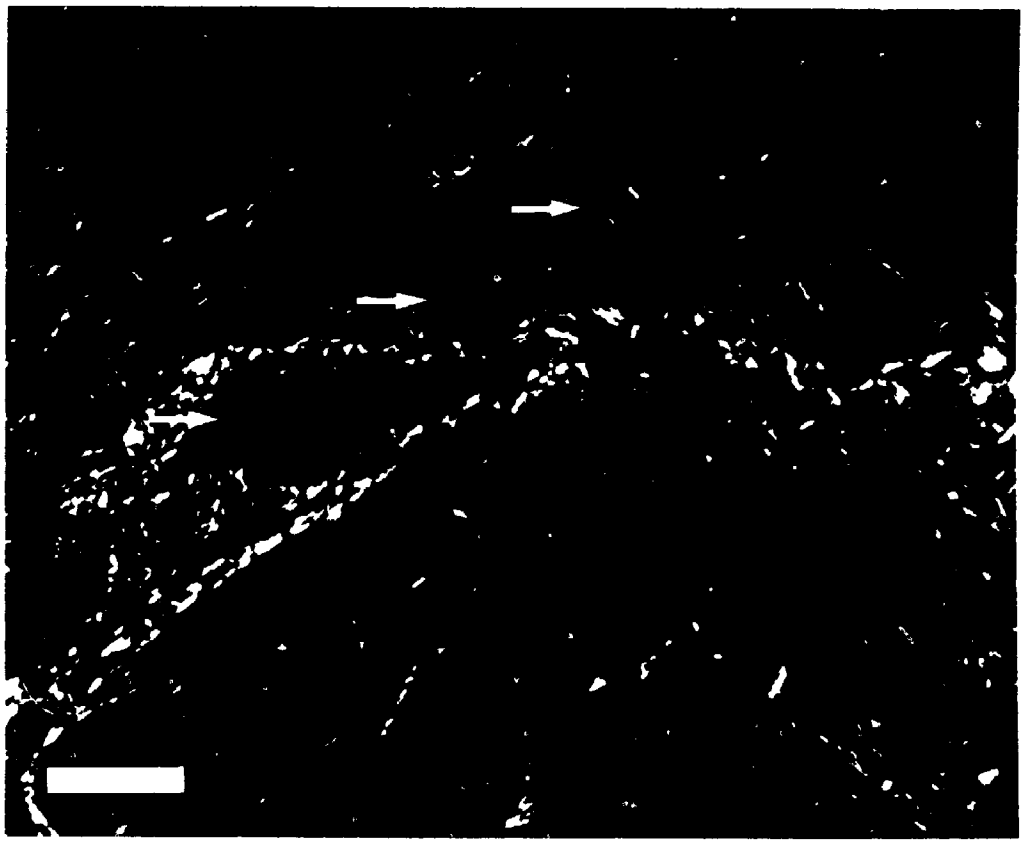

Plate 5.1: Surface of rat gracilis muscle 5 days after partial thickness injury There is a loose network of fibrotic collagen appearing eitner green or orange-red. Blood vessels are abundant (arrows) but appear dark since the luminal contents are nonbirefringent. Polar orientation is ⊗. Picrosirius red. Bar, 75μm.

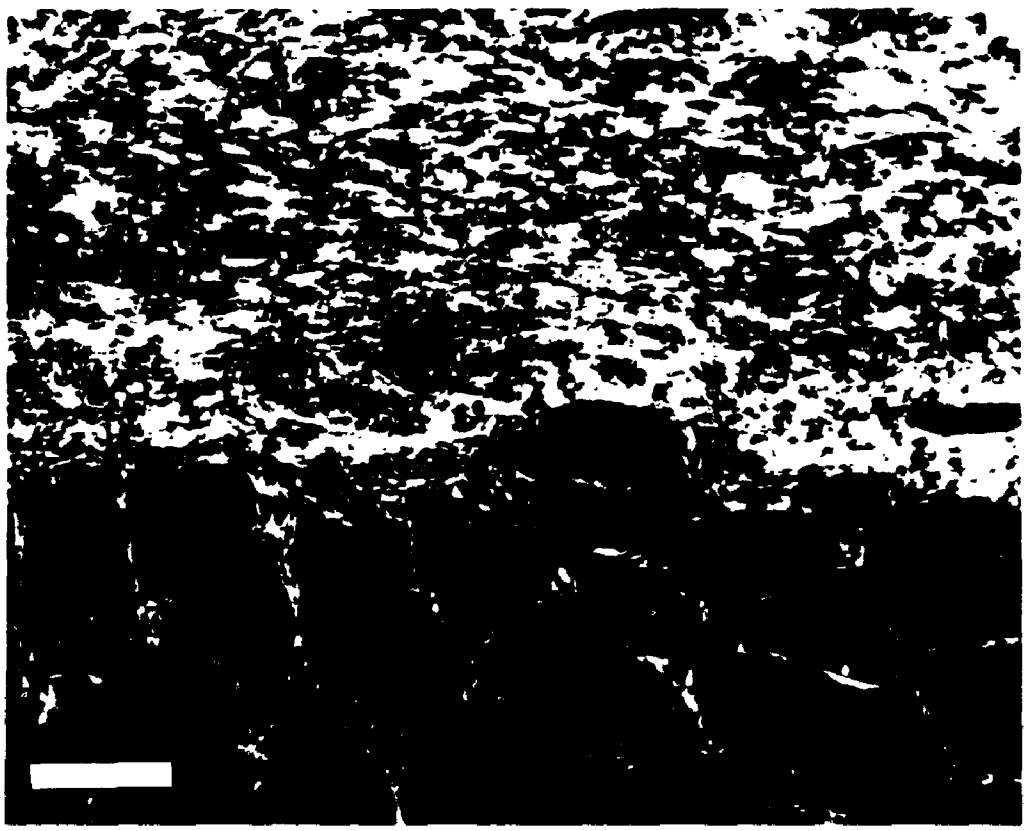

Plate 5.2: Surface of rat gracilis muscle 63 days after superficial injury. The collagen fibers have become progressively thicker, more densely packed, and generally appear brighter. Exposure time was 92% of that for plate 5.1. Polar orientation is ⊗. Picrosirius red. Bar, 75μm.

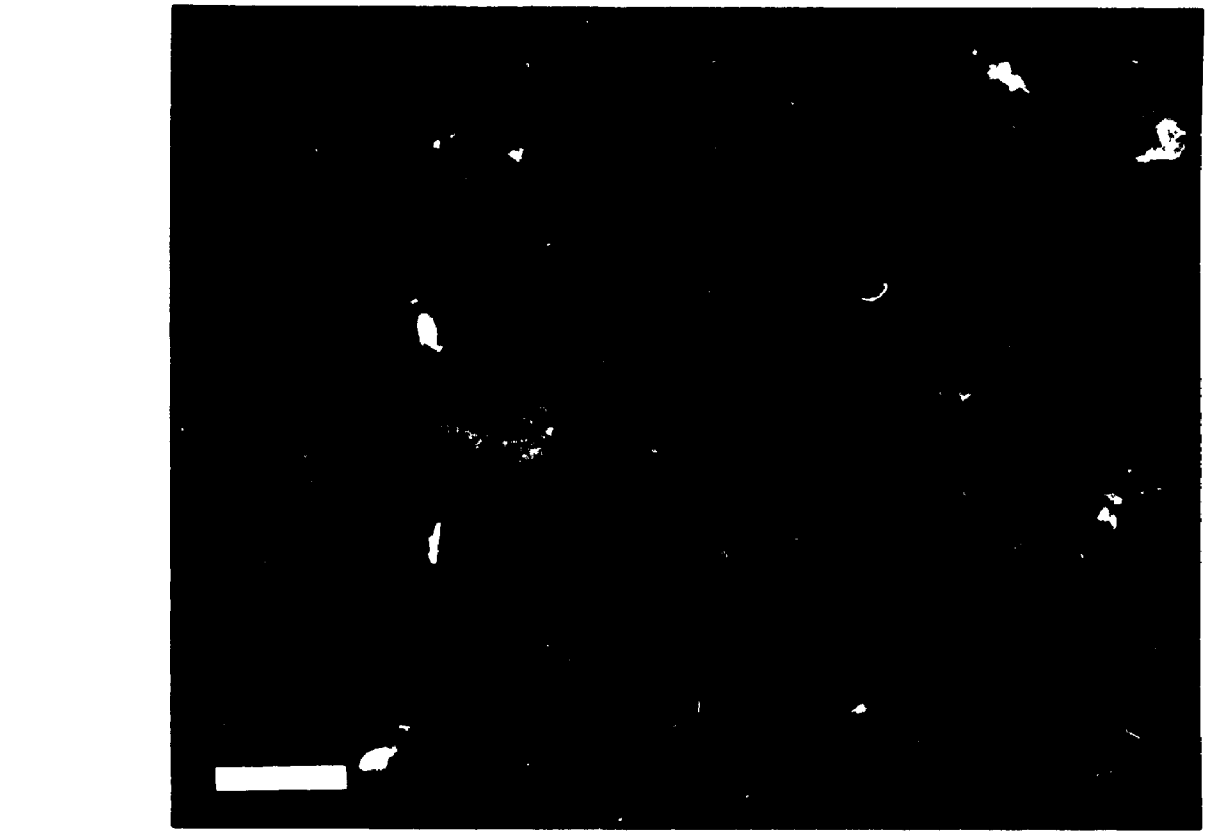

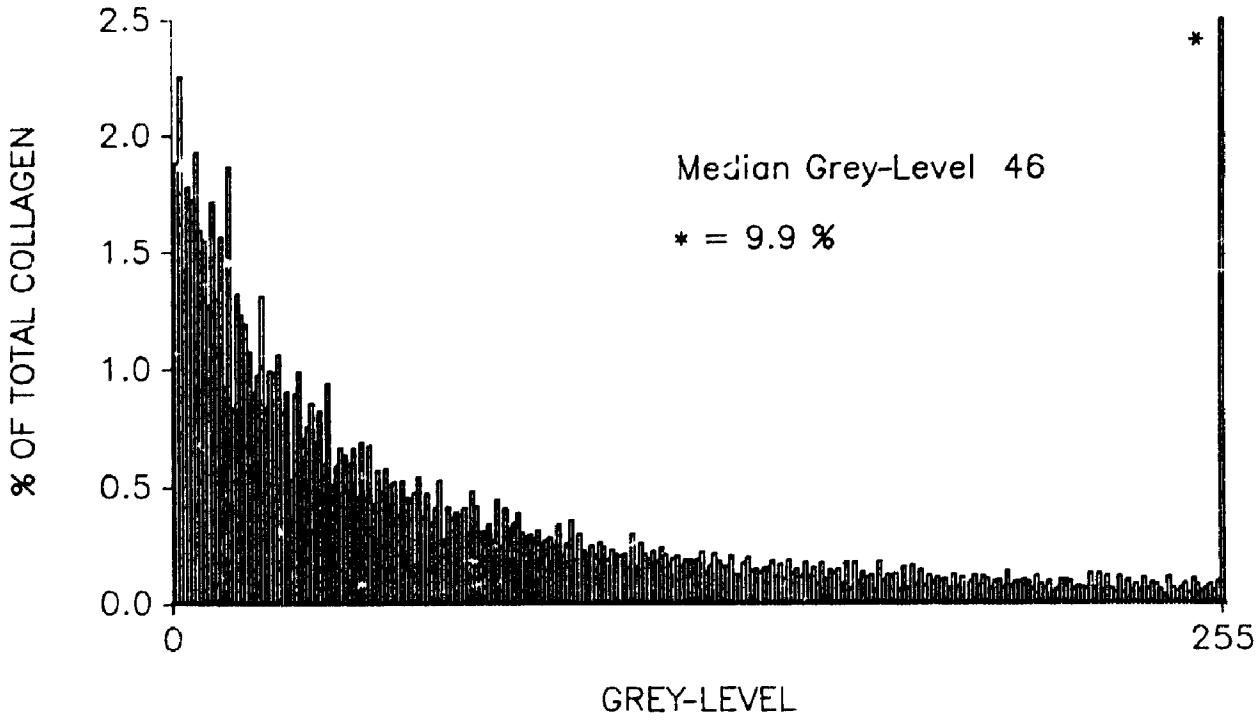

Plate 5.3: (Top panel) Colour-encoded image of healing rat muscle 5 days after injury. Bar, 100 μm. **Figure 5.2:** (Bottom panel) The corresponding grey-level histogram.

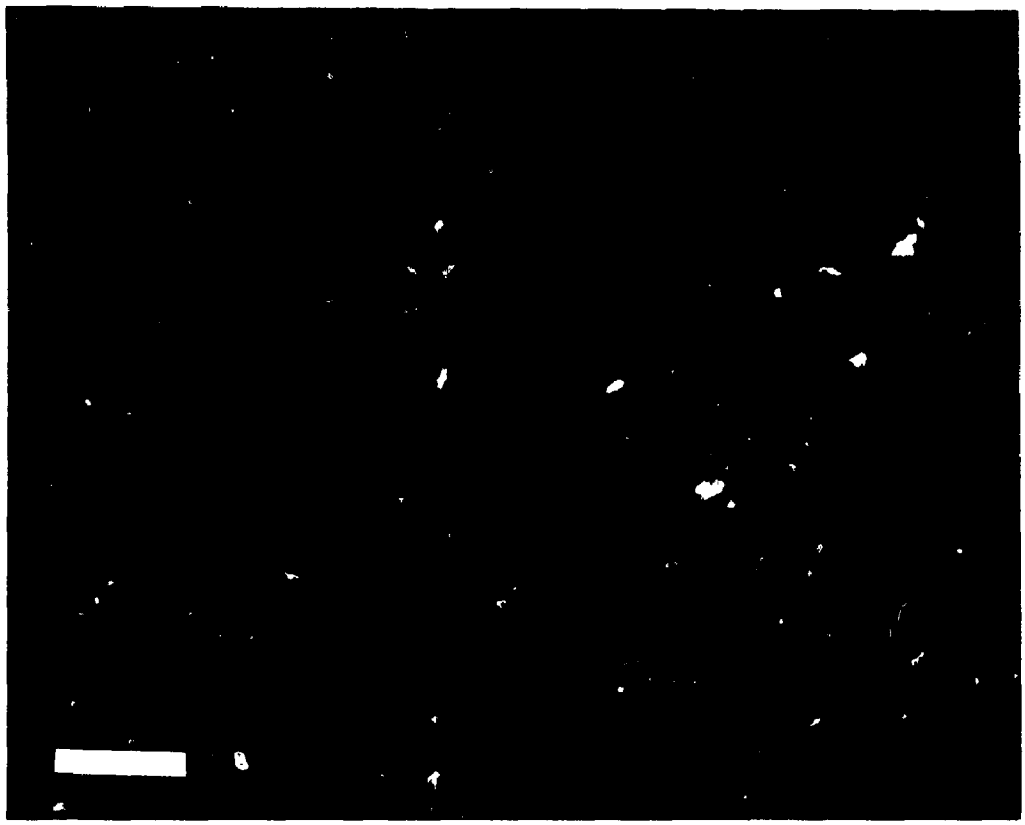

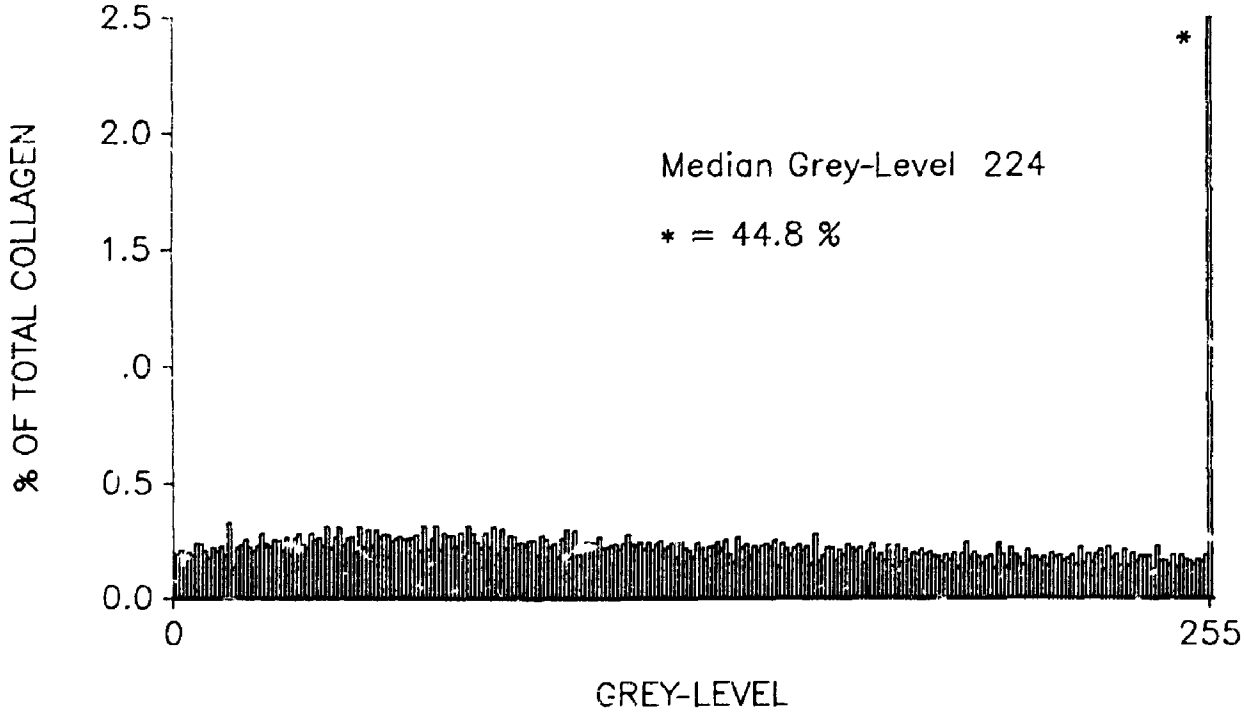

Plate 5.4: (Top panel) Colour-encoded image of healing rat muscle 63 days after injury. Bar 100µm. **Figure 5.3:** (Bottom panel) The corresponding grey-level histogram.

overall brightness was also evident from the grey-level histograms. For the 5-day specimen shown, the majority of collagen was depicted by pixels that were relatively less bright with a median grey-level of 46. Just under 10% of the collagen was at maximal detectable brightness. In contrast, in the 63 day specimen, the proportion of pixels at any given brightness was relatively uniform up to the spike at 255 which represented 45% of the total collagen area. The median grey-level in this case was 224. The profile for the scars of intermediate ages (9-42 days) had characteristics between these extremes.

Figure 5.4 shows the average median brightness value for fibrotic collagen expressed in terms of the median grey-level of fascial collagen and corrected for the grey-level offset of the video system. Brightness progressively increased throughout the study. Although only two rats were studied for each time period, the coefficient of variation was relatively small (14.4±11.1%) and statistical differences were seen between all time periods except days 5 and 9, 14 and 21, 21 and 42.

5.4 Discussion

This study shows that in fibrotic networks with variably oriented collagen fibers, time-dependent differences may still be detected using a histologic technique. While fiber alignment may be an important component of scar maturation in some instances, I chose a model of fibrosis where this, at least subjectively, was not a major component. In this way the model was qualitatively similar to interstitial myocardial fibrosis. Muscle was chosen as the tissue substrate, as opposed to skin or tendon, so that degenerating, pre-existing collagen was not present in the scar. It was important to avoid degraded collagen since its reduced birefringence would decrease the overall intensity of collagen brightness independent of fibrogenesis.

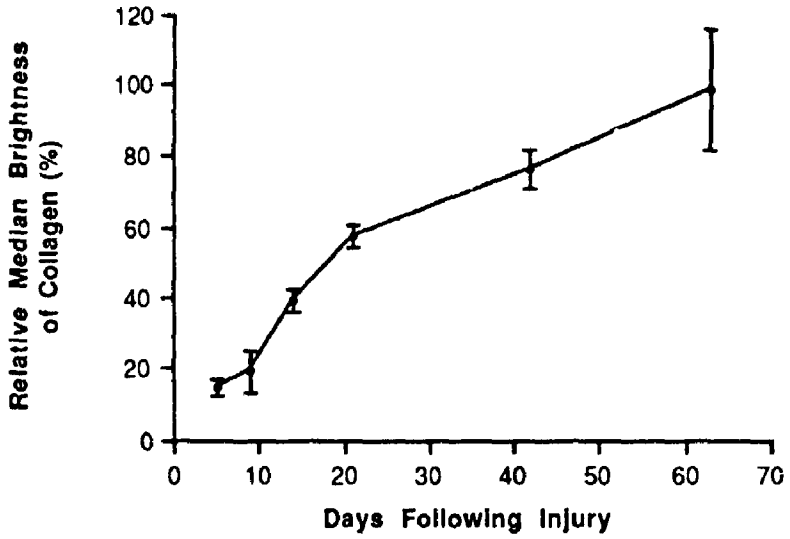

Figure 5.4: Time-course of the brightness of fibrotic collagen deposited on the surface of injured rat gracilis muscle. Brightness, initially less than 20 % of that of fascial collagen, increased progressively throughout the study period.

Interstitial myocardial fibrosis has been produced in experimental animals by inducing hypertension (Abrahams et al 1987, Kozlovskis et al 1987, Doering et al 1988) and following isoproterenol infusion (Jalil et al 1989, Pick et al 1989). While these methods are clearly more specific to the heart, the techniques are more involved and the precise time of the tissue insult causing fibrosis may be variable throughout the myocardium. This was not be the case for the relatively straightforward method used in this study.

In the fibrosis model employed, collagen content had plateaued by 21 days. This is consistent with previously reported findings of wound healing in rat skin (Madden and Peacock 1968, Cohen et al 1979). In contrast, the median intensity of brightness rose throughout the 63-day period. As discussed in Chapter 4, increased fiber packing likely contributed to this rise. However, by 21 days packing appeared complete evidenced by the plateau in the area fraction of collagen. The fact that collagen brightness continued to rise would support the suggestion that molecular changes within the collagen fibrils were being detected.

Structural reorganization after the initial phase of collagen deposition may be inferred from studies of mechanical function of healing wounds. Levinson et al (1965) have shown that the tensile strength of rat skin wounds does not reach a maximum until approximately 90 days after injury. The ability to quantitatively detect histologic changes associated with, and likely contributing to, the sustained augmentation of mechanical properties has here-to-fore not been possible.

For this study, I chose to evaluate the optical properties of all collagen fibers together within a given section. However, it would also be possible to assess regional differences within a tissue section. In this way, the observer could identify local areas with relatively less bright fibers amongst a bed of brighter, older fibers suggesting that active fibrosis was still occurring. Such an assessment would not be possible with biochemical techniques requiring tissue homogenization.

In summary, the changing birefringence of fibrotic collagen has been exploited to quantitatively assess collagen deposition and maturation following tissue injury. In the model used, collagen alignment was not a prominent feature. The technique might therefore be used to study the activity of interstitial fibrosis in patients with cardiac disease.

Chapter 6 Fibrosis in the Transplanted Heart and its Relation to Donor Ischemic Time

6.1 Introduction

Cardiac transplantation has become an important therapeutic alternative for patients with end-stage heart disease. Recipients of cardiac allografts achieve a level of comfort and quality of life much superior to their pretransplant condition (Copeland 1988). Yet while their exercise capacity is relatively good (McLaughlin 1978, Savin et al 1982) it is not entirely normal (Kavanaugh et al 1987, Pickering et al 1988) and there are several reports of impaired diastolic function of the transplanted heart (Humen et al 1984, Greenburg et al 1985, Frist et al 1987, Young et al 1987, Pflugfelder 1988). Recently, increased myocardial stiffness has been demonstrated after 1 year and found to be related to the length of time in which the donor heart was being transported, i.e., the ischemic time (Hausdorf et al 1989). This suggests that myocardial scarring may be a functionally important sequela of prolonged ischemic times. Yet, with the dramatic increase in frequency of cardiac transplantation (Fragomeni and Kaye 1988), reliance on off-site, long distance organ procurements is expected to increase (Copeland 1988).

It would therefore be useful to characterize the nature of the relationship between myocardial fibrosis and the ischemic time of the donor heart. Since endomyocardial biopsy samples are routinely obtained from transplant recipients, they can provide an excellent source of tissue for such an evaluation. Present methods for quantifying fibrosis in biopsy samples, however, are limited, either by unacceptable interobserver variability (Shanes et al 1986) or impracticality. Having established that the collagen videodensitometry system can accurately measure collagen content in biopsy specimens

(chapter 3), I set out to investigate the relation between cardiac fibrosis and ischemic time, in a consecutive series of heart transplant recipients.*

6.2 Methods

From a consecutive series of 40 orthotopic heart transplant recipients, 36 patients from whom at least 3 myocardial biopsies were available for analysis were studied. These patients were treated and followed at University Hospital, London, Canada. The mean donor age was 26 ± 11 years.

Graft excision was performed based on the technique of Shumway et al (1966) Twenty-six (72 %) of the donors required inotropic support prior to graft harvesting. The cardioplegia solution consisted of Ringer's lactate with dexamethasone (20 mg/l), heparin (3200 units/l), dextrose (25 g/l), regular insulin (10 units/l), and supplemented with sodium bicarbonate (3.6 mmol/l) and potassium chloride (20 mmol/l). The donor hearts were wrapped in sterile towels, placed in a plastic bag and immersed in an iced saline solution. During long distance transport, temperature was continuously monitored and maintained between 4 and 6°C. The total ischemic time was defined as the time from clamping of the donor aorta during harvesting to unclamping of the recipient aorta following aortic anastomosis.

Right heart hemodynamics using a Swan-Ganz thermodilution catheter were obtained one week following transplantation for the purpose of this and other ongoing studies at University Hospital. This was done by either W.J. Kostuk, P.W. Pflugfelder, or myself. On the same occasion, multiple right ventricular endomyocardial biopsy samples were taken using a Stanford-Caves bioptome. This set of biopsies was chosen for study as they were the initial biopsy samples for all patients thereby

* This work forms part of a publication (Pickering and Boughner, 1990). Permission to reproduce the table, figures, and portions of the text has been granted by the publisher.

eliminating the possibility of scarring from previous biopsy procedures and minimizing the likelihood of rejection-related fibrosis. Specimens were immediately fixed in 10% neutral buffered formalin, embedded as a single paraffin block, and sectioned at 5-μm thickness. Following the routine at University Hospital, slides were stained with hematoxylin and eosin, methyl-green pyronine, and Masson's trichrome. A diagnosis of rejection was made according to the criteria of Billingham (1981). For the purpose of this study, a slide adjacent to the hematoxylin and eosin-stained slide was stained with picrosirius red. This was done in 2 batches with concomitant staining of a section of rat tail tendon serving as a control tissue. When illuminated with polarized light, the median grey-levels of the digitized image of the tendons were identical and it was inferred that staining conditions were equal for both sets of biopsies.

The collagen content for each biopsy was determined by videodensitometry without knowledge of the corresponding ischemic time. The endocardium was carefully excluded from the analyzed field as were blood vessels and perivascular tissue. To give proportional weight to biopsy samples containing relatively more myocardium, the collagen estimate for each patient is expressed as the total collagen content for all biopsies divided by the total area of myocardium analyzed.

Histologic evidence for ischemic myocyte damage was sought based on focal myocytolysis in the absence of lymphocytic infiltration, with or without contraction bands. To assist in the early recognition of ischemic changes, the sections stained with hematoxylin and eosin were examined under polarized light for a loss of muscle birefringence (visibility) and for contraction bands which appear bright under these conditions. The presence of contraction bands alone was not considered sufficient to diagnose ischemic damage (Adioman et al 1978).

Seven autopsy hearts from patients free of cardiac disease were studied to ascertain the normal collagen content of the right ventricle. The mean age of the patients at the time of death was 28 ± 7 years. The cause of death was motor vehicle accident in

3, drug overdose in 2, chronic active hepatitis in 1, and lymphoma in another. Using a similar bioptome to that employed in the transplant patients, 3-4 endomyocardial biopsies from the right interventricular septum were taken from each heart, sectioned, and stained with picrosirius red. Staining conditions comparable to those of the transplant heart biopsy samples were verified using the rat tail tendon control tissue. The collagen estimate for each biopsy was made by videodensitometry.

6.3 Statistics

Means are presented ± 1 standard deviation. Ischemic times were analyzed in three categories: 0 120 minutes, 121 - 240 minutes, and > 240 minutes. Comparison between groups were done using one-way analysis of variance and Neuman-Keul's multiple range test. Noncontinuous variables were evaluated by contingency table analysis. Relations between the two methods of quantifying collagen, collagen content and ischemic time, and hemodynamics and collagen content were tested by linear regression analysis.

6.4 Results

From the seven normal autopsy hearts a total of 23 biopsies were taken (3.3 ± 0.5 biopsies/heart). The area of myocardium analyzed per biopsy was 1.9 ± 0.7 mm^2. The myocardial collagen content was 2.9 ± 0.6%.

From the 36 transplant recipients biopsy specimens were obtained 7.7 ± 1.6 (range 5 - 10) days after surgery. One hundred and fifteen biopsy specimens were evaluated (3.2 ± 0.4 fragments per patient), with the average area of myocardium analyzed per biopsy of 1.2 ± 0.6 mm^2. The mean collagen content was 4.7 ± 1.9 % (range 1.5 - 9.9 %) and was significantly greater than that of the control hearts (p =

0.02). Increased collagen typically appeared as focal patches of fibrosis that were best visualized with polarization microscopy (Plate 6.1).

Total allograft ischemic time was between 0 - 120 minutes in 12 patients, between 121 - 239 minutes in 14, and >240 minutes in 10. The age of the hearts and the proportion of donors requiring inotropic support were not different between groups (Table 6.1). Biopsy samples from hearts with the longest ischemic times (> 240 minutes) had significantly more myocardial collagen than those in the other groups ($p < 0.05$). Biopsy samples from hearts with an intermediate ischemic time (121-240 minutes) were more fibrotic than those from normal autopsy hearts ($p < 0.05$). Regression analysis revealed a linear correlation between myocardial collagen content and ischemic time ($r = 0.60$, $p < 0.001$) (Figure 6.1). There was no association between myocardial collagen and donor age. ($r = - 0.41$).

The mean right atrial pressure, pulmonary artery wedge pressure, and cardiac output were 9.0 ± 5.0 mm Hg, 14.9 ± 4.7 mm Hg, and 5.5 ± 1.0 l/min, respectively. Neither the pulmonary wedge pressure nor the cardiac output correlated with the collagen content ($r = 0.01$, $r = 0.04$, respectively) A trend was observed between the right atrial pressure and the collagen content although this did not attain statistical significance ($r = 0.18$, $p = 0.07$).

Myocyte necrosis was seen in biopsy specimens from eight patients. The mean ischemic time for this group was 244 ± 66 minutes and the collagen content was 5.7 ± 1.5 %. Damaged myocytes characteristically revealed reduced or absent birefringence (Plates 6.2, 6.3). Bright contraction bands were readily apparent at the periphery of the necrotic regions (Plate 6.3), although they were also commonly seen in biopsy samples without myocytolysis. In one patient a lymphocytic infiltrate with pyroninophilia (indicating messenger ribonucleic acid synthesis in activated lymphocytes) was associated with the myocytolysis. This was the only patient in whom rejection was identified.

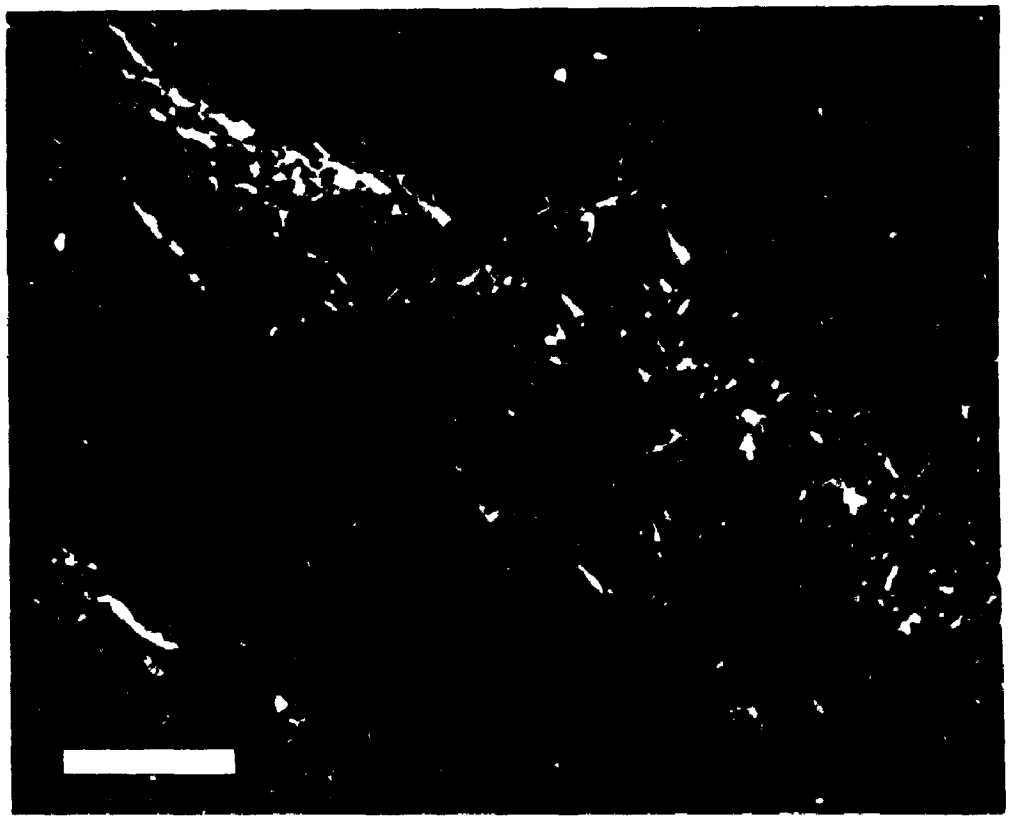

Plate 6.1: Polarization microscopy image of section of a biopsy sample taken 10 days after transplantation. The ischemic time for this allograft was 292 minutes. The bright yellow and green fibres depict a focal area of fibrosis. Bar, 50 μm. Polar orientation is ⊕ (Reproduced by permission of the American Heart Association)

	Normal	Transplant		
		Ischemic Time (min)		
	n=7	0-120 n=12	121-240 n=14	>240 n=10
Ischemic time (min)	-	96 ± 15	193 ± 29	295 ± 36
Age (yr)	28 ± 7	32 ± 14	23 ± 9	22 ± 5
Patients on inotropes	-	9	11	7
Collagen content (%)	2.9 ± 0.6	3.4 ± 1.3	4.4 ± 1.2*	6.7 ± 1.7†
Patients with myocyte necrosis	-	1	3	4

* $p<.05$ vs normal † $p<.05$ vs normal, 20, 121-240

Table 6.1: Characteristics of normal and transplanted hearts.

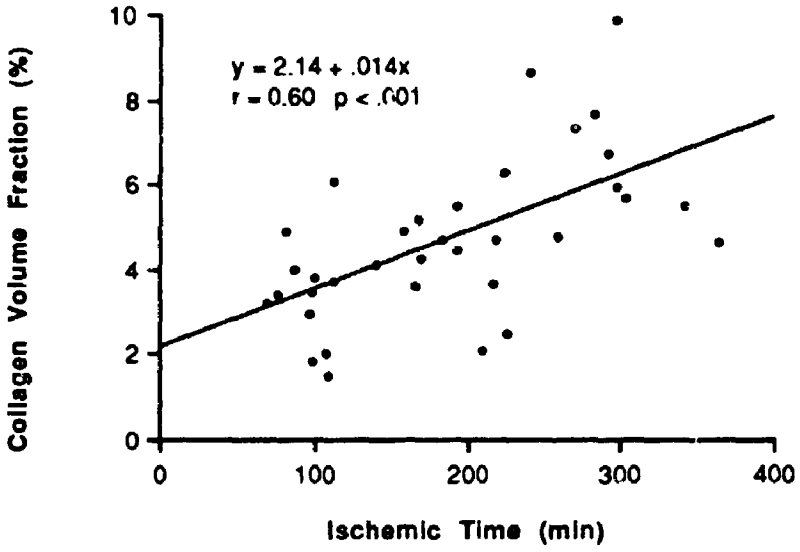

Figure 6.1: Association between total allograft ischemic time and myocardial collagen content of biopsy samples taken 5-10 days posttransplantation. One patient with an ischemic time of 225 minutes and a collagen content of 6.3% also had acute rejection.

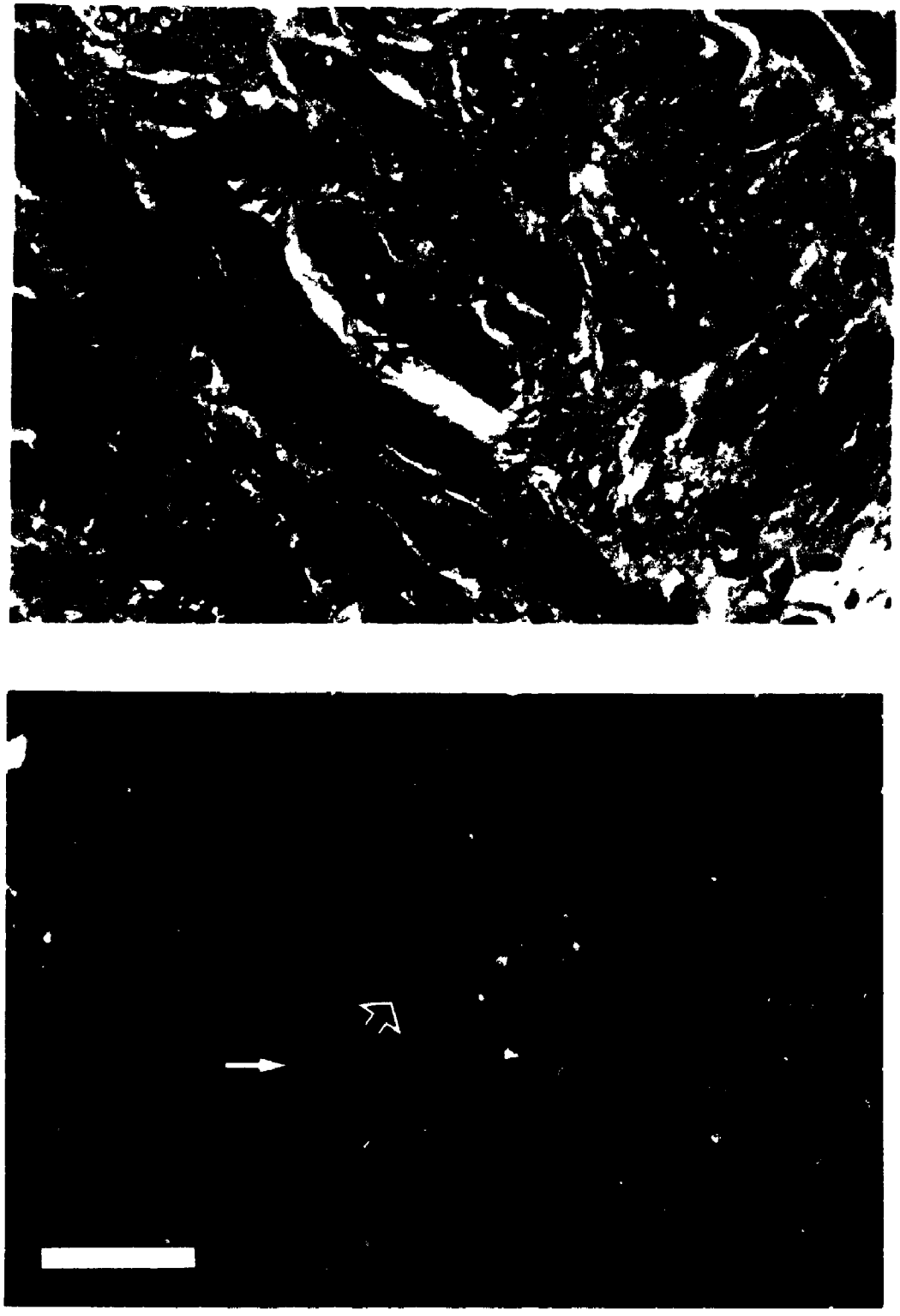

Plate 6.2: (Top panel) A section from the slide adjacent to that in Plate 6.1, stained with hematoxylin and eosin. Granulation tissue is present in the centre of the field. There is vacuolization within a myocyte suggesting early ischemic damage (open arrow) as well as multiple cc ntraction bands (arrow). The lower panel (**Plate 6.3**) shows the same specimen, now viewed with polarization microscopy. The contraction bands are highly birefringent and appear bright (arrow) while the injured myocyte is now invisible (open arrow). Polar orientation is ⊕. Bar, 50 μm.

6.4 Discussion

Diastolic abnormalities have been documented in the cardiac transplant recipient and include elevated right atrial and pulmonary wedge pressures (Greenburg et al 1985, Pflugfelder et al 1988), increased left ventricular end-diastolic pressures (Stinson et al 1972, Greenburg et al 1985, Frist et al 1987), and abnormal right atrial pressure wave forms (Humen et al 1984, Young et al 1987). Although ventricular relaxation appears to be normal, the passive stiffness of the ventricle has been shown to be increased (Hausdorf et al 1989). This is consistent with a significant increase in the fibrous component of the ventricle (Hess et al 1984). In turn, the relationship between conditions predisposing to scarring and the actual severity of myocardial fibrosis should be delineated. I chose to specifically examine the effect of the allograft ischemic time on fibrosis for two reasons: first, because of the pressure to utilize long distance procurements, and second, because the ischemic time is the only parameter to date that has been positively correlated with the passive diastolic properties of the ventricle (Hausdorf et al 1989).

A prerequisite for correlating histologic features with clinical parameters is the utilization of an objective approach yielding quantitative morphologic data. Such an approach has recently been employed for the assessment of myocyte hypertrophy in cardiac recipients (Imakita et al 1987). Fibrosis in heart allografts, however, has not previously been quantified although it has been reported by several investigators (Billingham 1981, Gokel et al 1985, Pomerance et al 1985).

Collagen Content Following Transplantation and Relation to Procurement Time

The dramatic increase in the worldwide frequency of cardiac transplantation (Fragomeni and Kaye 1988) has placed increased demands on the limited supply of

donor organs. To offset this problem, long distance procurement, with the attendant period of ischemia, has become increasingly employed (Copeland 1988). However this approach to expanding the pool of available organs must be balanced against the risks of ischemic injury, which are clearly time-dependant (Hearse et al 1981). Billingham et al (1981) have shown that with ischemic times below 3 hours capillary endothelial changes are prevalent after reperfusion and are worse in long distance procurements. In the immediate days following transplantation myocyte damage, presumably ischemic, is a biopsy finding common to several transplant centers (Gokel et al 1985, Billingham et al 1988, Copeland 1988). It is expected that any irreversibly injured myocytes would progress to focal fibrosis within several days.

By quantifying myocardial collagen in the initial biopsies of heart transplant recipients, I found that by 5 to 10 days the fibrous content was already greater than normal. Furthermore, a relationship existed between the collagen content and the total ischemic duration suggesting that the ischemic period is indeed an important etiology for allograft fibrosis and should be considered when scarring is identified in the weeks following surgery. Excess collagen was typically seen as fibrotic patches with abundant fibroblasts. Frequently, but not always, there was associated focal myocyte necrosis.

The one-week biopsy was chosen for analysis, in order to minimize interpretation difficulties arising from collagen deposition due to nonischemic etiologies. Myocardial fibrosis has been frequently observed in biopsy samples and may be related to resolved or resolving acute rejection (Billingham 1981, Gokel et al 1985, Pomerance et al 1985), chronic rejection (Bieber et al 1970), cyclosporin (Billingham 1981, Karch 1985), infection, and scarring from previous biopsies (Gokel et al 1985, Pomerance et al 1985). Thus, to specifically identify ischemia-induced fibrosis an early assessment is required. It is recognized that this may not be maximally sensitive because not all necrotic lesions may be at the fibrotic stage; however in the group studied, the mean time to the first biopsy was approximately 8 days which is somewhat later than in other

reports (Gokel et al 1985, Young et al 1987). It may be expected that with time the relation between ischemic time and ischemia-induced fibrosis may strengthen, although this would be difficult to determine for the above reason.

A potential limitation in interpreting data from endomyocardial biopsies, is the degree to which the samples reflect the morphology of the remainder of the myocardium. In the current study, patients were included if at least 3 satisfactory biopsies were available for analysis, although it has been suggested that 5 specimens may provide a more reliable sampling of the myocardium (Baandrup et al 1982).

Assessment of Ischemia-Related Myocyte Changes

Polarization microscopy offers a unique approach to the assessment of cardiac muscle damage. As myofibrils become structurally disorganized optical anisotropy is reduced resulting in a loss of myocyte birefringence. This becomes manifest as reduced muscle visibility when the microscope analyzer is inserted into the light path. While a mild reduction in birefringence may be reversible a complete absence suggests extensive fibrillar and molecular degradation consistent with cell death. At times we observed complete loss of visibility when only minor changes were evident on routine microscopy of the hematoxylin and eosin- and trichrome-stained sections. Thus the approach may be particularly useful in distinguishing reversible from irreversible myocyte damage shortly after ischemia. This hypothesis, however, has not been formally studied.

In total, myocyte necrosis was present in 8 (25%) patients and tended to be more prevalent in patients with ischemic times between 4 and 6 hours. This was not statistically significant, perhaps because of the relatively low frequency of the observation.

The enhanced birefringence of contraction bands is a polarized microscopy finding not previously described but clearly facilitates identification of this feature. It cannot be said for certain whether contraction bands represent early ischemic changes or

an artifact of the biopsy procedure. Adioman et al (1978) have proposed that these bands form following biopsy-induced myocardial depolarization with subsequent hypercontraction of the myocytes due to unopposed shortening. The increased birefringence seen in this study is consistent with excessive interdigitation of myofilaments, but in the absence of muscle protein disruption.

Functional Significance of Ischemia-Associated Fibrosis

The study did not reveal a relation between fibrosis and hemodynamics 5 to 10 days following transplantation. This lack of correlation may in part be due to the relatively mild degree of fibrosis seen at this time. Additionally, measurement of diastolic pressures alone is likely too insensitive to reliably detect the functional effects of early myocardial fibrosis. Rather, indices of the viscoelastic properties of the ventricle will more closely correlate with the degree of fibrosis (Hess et al 1984). In this regard, Hausdorf et al (1989) have found increased myocardial stiffness in patients greater than one year after surgery. Furthermore, they observed a correlation between the degree of both myocardial and chamber stiffness and the ischemic time. The current study therefore supports the hypothesis that prolonged ischemic times, by predisposing to myocardial fibrosis, may contribute to diastolic dysfunction in transplant recipients.

Elevated left ventricular end diastolic pressure (Stinson et al 1972, Greenburg et al 1985, Frist et al 1987) and atypical right atrial pressure responses to volume loading and inspiration (Humen et al 1984, Young et al 1987, Pflugfelder et al 1988) have sporadically been observed. The inconsistency of such observations may relate to the presence or absence of hypertension (Greenburg et al 1985) or graft atherosclerosis, (Giaudiani et al 1981) but may also reflect variations in the procurement time and the degree of ischemic necrosis at the time of transplantation.

Summary and Conclusions

In summary, the polarization-videodensitometry technique has been used to quantify myocardial fibrosis in the transplant recipient. As well, a novel assessment of myocyte injury following ischemia was made, using polarizing microscopy, based on the immediate loss of myocyte structural integrity. With these approaches, I have shown that ischemia-associated allograft fibrosis may be identified shortly after transplantation and its severity is dependent on the procurement time. Because fibrosis may contribute to impaired diastolic function, this relation should be considered when evaluating donor heart acceptability.

Chapter 7

Collagen Content and Fibrotic Activity in Heart Allografts: Relationships to Rejection

7.1 Introduction

In the past decade, the 1-year survival rates for patients undergoing cardiac transplantation have progressively increased, in part due to the use of the immunosuppressive agent cyclosporin (Frist et al 1987, Pomerance and Stovin 1985). Nevertheless, acute cardiac rejection is still prevalent among these patients (Thomson and McKenzie 1988) and most recipients experience at least one episode of rejection in the first six months after transplantation (Hunt and Stinson 1981). Through serial endomyocardial biopsies, these episodes can be identified and treatment can be adjusted accordingly. However, the long term effect of multiple episodes of rejection has not been established. Unless rejection is identified and successfully treated at a very early stage, myocyte destruction will ensue and will presumably progress to focal fibrosis. Indeed, scar tissue found in biopsy samples taken in the weeks following treatment for acute rejection is often believed to represent resolved rejection (Billingham 1981). Rejection, by inciting myocardial fibrosis, may therefore be an important factor limiting the exercise capabilities of these patients.

The precise relation between rejection and fibrosis has not, however, been characterized. Since there may be multiple causes of fibrosis in cardiac allografts, the relative contribution of rejection may be difficult to establish.

I felt that the polarization-video microscopy technique could offer a unique, quantitative approach with which to address this problem. To evaluate the relation between rejection and myocardial fibrosis, I retrospectively analyzed serial

endomyocardial biopsy samples, taken over a period of a year and a half, from five transplant recipients. Both the collagen content and the incidence and severity of rejection were quantified. Furthermore, since the biopsies formed a consecutive series there was a unique opportunity to follow the maturation of fibrotic collagen in a clinical setting. I therefore attempted to measure the activity of fibrosis in order to determine if active fibrosis was indeed temporally related to rejection.

7.2 Methods

A total of 201 endomyocardial biopsy specimens from five transplant recipients were analyzed. These were obtained using a Stanford-Caves bioptome, over the period from February 1987 to December 1988, by members of the Department of Cardiology at University Hospital. For each patient, the biopsy samples formed a consecutive series taken over a period of 1 to 1.5 years. Biopsies that yielded fewer than three separate endomyocardial fragments were excluded since the biopsy sensitivity with only two fragments is believed to be low (Rose and Uys 1984).

Specimens were fixed in 10% phosphate buffered formalin. All fragments from a given biopsy procedure –forming a biopsy-set– were embedded as a single paraffin block and were sectioned at 5 μm-thickness. I obtained three adjacent slides courtesy of Dr. C. Guiraudon. One had been stained with hematoxylin and eosin, another with methyl-green pyronine (to identify activated lymphoblasts) and the third, initially unstained, was stained with picrosirius red by Mrs. J. Dixon. In the latter case, the entire series of biopsy sections for a given patient were stained together.

All specimens were analyzed, in a blinded fashion, for three histologic findings:

1. Rejection

Rejection was evaluated based on previously reported features. Billingham (1981) first described the main morphologic features of rejection and proposed a system for grading the process. This is based on the presence of a lymphocytic infiltrate, edema, pyrininophilic lymphocytes (indicated by the red color of the cytoplasm of lymphocytes stained with methyl-green pyronine), focal myocyte damage, and the presence or absence of scar. While many investigators employ an approach similar to hers, there remains no uniform or quantitative criteria. While this may suffice in the clinical setting, quantitation is necessary for study purposes. I therefore considered rejection to be present if the mean number of interstitial lymphocytes in a high power (x400) microscopic field was greater than five *and* if there was either lymphocytic pyrininophilia or myocyte destruction. Edwards (1982) has demonstrated that a mean of between 1 and 5 lymphocytes per high power field may frequently be present in biopsy samples from patients with cardiac diseases other than lymphocytic myocarditis.

From the hematoxylin and eosin-stained sections the number of lymphocytes was systematically counted. Approximately 8 to 12 fields from each biopsy fragment were studied. Endocardial infiltrates of lymphocytes were not counted as this finding is not associated with the development of myocyte destruction (Billingham 1988). The presence of lymphocytic pyrininophilia was determined from the methyl green pyronine-stained sections (Plate 7.1). Myocyte integrity was determined from the hematoxylin and eosin-stained sections. If myocytes within a region of lymphocytic infiltration did not show obvious damage, they were also assessed using polarization microscopy to determine if there had been a reduction in birefringence, suggesting early degeneration (see chapter 6). Since resolution of the histologic findings of rejection may take up to two weeks (Billingham 1988), biopsy specimens taken within two weeks of a rejection episode were considered to show further rejection only if the mean lymphocyte count had increased with persistent pyrininophilia.

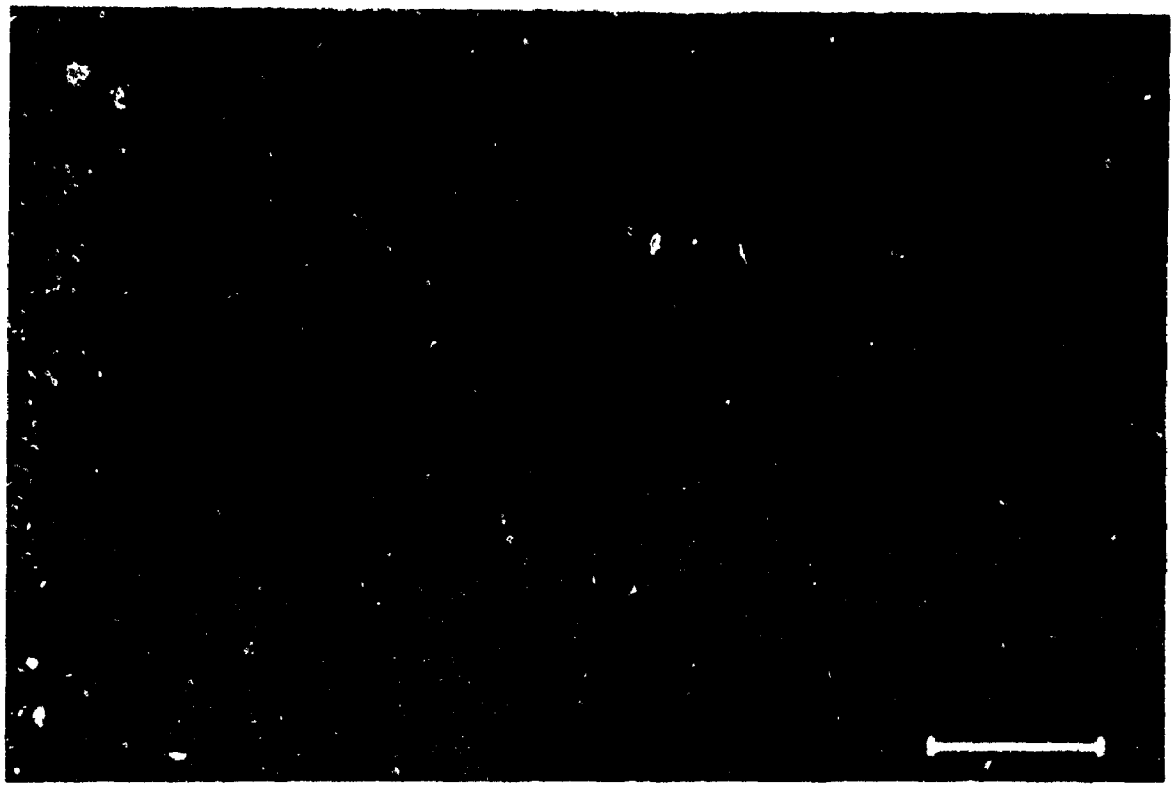

Plate 7.1: Section of myocardium stained with methyl green pyronine. The bright red (pyrininophilic) cytoplasm of the lymphocytes in the centre of the field denote immunologic activation which is a feature of rejection. Bar, 20 μm.

2. Collagen Content

Myocardial collagen content was assessed from the picrosirius red-stained sections by videodensitometry. For each biopsy, the collagen volume fraction was determined and expressed both in terms of the individual biopsy fragments and as an overall value for the biopsy-set (total collagen content divided by total area analyzed). A single biopsy fragment was considered fibrotic if the collagen content was greater than 4.5%. This value represents two standard deviations above the mean collagen content of the 23 biopsy samples from the seven normal autopsy hearts referred to in chapter 6. Using this criteria, 58 biopsy fragments from 29 biopsy-sets were determined to contain fibrosis.

3. Fibrotic Activity

Having identified these sections as fibrotic, they were then reexamined to determine the activity of fibrosis. Slides were redigitized and the specific regions considered to be fibrotic were circumscribed using the mouse. Typically, these areas appeared either as focal patches of interstitial fibrosis or as coarse bands of collagen bundles. The grey-level histogram for each of these areas was then determined. Histograms from a given biopsy-set were summed and the overall median grey-level was determined.

For each patient, a reference grey-level was determined based on the average median grey-level of 7 to 10 biopsy fragments free of fibrosis. In all but one patient, these were from biopsies performed in the first three weeks after transplantation. The median grey-levels of fibrotic and normal collagen were incremented by the black-level offset of the video system (determined from the grey-level versus transmittance plot) which for this study was 17. An index of fibrotic activity was then calculated as the corrected median grey-level of nonfibrotic myocardial collagen divided by that of fibrotic collagen. An index greater than 1 would indicate that the brightness of fibrotic collagen

was less than that of normal myocardial collagen, consistent with fibrosis at a relatively early stage of maturation. Conversely, an index less than 1 would describe a more mature network in which the fibers were brighter than normal myocardial collagen.

7.3 Statistics

Means are reported ± standard deviation. Relations between parameters of rejection and collagen content were tested by linear regression analysis. Comparisons between early and late fibrosis were made with paired t-tests.

7.4 Results

Characteristics of the five cardiac allografts studied are listed Table 7.1. The mean age of the donor was 32±12 years. Mean ischemic time was 146±67 minutes. Only one graft had been exposed to exogenous catecholamines prior to harvesting. In four of the five patients, at least one of the biopsy-sets obtained in the first year after transplantation showed fibrosis. One patient, with an ischemic time of 225 minutes, had fibrosis in the one-week biopsy but no fibrosis in the one-year biopsy. All other patients had a higher collagen content at one year than at one week. (Figure 7.1).

The quantitative data on the presence and severity of rejection is presented in Table 7.2. All patients had at least one episode of rejection and 11 episodes were identified in total. The mean lymphocyte count during a rejection episode was 14.5 ± 10.1 (range 5.3 to 37.3) cells per high-power field. The cumulative rejection-associated lymphocyte count, per patient, over the first year ranged from 5.3 to 72.2 cells per high-power field.

The amount of myocardial collagen present in biopsy samples taken at one year ranged from 3.7 to 6.2% (Table 7.2). There was no significant correlation between the

Patient	Donor Age (y)	Inotropic Therapy	Ischemic Time (min)	Fibrosis Within First Year
1	29	No	210	Yes
2	50	Yes	107	No
3	16	No	76	Yes
4	27	No	225	Yes
5	37	No	110	Yes

Table 7.1: Characteristics of the cardiac allografts of the five patients studied.

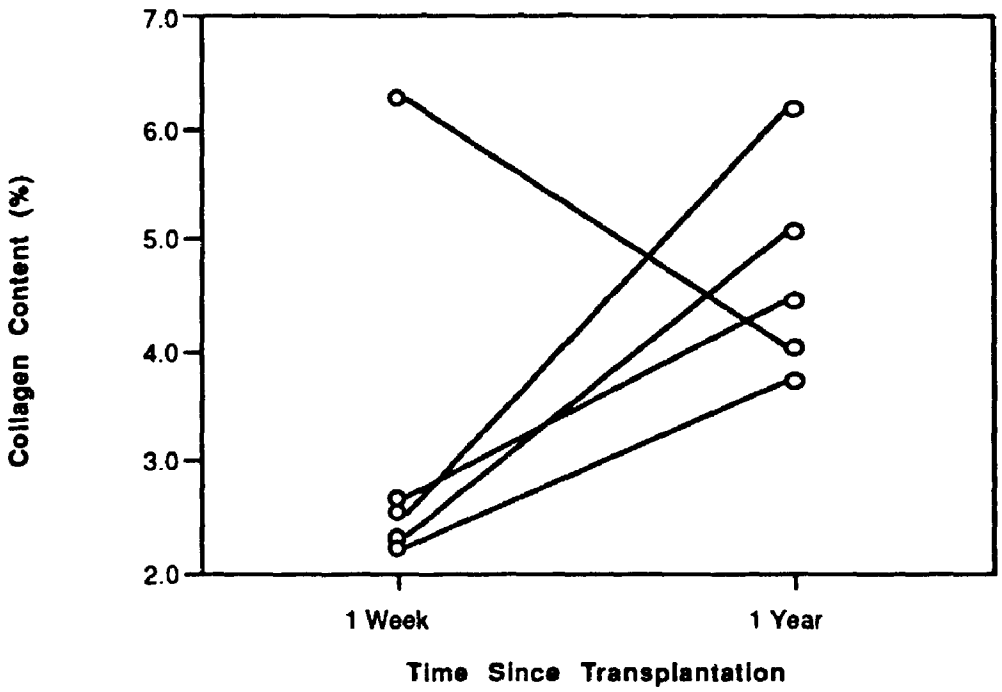

Figure 7.1: Myocardial collagen content in biopsy samples taken one week and one year after transplantation.

Patient	Number of Rejection Episodes	Cumulative Rejection-Associated Lymphocyte Count (per HPF)	Collagen Content of 1-Year biopsy (%)	Mean Collagen Content 4 Months-1 Year (%)
1	3	39.3	5.1	4.2 ± 1.7
2	1	5.3	3.7	3.5 ± 0.3
3	2	18.2	6.2	5.3 ± 1.1
4	2	24.0	4.0	4.7 ± 0.7
5	3	69.8	4.5	5.1 ± 0.8

Table 7.2: Prevalence and severity of rejection in five cardiac transplant recipients and the corresponding myocardial collagen content.

number of rejection episodes and the one-year collagen content ($r = 0.35$, $p = 0.57$) or between the cumulative rejection associated-lymphocyte count and the one year-collagen content ($r=0.06$, $p=0.9$). If the collagen content of the biopsy-sets taken between four months and one year were averaged, then there was a trend toward a relationship between the number of rejection episodes and collagen content ($r=0.73$) and between cumulative rejection associated-lymphocytes and collagen content ($r = 0.56$), but these did not attain statistical significance ($p=0.16$, $p=0.32$, respectively).

The index of fibrotic activity (brightness of normal myocardial collagen divided by that of fibrotic collagen) in those biopsy samples where scarring was identified is depicted in Figures 7.2 a, b, and c. In all four patients showing fibrosis, there was a downward trend in the activity index over the first year to year and a half after transplantation. For the group, the index at the final biopsy was 0.72 ± 0.15, significantly lower than that of the initial biopsy at 1.41 ± 0.18 ($p<0.01$). For a given patient the highest index of fibrotic activity was seen in biopsy samples temporally associated with rejection episodes (denoted in Figure 7.2 by the vertical arrows). In all four patients, the maximum value of fibrotic activity was either coincident with or occurred one week after a rejection episode. Sections showing fibrosis representative of that seen both early and late after transplantation are shown in Plates 7.2 and 7.3 respectively.

7.5 Discussion

The 1-year survival rate among heart transplant recipients is now over 90% (Fragomeni 1987, Copeland 1988) and attests to the success of present "anti-rejection" medications. The use of cyclosporin, in particular, has changed the nature of cardiac rejection from a severe acute event, to a more indolent and less life-threatening event

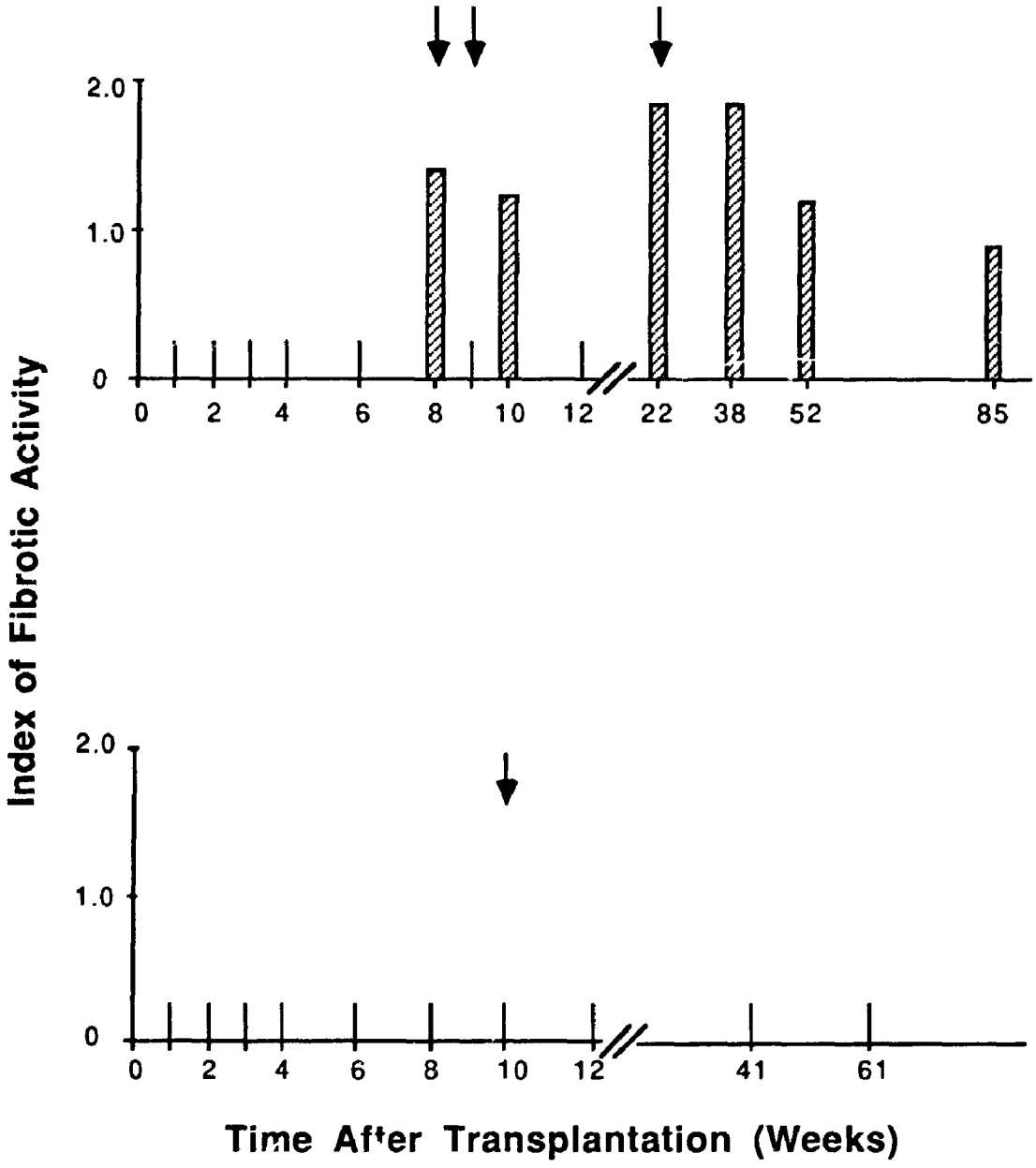

Figure 7.2a: Time-course of fibrotic activity in cardiac allografts. Biopsy specimens that were analyzed are depicted by a vertical line. Arrows denote episodes of acute rejection. Fibrotic activity is expressed as brightness of fibrotic collagen relative to normal myocardial collagen. In the first patient (top graph), fibrotic activity is maximum following 3 episodes of rejection and subsequently subsides. The second patient had only 1 episode of rejection and fibrosis was not identified.

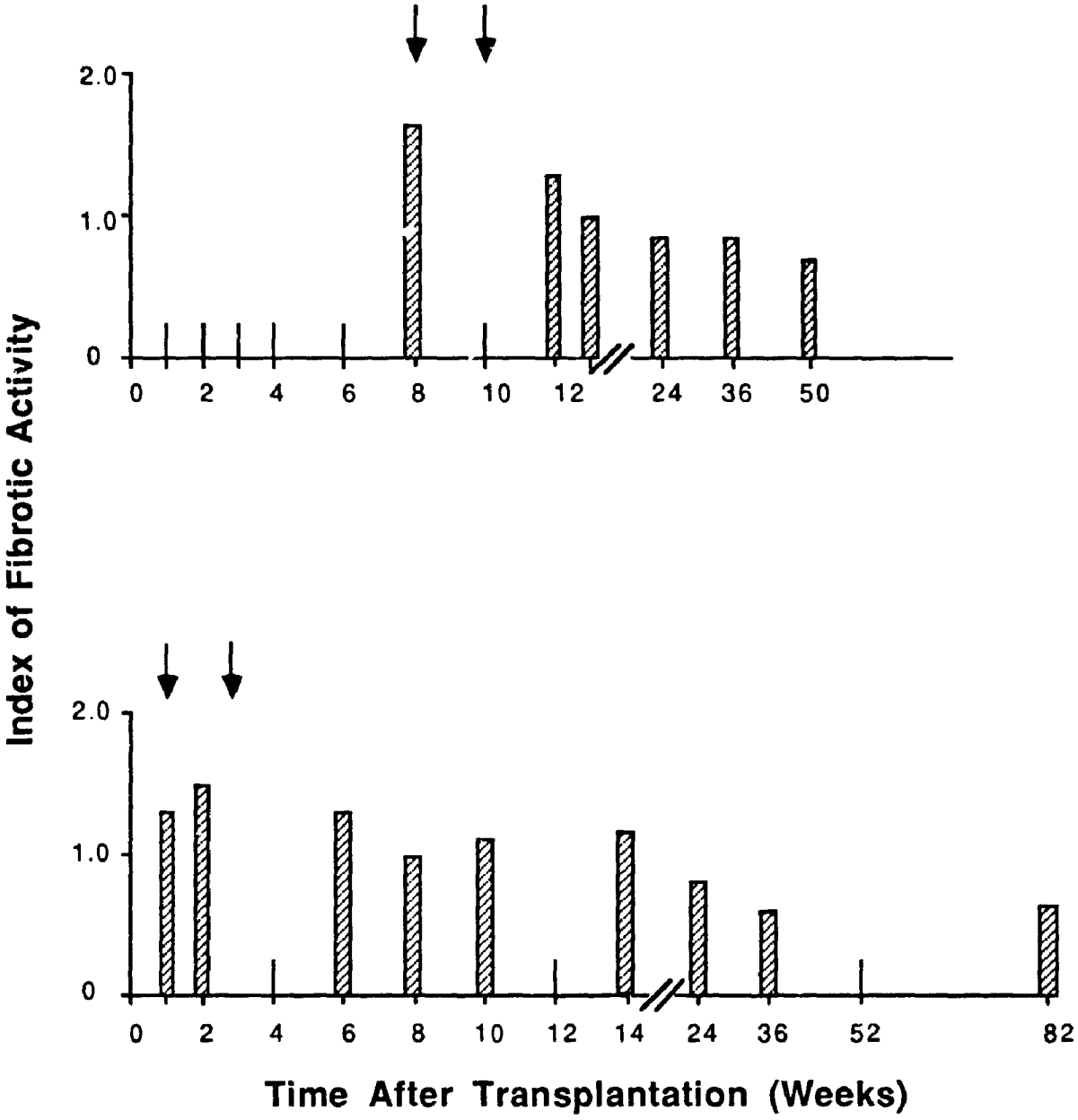

Figure 7.2b: Time-course of fibrotic activity (cont'd). In both patients the activity of fibrosis is greatest in association with rejection.

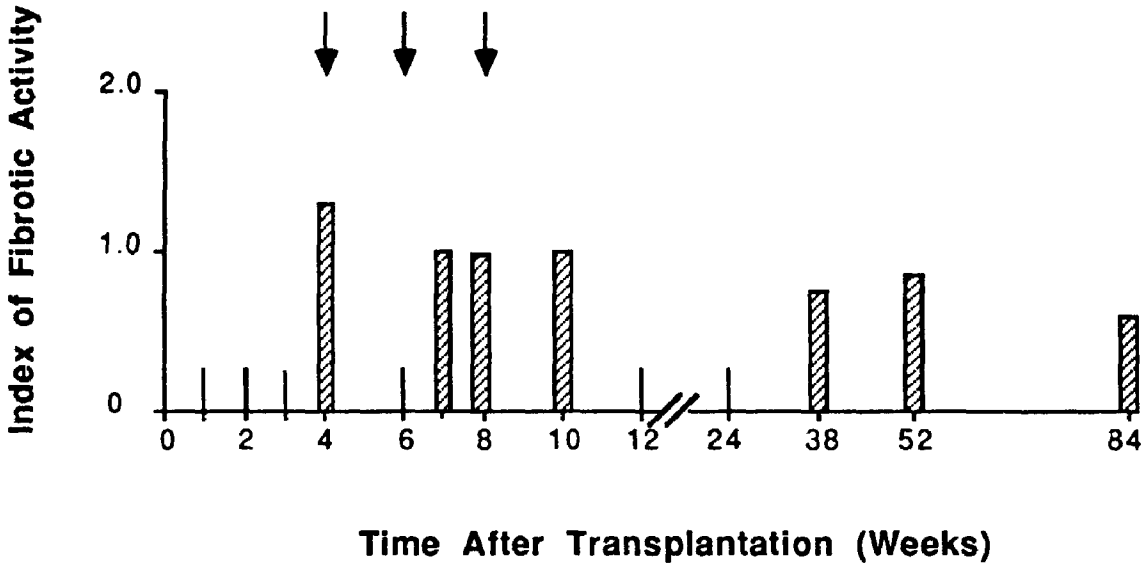

Figure 7.2c: Time-course of fibrotic activity (cont'd). In this patient the greatest activity coincides with the first episode of rejection and thereafter falls.

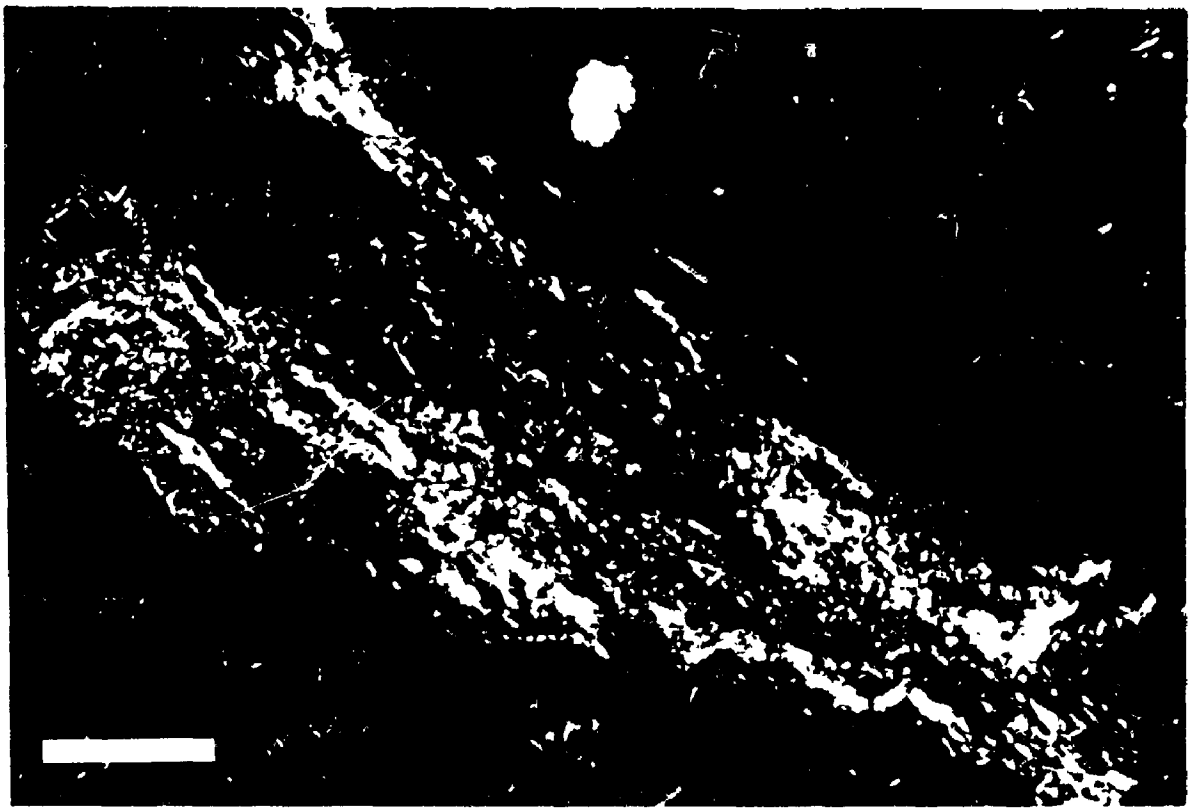

Plate 7.2: Section of a biopsy sample taken from patient number 1, 8 weeks after transplantion. A focus of fibrosis is present in the centre of the field. The collagen fibres are relatively thin, loosely packed, and are predominantly green. The activity index for this particular region was 1.8. Polar orientation is ⊕. Picrosirius red. Bar, 50 μm.

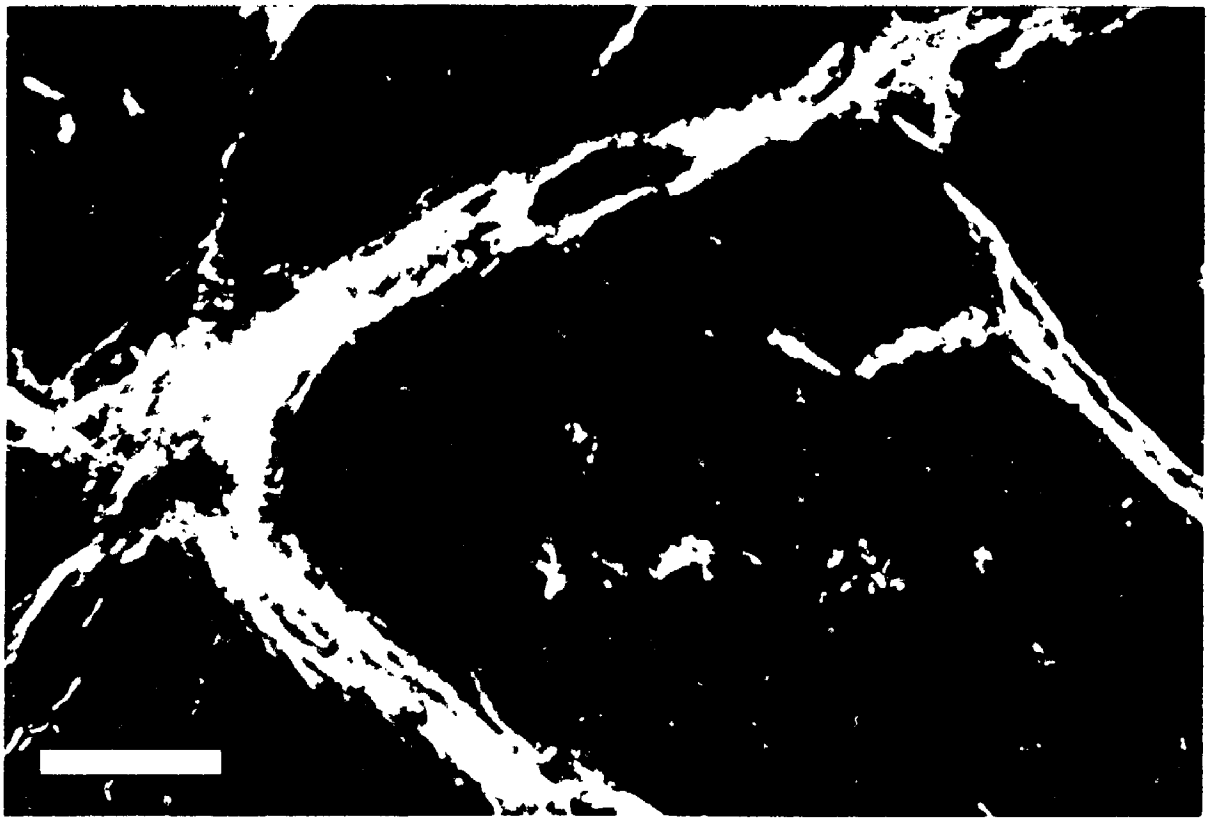

Plate 7.3: Polarization microscopy image of a section of a biopsy sample from patient 4, taken 82 weeks after transplantation. Coarse bands of bright collagen fibre bundles are present between myocytes. The activity index for these fibres was 0.6. Polar orientation is ⊕. Picrosirius red. Bar, 50 μm.

(Copeland 1988) that in most cases may be successfully treated (e.g., with bolus steroids). Nevertheless, although treatment of acute rejection is generally satisfactory, there is no evidence that the frequency of these events has significantly decreased in the "cyclosporin era" (Cooper and Novitsy 1984, White 1989). Patients generally have between one and three episodes of rejection in the first three months after transplantation (Hunt and Stinson 1981) with a declining incidence thereafter.

The long term sequela of rejection episodes has not been fully elucidated. Labovitz et al (1989) have shown that exercise capacity at 6 to 12 months after cardiac transplantation is inversely correlated to the number of rejection episodes during the first six months. This suggests that scarring due to rejection may adversely affect the mechanical function of the heart in the long term. The relation between rejection and fibrosis is, however, not clear. While it is suggested that rejection resolves by scar formation (Billingham 1981), the amount of fibrosis, in a given allograft, that is caused by rejection is unknown.

I have examined the relation between rejection and fibrosis in two ways. The first was to compare the amount of fibrosis with the number and severity of rejection episodes. Fibrosis was quantified using the polarization-videodensitometry technique, described and validated by studies presented in chapters 2 and 3. A quantitative approach to evaluating cardiac rejection was also deemed necessary although this has not previously been done. Limitations in subjective interpretation (e.g., due to old biopsy sites and slow resolution of immune-mediated damage) are, however, well documented (Billingham 1988, Copeland 1988). I based my approach on the actual number of myocardial lymphocytes and the presence or absence of lymphocyte activation and myocyte destruction. This approach incorporates the qualitative features of rejection (Billingham 1981) with the quantitative criteria previously applied to lymphocytic myocarditis (Edwards et al 1982). To reliably assess the long term effects of acute

rejection a quantitative assessment is necessary (Hausdorf et al 1988). In this way both the presence and severity of acute cardiac rejection could be quantified.

Using these approaches, no relation could be identified between rejection and amount of myocardial fibrosis. However, trends were seen in the data (the strongest being between the number of rejection episodes and collagen content) suggesting that a relation may exist but was not detected because of the small sample size. Since fibrosis late after transplantation is likely multifactorial, a much larger series of patients may be required to detect a significant effect of rejection.

The second approach to characterizing the relation between rejection and fibrosis was to serially determine the fibrotic activity in those biopsy specimens with scar tissue. This was done by determining the brightness of fibrotic collagen relative to nonfibrotic collagen. The inverse of this value served as the index of fibrotic activity. Although the number of patients studied was small, there were several notable features. In all patients the fibrotic activity progressively fell over the first year after transplantation. This decline suggests that events inciting fibrosis predominated in the early weeks (generally less than 12) following transplantation. This in fact was when all but one of the rejection episodes occurred, which is consistent with the reports of larger series (Hunt and Stinson 1981). Other factors leading to fibrosis may also be operating during this period of time. Myocardial damage secondary to prolonged procurement time has already been shown to be associated with early myocardial scarring (chapter 6). The one allograft in which scarring was identified in the first biopsy sample, had an ischemic time of 224 minutes. This patient, however, also experienced rejection in the first week.

The fact that the first approach failed to detect a significant relation between rejection and scarring while the second approach was strongly suggestive is not necessarily discordant. Active fibrosis does not imply that scarring is extensive, but that it is in an early stage. Thus in the 5 patients studied, there may not have been enough rejection-induced damage to cause a sufficient amount of scarring for a statistical

correlation to be found. However the temporal association between rejection and high fibrotic activity supports the concept that rejection resolves by the formation of a scar, albeit perhaps a small one.

The actual index of fibrotic activity may have predictive value in identifying rejection. In the present study, an index greater than 1.4 was associated with rejection occurring within the prior two weeks (including the time that rejection was identified) in at least four out of five (80%) instances. An index less than 1 was associated with at least a six week interval since the last rejection episode, in 10 out of 12 (83%) instances.

It must be emphasized that these "cut-off" levels for fibrotic activity have been identified in a post-hoc fashion and their use cannot be presently advocated. Determining the sensitivity and specificity of these parameters would require a prospective study. However, the fact that characteristics of fibrosis may independently identify, or exclude, an active disease process (in this case rejection) is a unique finding with important implications. There are clinical instances where direct histologic evidence of active cardiac damage is rarely found, usually because the acute changes are short-lived and not present at the time of biopsy. In these cases, fibrosis may be the predominant morphologic finding and determining the activity of fibrosis may be the only way of evaluating the activity of the disease process itself. This may be the case for idiopathic dilated cardiomyopathy where endomyocardial biopsy is characteristically unrewarding (Masson and O'Connel 1989) despite progressive deterioration in ventricular function. The emerging problem of accelerated coronary artery disease in transplant survivors (Hunt and Stinson 1989) may also be addressed by this type of approach. Here, the finding of active fibrosis late after transplantation may herald the onset of this important problem.

In summary, this study did not identify a clear relation between the amount of myocardial fibrosis and either the frequency or the severity of rejection. On the other hand, the time-course of fibrotic activity supports the proposal that rejection leads to

some scarring. In these patients therefore, the relative contribution of acute rejection to scarring was probably small.

Chapter 8 Discussion

The deposition of fibrotic collagen is an essential aspect of repair in any organ or tissue (Gillman 1968). Fibrosis in the heart, is generally regarded as a response to myocyte death occurring to maintain a degree of structural integrity (Robbins and Cotran 1979, p 95). While this is partly true, it is now apparent that the nature and extent of cardiac fibrosis can significantly influence ventricular performance (Weber 1989). To adequately study myocardial fibrosis, at both the basic and clinical level, the assessment of fibrosis must go well beyond the pathologist's interpretation of whether or not scarring exists. In this thesis, I have presented a new technique with which to study cardiac fibrosis. Using standard histologic sections, both the amount of fibrosis and the relative maturity of fibrotic collagen may readily be quantified.

8.1 Role of Polarization-Video Microscopy in Quantifying Myocardial Fibrosis

While a biochemical technique has long been a standard approach to quantifying collagen (Neuman and Logan 1950) and fibrosis (Chiarello et al 1983), its present role is limited by the need to solubilize the tissue. It is, therefore, a somewhat blunt instrument since precise information on the location of fibrosis is lost. Furthermore, its use is largely limited to the experimental model, or to postmortem hearts. Tissue specimens obtained from patients by biopsy cannot be analyzed biochemically since they are not generally large enough to have a portion digested for analysis. Stereologic methods may overcome these limitations yet the laborious nature of this assessment limits its practicality. As a result, cardiac fibrosis is infrequently quantified and is almost never quantified in the clinical setting.

The technique outlined in this thesis has been designed to overcome these limitations. By using standard histologic sections tissue architecture is preserved and the potential for wide applicability exists. The videodensitometry measurements correlated well with both hyroxyproline content and with collagen content determined stereologically from trichrome-stained histologic sections.

To develop the technique, two very different analysis techniques were incorporated: polarized light microscopy and digital image analysis. Polarizing microscopy has been used to study biologic material since the 1920's (Frey-Wyssling 1974). Its application requires that the material under study have two refractive indices and be therefore birefringent. Of the three most abundant birefringent structures in the human body (collagen, muscle, and elastin), collagen is the most intensely birefringent and is therefore well suited to study by polarized light techniques.

In contrast to polarizing microscopy, digital image processing has only recently developed into a discipline of its own. This has come about through the advent of inexpensive microprocessors, improved memory devices, and special purpose signal processing components. The primary goal of digital image processing is to enhance and analyze pictorial information. This information may come directly from a microscopic field of view.

In the digital domain, an image is represented by discrete points of defined brightness. Because the image seen through a polarizing microscope is already comprised of objects distinguishable by their brightness, it is well suited to analysis by digital processing.

To quantify collagen in cardiac tissue using digital techniques, there must be a threshold intensity of brightness (grey-level) that distinguishes collagen from all other myocardial components. To attain this I employed two approaches. The first was to stain the material with picrosirius red. This enhances collagen birefringence seven-fold, to a level approximately seven times that of cardiac muscle (Junqueira et al 1979). The

second was to illuminate the specimen with monochromatic light ($\lambda = 600 \pm 5$ nm) which further increased the collagen-muscle contrast. The net effect was the generation of an image that was effectively binary with respect to its grey-levels and to the morphologic components of the image. Pixels depicted collagen if they were bright (grey-level >0) and "noncollagen" if they weren't.

Because collagen may be identified using routine microscopy it could be argued that computerized analysis of a more conventional microscopal image would gain wider acceptance. There are several advantages to using polarized microscopy, however. The first is that contrast between collagen and the other tissue components is more readily attainable with polarization microscopy. As noted above, the differences in birefringence of materials may be readily translated into difference in brightness in the digital domain. With routine microscopy, features are typically identified on the basis of color. Differences in color may not always translate into clear differences in brightness (Jarvis 1988).* Hoyt et al (1984) have used a videodensitometric technique for quantifying collagen using routine microscopy of trichrome-stained material. To determine the threshold a careful analysis of the grey-level histogram was necessary and, in some instances, the grey-level distribution did not have discrete modes. I have found that a similar situation exists when analyzing picrosirius red-stained sections that were illuminated with nonpolarized light. Even with green-filtered light ($\lambda = 540 \pm 5$ nm, corresponding to the peak of the absorption spectra for collagen stained with sirius red (Junquiera et al 1978)), thin (< 5μm) collagen fibers were poorly discriminated from muscle on the basis of grey-levels. Jarvis (1988) has suggested that when using video techniques to examine standard microscopal images manual image editing is necessary if a thresholding technique is to be employed. Alternately, one might develop an image

* This applies to monochrome systems. Colour image analysis systems may prove to be of value in the analysis of images from standard light microscopic images. At present, these systems are considerably more expensive than monochrome ones and the analytical software is just becoming available.

processing routine in an attempt to enhance contrast after digitization. If an adequate threshold still can not be identified, an alternate approach, such as edge detection (Pratt 1978), would be necessary. Each of these approaches would significantly lengthen the time necessary to complete the evaluation. Using polarization microscopy, however, contrast between collage 1 all other components was sufficiently good that neither editing nor image processing, beyond the initial adjustment to the grey-level offset, were necessary. The number of steps and the computation requirements were therefore minimized.

The second advantage of the polarization approach is the superior sensitivity and specificity for collagen when the tissue is stained with picrosirius red. Since it was first used this stain has been considered superior to the widely-employed van Gieson's stain because of its ability to color fine collagen fibers and to its resistance to fading (Sweet et al 1964). I have observed that its sensitivity for collagen is also greater than that of the popular trichrome stain. The combination of picrosirius staining and polarized light microscopy is also specific for collagen (Junquiera et al 1979), unlike any stain used with routine microscopy (Weatherford 1972).

The final reason that the polarizing microscopy approach was chosen was that it offers much more than the identification of collagen. The intensity of collagen birefringence reflects its degree of structural organization at both the molecular and fibrillar level (Wolman et al 1972, Whittaker et al 1989). This principle was exploited in order to gauge fibrotic activity. Thus, by designing a video technique around a polarizing microscope, it was possible to evaluate fibrosis much more comprehensively than it would be if standard light microscopy were used.

In spite of the advantages of polarizing microscopy, the phenomenon of extinction that is seen with polarized light techniques could in theory lead to an underestimation of collagen content. A birefringent structure lying parallel or perpendicular to the plane of polarization will not be visualized since the incident light

will "see" only one refractive index. Its state of polarization will not be altered and it will therefore be invisible. From a practical standpoint, I considered this possibility in two settings. The first was in sections from autopsy hearts where extinction was not felt to be important since fibers aligned with each other may be easily rotated out of extinction. The second was in biopsy specimens. Here, the smaller tissue size and the less controlled procurement method produce a greater variability in fiber alignment following embedding and sectioning. It could therefore be more difficult to ensure that all fibers were out of the extinction position during analysis. Nevertheless, for both types of specimens, collagen content estimated using the polarization videodensitometry method correlated well with an independent quantitative measurement technique. Furthermore, in biopsy specimens, the degree of difference between any two estimates taken at different orientations was very small (mean of 5%) and declined as the total collagen content went from the normal to the fibrotic range. Thus, in practice, the effect of collagen extinction was quite small. This corresponds to the subjective visual assessment. While the intensity of brightness of fibrotic collagen clearly varies with orientation, the proportion of fibers that become truly invisible is small (Dolber and Spach 1987). It is l .ely that the constituent fibrils of fibrotic collagen do not lie in perfectly parallel planes as do the components of nonbi logic birefringent materials such as crystals.*

8.2 Role of Polarization-Video Microscopy in Assessing Fibrotic Maturity and Activity

Evaluating the activity of a disease is of considerable importance when planning treatment strategies. Since all therapeutic interventions have their limitations their risk-

* While the imperfect alignment of the light absorbing elements of fibrotic collagen has proven to be advantageous for the measurement of collagen content, it does render the measurement of retardation more difficult.

benefit ratio is optimized when given during the active phase of the disease, since they are most likely to be effective at this time. Assessments of disease activity are routinely made in such systemic conditions as rheumatoid arthritis, cancer, and leukemia and therapy is adjusted accordingly.

In the heart, while the disease activity is important, there are few instances where it can be satisfactorily monitored. Frequently, myocyte damage occurs abruptly and the predominant pathologic finding is fibrosis. Because fibrosis has classically been interpreted as the final stage of the disease process its presence has been considered to imply that the "window of opportunity" for useful therapeutic intervention has passed. This is no longer the case. For example, it is now believed that the nature of the healing process following myocardial infarction may significantly affect short and long term mortality (Lerman et al 1983, Jugdutt and Amy 1986). In other conditions, such as dilated cardiomyopathy, the disease process may be progressive but direct histologic evidence for this, other than scarring, may not be available (Katz 1990). In many instances, therefore, the activity of the disease may be gauged by the activity of the associated cardiac fibrosis.

In this thesis, I have shown that the polarization-video microscopy technique is a tool with which an assessment of fibrotic activity can be made. Changes in both collagen packing and in molecular and fibrillar organization will occur as a fibrotic network matures (Prockop et al 1979a, Bailey and Light 1985) and these may be reflected by the degree to which the collagen retards linearly polarized light (Wolman et al 1972, Mello et al 1975, Whittaker et al 1989). While the video microscopy technique cannot measure retardation, it can be used to evaluate the intensity of brightness. I have shown that over the range of retardation values generally seen for collagen stained with picrosirius red, intensity and retardation are closely associated.

Brightness is also affected by collagen fiber orientation and this must be considered when applying the video technique to measure fibrotic activity. I have proposed that a practical way of taking this into account is to first establish, in general terms, whether the collagen is deposited as a highly aligned network (e.g., as in replacement fibrosis) or as one with a more diffuse arrangement (e.g., most cases of interstitial fibrosis). In both of these cases, the brightness of the network increases over time. The precise relation between fibrotic maturity and brightness however will not necessarily be the same in each instance. One may not, for instance, compare the age or activity of fibrosis associated with left ventricular hypertrophy, which is interstitial (Tanaka et al 1986), with that of fibrosis seen following a myocardial infarction. Rather, the approach is best suited to following a particular fibrotic process in a single individual, or in a group of individuals (or experimental animals) with the same condition.

In recent years, several methods of altering the fibrotic process have been proposed. Interventions that may accelerate fibrosis include the addition of cofactors normally involved in collagen synthesis (e.g., α-ketoglutarate, ferrous ions, ascorbate (Goldberg and Rabinovitch 1983)) or of topical treatment with epidermal growth factor (Brown et al 1989). Agents that decelerate the process include corticosteroids (Oikarine 1977), D-penicillamine (Grant and Prockop 1972), beta-aminopropionitrile (Madden et al 1973), proline analogues (Prockop et al 1979a), and colchicine (Diegelmann and Peterkofsky 1972). None of these approaches have as yet gained wide acceptance since results have been variable. With the polarization video technique, however, one may be able to define a period of time during which these measures are most likely to be effective. In this way, the role of these and other putative measures for modifying the fibrotic response, may be reappraised.

8.3 Use of Polarization-Video Microscopy in Evaluating Fibrosis in Cardiac Transplant Recipients

The utility of quantifying fibrotic content and activity may be best brought into focus through its application to a known clinical problem. While there is an abundance of conditions that may be adversely affected by fibrosis, scarring in the human transplanted heart is perhaps the most recent example. In the past decade, there has been a dramatic increase in the number of cardiac transplantations worldwide (Fragomeni and Kaye 1987, Copeland 1988). While almost all transplant survivors achieve a quality of life superior to their pretransplant condition, their exercise capacity remains subnormal (Kavanaugh et al 1977). To a considerable extent this may be due to impaired diastolic function of the transplanted heart, a feature indicated by the abnormally elevated left ventricular filling pressures that occur with exercise (Stinson et al 1972, Greenberg et al 1985, Young et al 1987). Hausdorf et al (1989) have recently observed an increase in the passive diastolic properties of the transplanted heart one year after surgery. Their data, in combination with several reports of allograft fibrosis (Billingham 1981, Gokel et al 1985, Pomerance et al 1985) suggest that scarring in the transplanted heart may be an important factor limiting the exercise capabilities of allografts recipients.

The results of the studies presented in Chapters 6 and 7 indicate that: 1) there is a significant correlation between graft procurement time and myocardial fibrosis early after transplantation and 2) allograft rejection is followed by active fibrosis during the first year after transplantation. Establishing a relation between fibrosis and rejection is particularly challenging because there are multiple potential etiologies of scarring in the months following transplantation. However, by examining fibrosis in a comprehensive fashion, i.e., both content and age, the nature of these complex relations may be characterized.

The above studies were possible because of the ease with which endomyocardial biopsy can presently be performed. The ability to evaluate fibrosis on biopsy samples is of considerable importance because it enables one to follow cardiac morphology over time. It is cautioned, however, that the small tissue samples taken by bioptome may not always represent the remainder of the myocardium, particularly if the disease process is patchy. Baandrup (1982) has observed that the coefficient of variation of the collagen volume-fraction decreases until at least five samples are studied. I found, examining three or four samples per patient, that the mean coefficient of variation of collagen content was approximately 25%. This degree of variability may impair one's ability to establish differences between any two patients, although inferences under these circumstances are frequently made. However, if the analysis is confined to examining relationships within a specific patient population then important information may still be gathered.

8.4 Future Directions

Having established the validity and utility of the polarization-image analysis technique, it may now be employed to quantitatively study a number of problems associated with cardiac fibrosis at both the basic or clinical level. Much remains unknown about the relation between cardiac structure and function (or dysfunction), and the technique could, for example, be very useful in characterizing this relationship. In contrast to the limited modes for studying fibrosis, there is a plethora of quantitative approaches for evaluating systolic and diastolic function in the human heart (Nakayama et al 1987, Hess et al 1984, Brutsaert et al 1984, Grossman 1986). Therefore the manner in which scarring alters cardiac performance may be quantitatively studied. The relation between myocardial fibrosis and diastolic function was evaluated in a preliminary manner in transplant recipients (see Chapter 6). Using a more precise

method of evaluating passive diastolic properties of the heart (Hausdorf et al 1989) and a quantitative approach to determining exercise capacity (e.g., oxygen uptake parameters), the relationships between exercise performance, diastolic cardiac function, and myocardial fibrosis could be characterized. This has not been fully evaluated in any patient population.

Fibrosis in dilated cardiomyopathy is another problem requiring further investigation. In this condition, a large amount of scarring has been associated with more severe symptoms of heart failure (Unverferth et al 1983) and reduced ejection fraction (Mall et al 1982). Recently, Nakayama et al (1987) suggested that collagen proliferation may have a pivotal role in the deterioration of cardiac contractility. By quantifying, in a serial fashion, the content and activity of fibrosis in patients with this disorder, one may be able to further evaluate this relationship. The stage might then be set for the study of appropriately-timed interventions to retard progression of this often fatal disease.

The assessment of fibrosis by the video technique is by no means limited to the heart. A quantitative study of collagen deposition in the lung, liver, and blood vessel walls could provide important insights into the pathogenesis of diseases within these organs. Application to the study of patients with scleroderma (a progressive disease characterized by progressive collagen deposition in the skin and internal organs), is particularly attractive because of the ease of obtaining tissue for study (from the skin) and the very poor prognosis of patients with the systemic form of this condition (Medsger et al 1971).

Although the polarization-video microscopy system has been designed to study fibrosis, there is the potential to expand its application. For example, the technique may be modified to study the thin collagen fibers comprising the normal collagen framework of the heart. In recent years, this network has been characterized using scanning electron microscopy (Caulfield and Borg 1979, Borg and Caulfield 1981, Robinson et al 1987).

However, these structures may also be appreciated with high power light microscopy (Weber 1989). The small diameter of these fibers (< 500 nm (Caulfield and Borg 1979)) implies that retardation, and therefore visibility with polarizing microscopy, may be low. This could be overcome through adjustments to the compensator settings and manipulation of the grey-level offset, in a manner similar to that used by Allen et al (1981) to study ciliary motion. Quantitation of the components of the fibrous network may then be possible.

Finally, the assessment of muscle birefringence may also be exploited by this video technique. At present, there are several circumstances where the histologic appearance of the myocyte is discordant with its functional status. For example, in the early hours of cell death, the light microscopic appearance of the myocyte may be unremarkable (Hearse et al 1981). Also, it is hypothesized that myocytes may exist, for prolonged periods, in an injured but viable state. These cells have been referred to as "stunned" or "hibernating" and under the appropriate conditions may restore their function, with a coincident improvement in cardiac performance (Rahimtoola 1985). There is presently no satisfactory means of distinguishing these reversibly damaged myocytes from normal cells.

The possibility that the intensity of birefringence may reflect muscle cell viability was introduced in Chapter 6. This hypothesis could be tested by quantifying muscle brightness in a model of myocardial ischemia. Ultimately, with polarization-video microscopy, it may be possible to differentiate between normal myocytes, reversibly damaged myocytes, and early cell death. This could have considerable clinical value, for instance, in selecting those patients with coronary disease whose ventricular function would be most likely to improve after coronary revascularization.

In conclusion, the content and activity of myocardial fibrosis may be quantified using polarization-video microscopy.

Appendix Measurement of Retardation of Polarized Light

Retardation was measured using the method of de Sénarmont with monochromatic light (λ = 546 nm). In this approach, the fiber is brought to extinction and rotated through 45°. A quarter-wave plate is then inserted above the fiber. This plate consists of a birefringent substance that introduces a phase difference of 90° ($\lambda/4$) between the orthogonal rays that traverse it. Its slow axis is parallel to the transmission axis of the polarizer. The effect is to convert the elliptically polarized light that emerges from the specimen to linear polarized light, the azimuth of which depends on the relative phase of the 2 beams leaving the specimen, i.e., retardation. The analyzer is then rotated until its transmission axis is perpendicular to the plane of polarization of the emerging light and the fiber appears dark. Retardation in degrees is equal to twice the angle through which the analyzer was rotated (Slayter 1970, p 335).

The specific action of the quarter-wave plate may be understood if one considers the orthogonal beams emerging from the specimen independent of each other. Each beam will be resolved by the quarter-wave plate into two mutually perpendicular rays. These component beams will be of equal amplitude (because the vibration azimuths of the quarter-wave plate are 45° to those of the specimen) and the phase shift between them will be 90°. Upon exiting the plate they therefore recombine to form circularly polarized light. Since there are two, mutually perpendicular rays that emerge from the specimen there will be two circularly polarized beams exiting from the quarter wave plate, and these will have opposite senses. The resultant of two circularly polarized beams with opposite senses is a vibration which is linearly polarized in a plane determined by the relative phase of the two circular motions.* This in turn is determined

* This is in effect a corollary to the phenomona of circularly or elliptically polarized light forming as the resultant of two beams of plane-polarized light.

by the relative phase of the beams leaving the specimen, i.e., the retardation produced by the fiber. These features are depicted in Figure A.1.

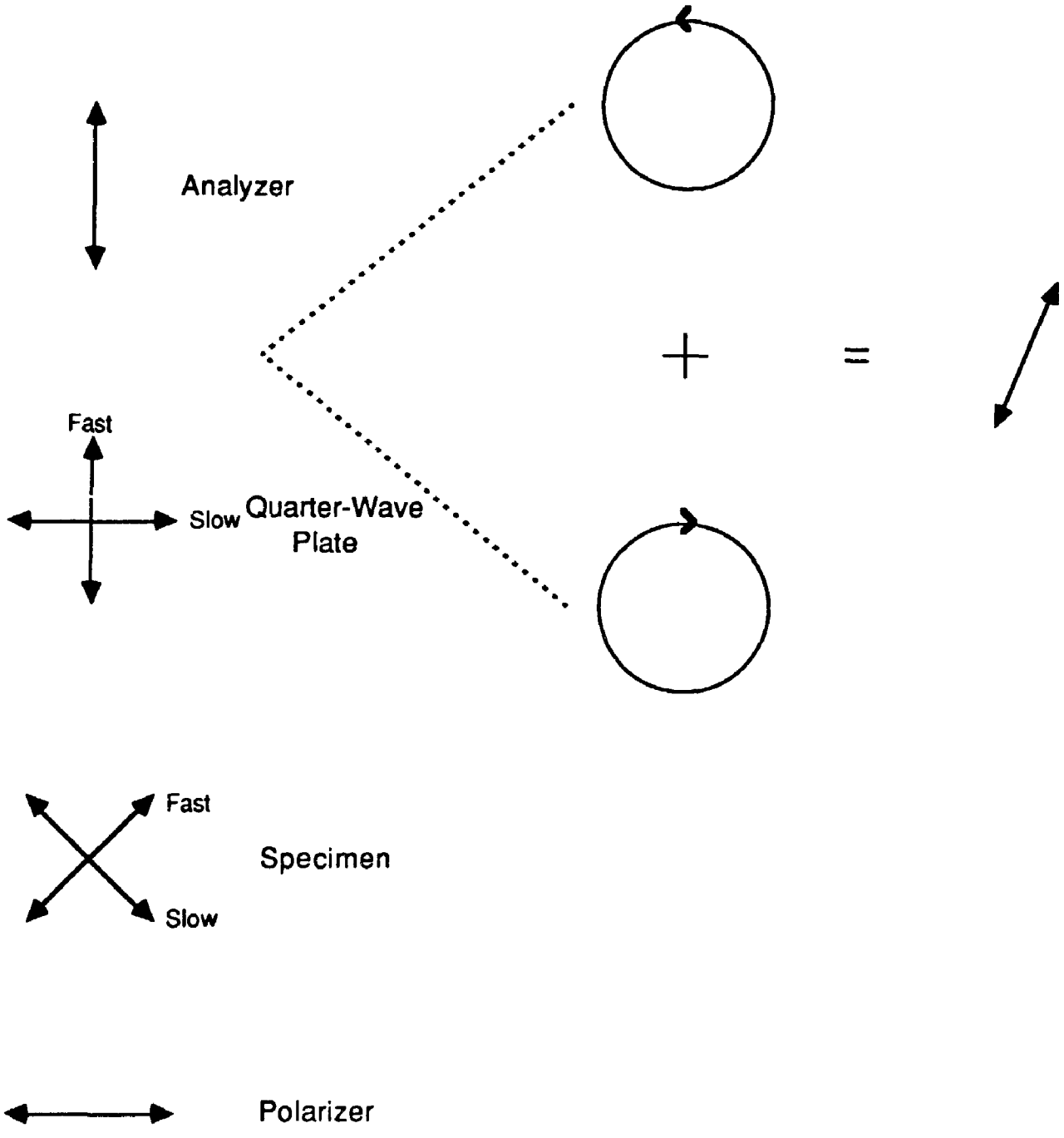

Figure A.1: Schematic diagram showing the effect of the quarter wave plate compensator. Adapted from Slayter 1980, p 335.

References

Abrahams C, Janicki JS, Weber KT. (1987) Myocardial hypertrophy in *Macaca fascicularis*. Structural remodelling of collagen matrix. Lab Invest 56: 676-683.

Adomian GE, Laks MM, Billingham ME. (1978) The incidence and significance of contraction bands in endomyocardial biopsies from normal human hearts. Am Heart J 96: 348-351.

Allain JC, Le Lous M, Bazin S, Bailey AJ, Delaunay A. (1978) Isometric tension developed during heating of collagenous tissues. Relationships with collagen cross-linking. Biochim Biophys Acta 533: 147-155.

Allen RD, Allen NS. (1983) Video-enhanced microscopy with a computer frame memory. J Microscopy 129: 3-17.

Allen Rd, Travis JL, Allen NS, Yilmaz H. (1981) Video-enhanced contrast polarization (AVEC-POL) microscopy: a new method applied to the motile reticulopodial network of *Allogromia caticollaris*. Cell Motil 1: 275-289.

Anttinen H. (1977) Collagen glucosyltransferase activity in human serum. Clin Chim Acta 77: 323-330.

Baandrup A, Florio RA, Olsen EJC. (1982) Do endomyocardial biopsies represent the morphology of the rest of the myocardium? A quantitative light microscopic study of single v. multiple biopsies with the King's bioptome. Eur Heart J 3: 171-178.

Bailey AJ, Light ND. Intermolecular crosslinking in fibrotic collagen. In: D Evered and J Whelen (Ed.), Fibrosis, CIBA Foundation Symposium 114. London, Pitman, 1985, pp 80-96.

Bates RJ, Beutler S, Resnekov L, Anagnostopoulos CE. (1977) Cardiac rupture - challenge in diagnosis and management. Am J Cardiol 40: 429-437.

Bennett HS. The Microscopal Investigation of Biological Materials with Polarized Light. In: R McClung-Jones (Ed.), McClung's Handbook of Microscopal Technique. New York, Harper and Row, 1950, pp 591-677.

Bieber CP, Stinson EB, Shumway N, Payne R, Kosek J. (1970) Cardiac transplantation in man. Cardiac allograft and pathology. Circulation 41: 753-772.

Billingham ME, Baumgartner WA, Watson DC, Reitz BA, Masek MA, Raney AA, Oyer PE, Stinson EB, Shumway WE. (1981) Distant heart procurement for heart transplantation. Ultrastructural studies. Circulation 62 (suppl I): 11-19.

Billingham ME. (1981) Diagnosis of cardiac rejection by endomyocardial biopsy. Heart Transplantation 1: 25-30.

Billingham ME. Cardiac transplantation. In: Waller BF (Ed.), Contemporary Issues in Cardiovascular Pathology, Philadelphia, FA Davis, 1988, pp 185-199.

Borg TK and Caulfield JB. (1981) The collagen matrix of the heart. Federation Proc 40: 2037-2041.

Brecher GA. (1956) Experimental evidence of ventricular diastolic suction. Circ Res 4: 513-518.

Brown GL, Nanny LB, Griffen J, Cramer AB, Yancey JM, Curtsinger LT, Holtzin L, Schultz G, Jurkievicz MJ, Lynch JV. (1989) Enhancement of wound healing by topical growth factor. New Engl J Med 321: 76-79.

Brunner G, Schubothe M. (1976). Prolylhydroxylase activity in liver biopsy specimens: an indicator for the activity of connective tissue formation? Digestion 14: 463.

Brutsaert L, Rademakers FE, Sys SU. (1984) Triple control of relaxation: implications in cardiac disease. Circulation 69: 190-196.

Burton AC (1954). Relation of structure to function of the tissues of the wall of vessels. Physiol Rev 34: 619-642.

Butzow JJ, Eichhorn GL. (1968) Physical chemical studies on the age changes in rat tail tendon collagen. Biochim Biophys Acta 154: 208-219.

Carrier M, Paplanus SH, Graham AR, Copeland JG. (1987) Histopathology of acute myocardial necrosis: effects of immunosuppression therapy. J Heart Transplantation 6: 218-221.

Caspari PG, Newcomb M, Gibson K, Harris P. (1977) Collagen in the normal and hypertrophied human ventricle. Cardiovasc Res 11: 554-558.

Caulfield JB and Borg TK. (1979) The collagen network of the heart. Lab Invest 40: 364-372.

Chiariello M, Ambrosio G, Capelli-Bigazzi M, Perrone-Filardi P, Brigante F, Sifola C. (1986) A biochemical method for the quantitation of myocardial scarring after experimental coronary occlusion. J Moll Cell Cardiol 18: 283-290.

Clore JN, Cohen IK, Diegelmann RF. (1979) Quantitation of collagen types I and III during would healing in rat skin. Proc Soc Exp Biol Med 161: 337-340.

Cohen IK, Moore CD, Diegelmann RF. (1979) Onset and localization of collagen synthesis during wound healing in open rat skin. Proc Soc Exp Biol Med 160: 458-462.

Constantine VS, Mowry RW. (1968). The selective staining of human dermal collagen. II. The use of picrosirius red F3BA with polarization microscopy. J Invest Derm 50: 419-423.

Cooper DKC, Novitzky D. Diagnosis and management of acute rejection. In: DKC Cooper and RB Lanza (Eds.), Heart Transplantation. Boston, MTP Press, 1984, pp 157-176.

Copeland JG. (1988) Cardiac Transplantation. Curr Probl in Cardiol 13: 157-224.

Dick MR, Unverferth DV, Baba N. (19^2) The pattern of myocardial degeneration in nonischemic congestive cardiomyopathy. Hum Pathol 13: 740-744.

Diegelmann RF, Peterkofsky B. (1972) Inhibition of collagen secretion from bone and cultured fibroblasts by microtubular disruptive drugs. Proc Natl Acad Sci 69: 892-896.

Doering CW, Jalil JE, Janicki JS, Pick R, Aghili S, Abrahams C, Weber KT. (1988) Collagen network remodelling and diastolic stiffness of the rat left ventricle with pressure overload hypertrophy. Cardiovasc Res 22: 686-695.

Drury RAB, Wallington EA. Carlton's Histological Technique. London, Oxford University Press, 1967, pp 166-181.

Edwards WD, Holmes DR, Reeder GS. (1982) Diagnosis of active lymphocytic myocarditis by endomyocardial biopsy. Quantitative criteria for light microscopy. Mayo Clin Proc 57: 419-525.

Eghbali M, Blumefeld OO, Seifter S, Butterick PM, Leinwand LA, Robinson TF, Zern MA, Gambrone MA. (1989) Location of types I, III and IV collagen mRNAs in rat heart cells by *in situ* hybridization. J Mol Cell Cardiol 21: 103-113.

Factor SM and Robinson TF. (1988) Comparative connective tissue structure-function relationships in biologic pumps. Lab Invest 58: 150-156.

Fragomeni LS, Kaye MP. (1988) The registry of the International Society for Heart Transplantation: fifth official report - 1988. J Heart Transplantation 7: 249-253.

Frey-Wyssling A. (1974) Ultrastructure research in biology before the electron microscopy. J Microsc 100: 21-34.

Fuster V, Danielson MA, Robb RA, Brodvent JC, Brown AL, Eleveback LR. (1977) Quantitation of left ventricular myocardial fiber hypertrophy and interstitial tissue in human hearts with chronically increased volume and pressure overload. Circulation 55: 504-508.

Gardner PI, Ursell PC, Pham TD, Fenoglio JJ, Wit AL. Experimental chronic ventricular tachycardia: anatomic and electrophysiologic substrates. In: ME Josephson, HJJ Wellens (Eds.), Tachycardias: Mechanisms, Diagnosis and Treatment. Philadelphia, Lea and Febiger, 1984, pp 29-40.

Gillman T. On some aspects of collagen formation in localized repair and in diffuse fibrotic reactions to injury. In: BS Gould (Ed.), Treatise on Collagen, Volume 2 Biology of Collagen, Part B. New York, Academic Press, 1968, pp 331-407.

Gokel JM, Reichart B, Struck E. (1985) Human cardiac tranpslantation - evaluation of morphologic changes in serial endomyocardial biopsies. Path Res Pract 178: 354-364.

Goldberg B, Rabinovitch M. Connective tissue. In: L Weiss (Ed.), Histology: Cell and Tissue Biology. New York, Elsevier Biomedical, 1983, pp 139-177.

Grant ME, Prockop DJ. (1972) The biosynthesis of collagen. N Engl J Med 286: 194-199.

Grossman W. Evaluation of systolic and diastolic function of the myocardium. In W Grossman (Ed.), Cardiac Catheterization and Angiography. Philadelphia, Lea and Febiger, 1986, pp 301-319.

Hearse DJ, Baimbridge MV, Jynge P: Protection of the Ischemic Myocardium: Cardioplegia. New York, Raven Press, 1981, pp 21-95.

Herskowitz A, Soule LM, Mellits ED, Traill TA, Achuff SC, Reitz BA, Borkon AM, Baumgartner WA, Baughan KL. (1987) Histologic predictors of acute cardiac rejection in human endomyocardial biopsies: a multivariate analysis. J Am Coll Cardiol 9: 802-810.

Hess OM, Ritter M, Schneider J, Grimm J, Turina M, Krayenbuehl HP. (1984) Diastolic sitffness in myocardial structure in aortic valve disease before and after valve replacement. Circulation 69: 855-865.

Hoyt RH, Ericksen E, Collins SM, Skorton DJ. (1984). Computer-assisted quantitation of myocardial fibrosis in histologic sections. Arch Pathol Lab Med 108: 280-283.

Hunt SA, Stinson EB. (1981) Cardiac transplantation. Ann Rev Med 32: 213-220.

Hunt SA, Stinson EB. Accelerated atherosclerosis in the cardiac allograft. In: J Wallwork (Ed.), Heart and Heart-Lung Transplantation. Toronto, WB Saunders, 1989, pp 359-368.

Imakita M, Tazelaar HD, Rowan RA, Masek MA, Billingham ME. (1887) Myocyte hypertrophy in the transplanted heart. A morphometric analysis. Transplantation 43: 839-842.

Inoué S. (1981) Video image processing greatly enhances contrast, quality, and speed in polarization-based microscopy. J Cell Biol 89: 346-356.

Inoué S. Video Microscopy. New York Plenum, 1986.

Inoué S, Hyde W. (1957) Studies on depolarization of light at microscope lens surfaces. II. The simultaneous realization of high resolution and high sensitivity with the polarizing microscope. J Biophys Biochem Cytol 3: 831-844.

Jalil JE, Doering CW, Janicki JS, Pick R, Schroff SG, Weber KT. (1989) Fibrillar collagen and myocardial stiffness in the intact hypertrophied rat ventricle. Circ Res 64: 1041-1050.

Jarvis LR. (1988) Microcomputer video image analysis. J Microscopy 150: 83-97.

Jozsa L, Reffy A, Balint JB. (1984) Polarization and electron microscopic studies on the collagen of intact and ruptured human tendons. Acta Histochem 74: 209-215.

Jugdutt BI and Amy RM. (1986). Healing after myocardial infarction in the dog. Changes in infarct hydroxyproline and topography. J Am Coll Cardiol 7: 91-102.

Junqueira LCU, Bignolas JG, Brentani RR. (1979) Picrosirius staining plus polarization microscopy, a specific method for collagen detection in tissue sections. Histochem J 11: 447-455.

Junqueira LCU, Cossermelli W, Brentani R (1978) Differential staining of collagens type I, II and III by sirius red and polarization microscopy. Arch Histol Jap 41: 267-274.

Junqueira LCU, Montes GS, Sanchez EM. (1982) The influence of tissue section thickness on the study of collagen by the picrosirius-polarization method. Histochem 74: 153-156.

Karch SB, Billingham ME (1985) Cyclosporine induced myocardial fibrosis: a unique controlled case report. Heart Tranplantation 4: 210-212.

Kastelic J, Baer,E. Deformation in tendon collagen. In: JFV Vincent, JD Currie (Eds.), The Mechanical Properties of Biologic Materials. London, Cambridge University Press, 1980, pp397-435.

Katz AM. (1990) Cardiomyopathy of overload. A major determinant of prognosis in congestive heart failure. N Engl J Med 322: 100-110.

Kavanagh T, Yacoub MH, Mertens DJ, Kennedy J, Campbell RB, Sawyer P. (1988) Cardiorespiratory responses to exercise training after orthotopic cardiac transplantation. Circulation 77: 161-171.

Kozlocskis PL, Fieber LA, Pruitt DK, Bailey BK, Smets MJD. Baset AL, Kimura S, Myerburg RJ. (1987) Myocardial changes during the progression of left ventricular pressure-overload by renal hypertension on aortic constriction: myosin, myosin ATPase and collagen. J Mol Cell Cardiol 19: 105-114.

Krayenbuehl HP, Hess OM, Monrad ES, Schneider J, Mall G,Turina M. (1989) Left ventricular myocardial structure in aortic valve disease before, intermediate and late after aortic valve replacement. Circulation 79: 744-755.

Labovitz AJ, Drimmer AM, McBride LR, Pennington DG, Willman VL, Miller LW. (1989) Exercise capacity during the first year after cardiac transplantation. Am J Cardiol 64: 642-645.

Lenkiewicz JE, Davies MJ, Rosen D. (1972) Collagen in human myocardium as a function of age. Cardiovasc Res 6: 549-555.

Lerman RH, Apstein CS, Kagan HM, Osmers EL, Chichester CO, Vogel WM, Connolly CM, Steffee WP. (1983) Myocardial healing and repair after experimental infarction in the rabbit. Circ Res 53: 378-388.

Levenson SM, Geever EF, Crowley LV, Oates JF, Berard CW, Rosen H. (1965) The healing of rat skin wounds. Ann Surg 161: 293-308.

Light ND, Bailey AJ. Molecular structure and the stabilization of the collagen fibre. In: A Viddik, J Vuust (Eds.), Biology of Collagen. London, Academic Press, 1980, pp 15-38.

Madden JW, Davis WM, Butler C. (1973). Experimental esophageal lye burns. II Correcting established structures with beta-aminopropionitrile and bougienage. Ann Surg 178: 277-284.

Madden JW, Peacock EE.(1968) Studies on the biology of collagen during wound healing. I Rate of collagen synthesis deposition and cutaneous wounds of the rat. Surgery 64: 288-294.

Mall G, Schwarz F, Derks H. (1982) Clinical pathologic correlations in congestive cardiomyopathy. A study on endomyocardial biopsies. Virchows Arch 397: 67-82.

Mallory GK, White PD, Salcedo-Salgar J. (1939) The speed of healing of myocardial infarction: a study of the pathologic anatomy in 72 cases. Am Heart J 18: 647-671.

Medsgers TA, Masi T, Rodnan GP, Benedek TG, Robinson H. (1971) Survival with systemic sclerosis. A life-table analysis of clinical and demographic factors in 309 patients. Ann Int Med 75: 369-371.

Medugorac I and Jacob R. (1983) Characterization of left ventricular collagen in the rat. Cardiovasc Res 17: 15-21.

Mello ML, Godo C, Vidal BC, Abujadi JM. (1975) Changes in macromolecular orientation on collagen fibres during the process of tendon repair in the rat. Ann Histochim 20: 145-152.

Mezey E, Potter JJ, Maddrey WC. (1976) Hepatic collagen proline hydroxylase activity in alcoholic liver disease. Clin Chim Acta 68: 313-320.

Moore GW, Hutchins GM, Bulkley BH, Tseng JS, Kai PF. (1980) Constituents of human ventricular myocardium; connective tissue hyperplasia accompanying muscular hypertrophy. Am Heart J 100: 610-616.

Mortensen SA, Baandrup U. (1987) Endomyocardial biopsy with a modified bioptome introducer sheath: focus on diagnostic yield and prevention of complications. Cath Cardiovasc Diag 13: 194-203.

Nakayama Y, Shimizu G, Hirota Y, Saito T, Kino M, Kitaura Y, Kawmaura K. (1987) Functional and histopathologic correlation in patients with dilated cardiomyopathy: an integrated evaluation by multivariate analysis. J Am Coll Cardiol 10: 186-192.

Neuman RE, Logan MA. (1950) The determination of hydroxyproline. J Biol Chem 184: 299-306.

Nimni ME, Harkness RD. Molecular structures and functions of collagen. In: ME Nimni (Ed.), Collagen, Volume 1, Biochemistry. Boca Raton, CRC Press, 1988, pp 1-78.

Nimni ME. (1980) The molecular organization of collagen and its role in determining the biophysical properties of the connective tissues. Biorheology 17: 51-82.

Oikarinen A. (1977) Effect of cortisol acetate on collagen biosynthesis and on the activities of prolylhydroxylase, lysylhydroxylase, collagen galactosyltransferase, and collagen glucosyltransferase in chick-embryo tendon cells. Biochem J 164: 533-539.

Oken DE, Boucek RJ. (1957) Quantitation of collagen in human myocardium. Circ Res 5: 357-361.

Oldershaw PJ, Brookspy IAB, Davies MJ, Coltart DJ, Jenkins BS, Webb-Peploe MM. (1980) Correlations of fibrosis in endomyocardial biopsies from patients with aortic valve disease. Br Heart J 44: 609-611.

Olsen EGJ. (1975) Pathological recognition of cardiomyopathy. Postgrad Med J 51: 277-281.

Pearlman ES, Weber KT, Janicki JS, Pietra GG, Fishman AP. (1982) Muscle fiber orientation and connective tissue content in the hypertrophied human heart. Lab Invest 46: 158-164.

Perez-Tamayo R, Montfort I. (1980) The susceptibility of hepatic collagen to homologous collagenase in human and experimental cirrhosis of the liver. Am J Pathol 100: 427-442.

Pfeffer MA, Lamas GA, Vaughan DE, Parisi AF, Braunwald, E. (1988) Effect of captopril on progressive ventricular dilatation after anterior myocardial infarction. N Engl J Med 319: 80-86.

Pick R, Jalil JE, Janicki JS, Weber KT. (1989) The fibrillar and nature and structure of isoproterenol-induced myocardial fibrosis in the rat. Am J Pathol 134: 365-371.

Pickering JG, Boughner, DR. (1990) Fibrosis in the transplanted heart and its relation to donor ischemic time. Assessment with polarized light microscopy and digital image analysis. Circulation 81: 949-958 .

Pickering JG, Cunningham DJ, Patterson D, Boughner DR. (1988) Cardiorespiratory response to exercise in cardiac transplant recipients. Clin Invest Med 11: D72.

Pomerance A, Stovin PGI. (1985) Heart transplant pathology: the British experience. J Clin Pathol 38: 146-159.

Porter RR, Reid KBM. (1978) The biochemistry of complement. Nature 275: 699-704.

Pratt, WK. (1978) Digital Image Processing. J Wiley and Sons, New York.

Prockop DJ, Kivirikko KI, Tuderman L, Guzman N. (1979a) The biosynthesis of collagen and its disorders. N Engl J Med 301: 77-85.

Prockop DJ, Kivirikko KI, Tuderman L, Guzman NA. (1979b) The biosynthesis of collagen and its disorders. N Engl J Med 301: 13-23.

Prockop DJ, Kivirikko KI. (1984) Heritable diseases of collagen. N Engl J Med 311: 376-386.

Prockop DJ, Udenfriend S. (1960) A specific method for the analysis of hydroxyproline in tissue and urine. Anal Biochem 1: 228-239.

Rahimtoola SH. (1985) A perspective on the three large multicenter, randomized clinical trials of coronary bypass surgery for chronic stable angina. Circulation 72 (Suppl V): V123-V135.

Richards DA. Blake GJ, Spear JF, Moore EN. (1984) Electrophysiologic substrate for ventricular tachycardia: correlation of properties in vivo and in vitro. Circulation 69: 369-381.

Robbins SL and Cotran RS. Pathologic basis of disease. Toronto, WB Saunders, 1979.

Robinson TF, Cohen-Gould L, Factor SM. (1983) Skeletal framework of mammalian heart and muscle. Arrangement of inter- and pericellular connective tissue strcutures. Lab Invest 49: 482-498.

Robinson TF, Factor SM, Capasso JM, Wittenberg BA, Blumenfeld OO, Seifter S. (1987) Morphology, composition and function of struts between cardiac myocytes of rat and hamster. Cell Tissue Res 249: 247-255.

Robinson TF, Factor SN, Sonnenblick EH. (1986) The heart as a suction pump. Scientific American 254: 84-91.

Rose AG, Uys CJ. Pathology of acute rejection. In: DKC Cooper and RP Lanza (Eds.), Heart Transplantation. Lancaster MTP Press Limited, 1984, pp 157-76.

Schwarz F, Mall G, Zebe H, Blickle J, Derks H, Manthey J, Kubler W. (1983) Quantitative morphologic findings of the myocardium in the idiopathic dilated cardiomyopathy. Am J Cardiol 51: 501-506.

Shanes JG, Ghali J, Billingham ME, Ferrans VJ, Fenoglio JJ, Edwards WD, Tsai CC, Saffitz JE, Isner J, Furner S, Subramanian R. (1987) Interobserver variability in the pathologic interpretation of endomyocardial biopsy results. Circulation 75: 401-405.

Shurcliff WA. Polarized Light. Cambridge Massachusetts, Harvard University Press, 1962.

Silbert JE. Biosynthesis of mucopolysaccharides and protein polysaccharides. In: R Perez-Tamayo and M. Rojkind (Eds.), Molecular Pathology of Connective Tissues, New York, Marcel-Dekker, 1973, pp 323-353.

Sinex FM. The role of collagen in aging. In: BS Gould (Ed.) Treatise on Collagen, Volume 2, Biology of Collagen, Part B. New York, Academic Press, 1968, pp 409-448.

Slayter EM. Optical Methods in Biology. New York, Wiley-Interscience, 1970.

Sweet F, Puchtler H, Rosenthal SL. (1964) Sirius red F3BA as a stain for connective tissue. Arch Path 78: 69-72.

Tanaka M, Fujiwara H, Onodera T, Wu DJ, Hamashima Y, Kawai C. (1986) Quantitative analysis of mycoardial fibrosis in normals, hypertensive hearts and hypertrophic cardiomyopathy. Br Heart J 55: 575-81.

Thomson D, McKenzie FN. (1988) Examining the growing success of heart transplantation. Persp Cardiol 4: 39-50.

Timpl R, Vondermark K, Vondermark H. Immunochemistry and immunohistology of collagens. In: A Viidik and J Vuust (Eds.), Biology of Collagen. London, Academic Press, 1980, pp 211-222.

Tomanek RJ, Taunton CA, Liskop KS. (1972) Relationship between age, chronic exercise and connective tissue of the heart. J Gerontol 27: 33-38.

Topel EJ, Traill TA, Fortuin NJ. (1985) Hypertensive hypertrophic cardiomyopathy of the elderly. N Engl J Med 312: 277-283.

Tsellarius YG. (1967) Changes in muscle fibers of the heart in adrenalic injuries. Arkh Patol 29: 34-40.

Unverferth DV, Fetters JK, Unverferth DJ, Leier CV, Magoren RD, Arn AR, Baker PB. (1983) Human myocardial histologic characteristics in congestive heart failure. Circulation 68: 1194-1200.

Vesely I, Boughner DR. (1989) Analysis of the bending behaviour of porcine xenograft leaflets and of natural aortic valve material: bending stiffness, neutral axis and shear measurements. J Biomech 22: 655-671.

Weber KT, Janicki JS, Pick R, Abrahams C, Schroff SG, Bashey RI, Chen RM. (1987) Collagen in the hypertrophied, pressure-overloaded myocardium. Circulation 75(suppl I): I40-I47.

Weber KT, Pick R, Janicki JS, Gadodia D, Lakier JB. (1988) Inadequate collagen tethers in dilated cardiomyopathy. Am Heart J 6: 1641-1646.

Weber KT. (1989) Cardiac interstitium in health and disease: the fibrillar collagen network. J Am Coll Cardiol 13: 1637-1652.

Weibel ER. Morphometry of the Human Lung. New York Academic Press, 1963, pp 9-39.

White DJG. Immunosuppression for cardiac tranpslantation. In: J Wallwork (Ed.), Heart and Heart Lung Transplantation. Toronto, WB Saunders, 1989, pp 155-172.

Whittaker P, Boughner DR, Kloner RA. (1989) Analysis of healing after myocardial infarction using polarized light microscopy. Am J Pathol 134: 879-893.

Whittaker P. (1986) Structural analysis of cardiovascular tissue using quantitative polarized light microscopy. Ph.D.Thesis The University of Western Ontario, London, Canada.

Williams IF, McCullagh KG, Silver IA. (1984) The distribution of types I and III collagen and fibrinectin in the healing equine tendon. Conn Tiss Res 12: 211-227.

Woessner JF. (1961) The determination of hydroxyproline in tissue and protein samples containing small proportions of this iminoacid. Arch Biochem Biophys 93: 440-447.

Wolman M. (1970) On the use of polarized light in pathology. Pathol Ann 5: 381-416.

Wolman M. (1975) Polarized light as a tool of diagnostic pathology. J Histochem Cytochim 23: 21-50.

Wolman M, Gillman T. (1972) A polarized light study of collagen in dermal wound healing. Br J Exp Pathol 53: 85-89.

Wolman M, Kasten FH. (1986) Polarized light microscopy in the study of the molecular structure of collagen and reticulin. Histochem 85: 41-49.

Yonesaka S, Becker AE. (1987) Dilated cardiomyopathy: diagnostic accuracy of endomyocardial biosy. Br Heart J 58: 156-161.

Young JB, Leon CH, Short HD, Noon GP, Lawrence EC, Whisennand HH, Pratt CM, Goodman DA, Weilbaecher D, Quinones MA, De Bakey ME. (1987) Evolution of hemodynamics after orthotopic heart and heart-lung transplantation: early restrictive patterns persisting in occult fashion. J Heart Tranpslantation 6: 34-43.